Hydrothermal Alteration, gold distribution and geochronology of epithermal gold mineralization in the Copiapo volcanic complex, Chile

A thesis submitted in partial fulfillment of the requirements for the degree of Bachelor of Science with Honours at Dalhousie University, Halifax, Nova Scotia, Canada

by

Thomas Mulja

March 7, 1986.

Distribution License

DalSpace requires agreement to this non-exclusive distribution license before your item can appear on DalSpace.

NON-EXCLUSIVE DISTRIBUTION LICENSE

You (the author(s) or copyright owner) grant to Dalhousie University the non-exclusive right to reproduce and distribute your submission worldwide in any medium.

You agree that Dalhousie University may, without changing the content, reformat the submission for the purpose of preservation.

You also agree that Dalhousie University may keep more than one copy of this submission for purposes of security, back-up and preservation.

You agree that the submission is your original work, and that you have the right to grant the rights contained in this license. You also agree that your submission does not, to the best of your knowledge, infringe upon anyone's copyright.

If the submission contains material for which you do not hold copyright, you agree that you have obtained the unrestricted permission of the copyright owner to grant Dalhousie University the rights required by this license, and that such third-party owned material is clearly identified and acknowledged within the text or content of the submission.

If the submission is based upon work that has been sponsored or supported by an agency or organization other than Dalhousie University, you assert that you have fulfilled any right of review or other obligations required by such contract or agreement.

Dalhousie University will clearly identify your name(s) as the author(s) or owner(s) of the submission, and will not make any alteration to the content of the files that you have submitted.

If you have questions regarding this license please contact the repository manager at dalspace@dal.ca.

Grant the distribution license by signing and dating below.

_____ _____

Name of signatory Date

FRONTISPIECE. Cone Azufre (6042 m) of Volcan Copiapo.

Hydrothermal alteration, gold distribution and geochronology of epithermal mineralization in the Copiapo volcanic complex, Chile.

by Thomas Mulja

Abstract

This thesis is a pilot project of an ongoing investigation into the gold metallogenesis in the Copiapo volcanic complex, Chile. The study is aimed at understanding the pattern of hydrothermal alteration and its relation to the gold mineralization in a local geological context at latitutes 27° 08' to 27°24' South and longitutes 69° 00' to 69° 20' west.

Petrographic, chemical and X-ray diffraction studies have led to the recognition of three types of altered mineral assemblages: I. montmorillonite ± jarosite ± kaolinite, II. sericite + quartz ± kaolinite ± chlorite and III. alunite + quartz ± dickite ± prehnite. Field relations of these assemblages do not suggest any direct spatial and/or temporal relationships. Type III assemblage flanks a gold bearing quartz-alunite vein system. The most significant geochemical transfers are : 1. addition of silicon, potassium and iron in alteration type I; 2. removal of magnesium, manganese and calcium in all assemblages, and 3. exchange of other elements for silicon in type III.

Gold, arsenic, lead, antimony, selenium, molybdenum and sulfur are enriched in all altered rocks. Gold is progressively enriched from fresh to altered rocks and to veins. The highest gold grade is 4.5 ppm, compared with 10 ppb in fresh rocks. Alteration-mineralization systems are restricted to north-south trending fracture zones, which appear to be the structural control for hydrothermal activity.

On the basis of new radiometric dates on volcanic rocks and on altered/mineralized rock, the volcanological evolution of the complex during the last 14 Ma or so is characterized by explosive volcanism, in which major eruptions occurred at about 14, 10 and 8.6 Ma. Two lava flows were erupted in different localities, but almost at the same time: 13.8 $\pm$ 0.6 and 13.29 $\pm$ 0.05 Ma. Caldera formation and resurgence, alteration and gold mineralization are related to volcanism. A radiometric date on alunite, which is associated with gold mineralization, yields a K/Ar age of 12.0 $\pm$ 0.6 M.a.

The Geologic characteristics, alteration and gold mineralization patterns are comparable to those recognized elsewhere in the world.

Acknowledgements

This thesis would not have been written without the supports from both my family and Dr. Marcos Zentilli who initiated and supervised this work. Major fund for this thesis came from the NSERC operating grant (No. A9036) to Dr. Zentilli.

The writer would like to acknowledge the generous assistance and cooperation given by the following individuals;

Dr. P. Reynolds and Mr. K. Taylor : geochronology

Mr. S. Parikh : technique of analytical geochemistry

Ms. K. Gillis and Dr. G.k. Muecke : alteration geochemistry

Mr. P. Wallace : photomicrograph technique

Mr. G. Oakey, Mr. R. Hingston and Mr. I. MacInnis : computer text editing,

and numerous people in the geology department.

A special thank is directed to Ms. L. Young who read the entire text and gave constructive suggestions. Nevertheless, the writer is solely responsible for all the contents of this thesis.

Table of Contents

	Page
Abstract	i
Acknowledgements	iii
List of Figures	vi
List of Tables	vii
List of Plates	viii
Chapter I. Introduction	
1.1 General statement	1
1.2 Geography	1
1.3 Previous and current work	6
1.4 The present study :	
A. Objectives, methods and limitations	6
B. Sampling and analytical methods	9
C. Organization of this thesis	11
Chapter II. Caldera resurgence : a review of volcanogenic epithermal ore deposits	
2.1 Introduction	12
2.2 Caldera resurgence	12
2.3 Mineralization	15
Chapter III. Geology and Petrology	
3.1 Introduction	20
3.2 Geology of Copiapo volcanic complex	24
A. Pre-Tertiary basement	27
B. Tertiary lithologies	27
C. Structural geology	29
3.3 Petrology and geochemistry of Tertiary lithologies	
A. Pyroclastic rocks	31
B. Lavas	34
C. Intrusive rocks	38
D. Vein and cap rocks	39
E. Summary	39
F. Geochemistry	41
Major Elements	43
Trace elements	51
G. Summary	58
Chapter IV. Hydrothermal Alteration	
4.1 Introduction	59
4.2 Physical changes	59
4.3 Mineralogical changes	61
4.4 Chemical changes	70
4.5 Discussion	79
4.6 Conclusions	82
Chapter V. Gold distribution	
5.1 Introduction	84
5.2 Results and discussion	84
A. Gold	84
B. Arsenic and antimony	87

C. Molybdenum, lead and selenium..... 89
D. Potassium and sulfur..... 89
5.3 Discussion..... 89
5.4 Conclusions..... 92

Chapter VI. Geochronology
6.1 Introduction..... 93
6.2 The K-Ar and Ar-Ar dating methods..... 93
6.3 Results and discussions..... 95
6.4 Conclusions..... 102

Chapter VII. General discussion, Conclusions and Recommendations.
7.1 General discussion..... 103
7.2 Conclusions..... 104
7.3 Recommendations..... 106

References

Appendices

I. Analytical methods
II. Petrography
III. X-ray Diffraction patterns
IV. Gains and losses of elements

List of Figures

		Page
I.1	Setting of Copiapo volcanic complex.....	2
I.2	Location of the study area.....	3
I.3	Physiographic regions of part of northern Chile and Argentina.....	5
I.4	Sample location map.....	10
II.1	Model of ore deposits associated with a caldera..	13
II.2	Evolution of a resurgent caldera.....	14
II.3	Generalized model of an epithermal deposit and its alteration patterns.....	17
III.1	Seismic map of the Andes.....	21
III.2	Distribution of late Cenozoic volcanisms in the central Andes.....	22
III.3	Regional geology of the Andes (26°-29° S).....	23
III.4	Geochronology map of the Andes (26°-29° S).....	25
III.5	Chemical variations along the Chilean-Argentinian transect.....	26
III.6	Geology of Copiapo volcanic complex.....	28
III.7	Satellite image of Copiapo volcanic complex.....	30
III.8	$Na_2O + K_2O$ vs SiO_2 diagram.....	44
III.9	K_2O vs SiO_2 diagram.....	45
III.10	The AFM diagram.....	46
III.11	The Harker variation diagrams.....	47
III.12	Zr vs TiO_2 diagram.....	50
III.13	Rb and Ba vs SiO_2 diagram.....	52
	Rb and Ba vs K_2O diagram.....	52
III.14	Ni, Cr and V vs SiO_2 diagam.....	54
	Ni vs MgO diagram.....	54
III.15	Cu vs SiO_2 diagram.....	56
IV.1	Distribution of alteration assemblages.....	67
IV.2	Ti/Zr ratio in the altered rocks.....	72
IV.3	Gains and losses of geochmical elements.....	76
V.1	Comparison of gold and associated elements.....	86
VI.1	Location of radiometrically dated rocks.....	98
VI.2	Evolution of the Copiapo volcanic complex.....	100

List of Tables

page

I.1 Selected publications on Central Andes (26°- 29° Lat. S)..... 7

II.1 Characteristics of volcanogenic epithermal deposits. 18

III.1 Chemical analyses of unaltered rocks 42

III.2 Simple statistics of copper..... 55

IV.1 Alteration mineralogy..... 62

IV.2 Chemical analyses of altered rocks..... 71

IV.3 Original lithology of altered rocks..... 73

IV.4 Comparison of chemical analyses between alteration type III and vein rocks..... 79

V.1 Analytical results of gold and other selected trace elements..... 85

VI.1 Radiometric data for Copiapo rocks..... 96

List of Plates

page

Plate

1. Andesitic ignimbrite (TS) 32
2. Andesitic lava flow (HS) 35
3. Andesitic lava (TS) 35
4. Quartz-Alunite vein (HS) 40
5. Altered rock (HS)..... 60
6. Altered glass (TS) 63
7. Altered ignimbrite (TS) 63
8a,b. Silicified rock (TS) 64
9. Sericitized feldspar (TS) 65
10. Prehnite replacing feldspar (TS) 65
11,12. Crustified texture of quartz veinlet (TS) 88

TS: Thin section, HS: Hand specimen

Chapter I

Introduction

1.1 General statement

The interest in epithermal gold deposits in volcanic terrains has recently increased but this kind of deposit is still poorly understood. Recently, Sillitoe and Bonham (1981) and Buchanan (1981) have suggested generalized models which outline the host rocks, vertical and horizontal patterns of wall-rock alteration, mineralization, level of deposition, and chemical and physical ore controls of epithermal precious metal deposits. This thesis is the first attempt to understand epithermal gold mineralization associated with volcanic activity in the Copiapo volcanic complex in the Central Andean Cordillera of Chile (Figure I.1). The complex is possibly part of a resurgent caldera of Miocene age. Rocks in Copiapo volcanic Complex have not been intensely weathered thus the original alteration patterns are still retained. It was hoped that thwas theswas would provide some useful guides for exploration of epithermal gold in the study area.

1.2 Geography

The area of this study is located in the Chilean volcanic belt between latitudes 27° 08' and 27° 24' South and longitudes 69° 00' and 69° 20' West (Figure I.2). The products of the Copiapo volcanic Complex cover an area of about 200 square kilometers. The highest peak Azufre (6042 m) of Copiapo volcanic Complex (hereafter referred to as Copiapo) is located at latitute 27° 15' South and 69° 08' Longitude, about 100 kilometers east of the

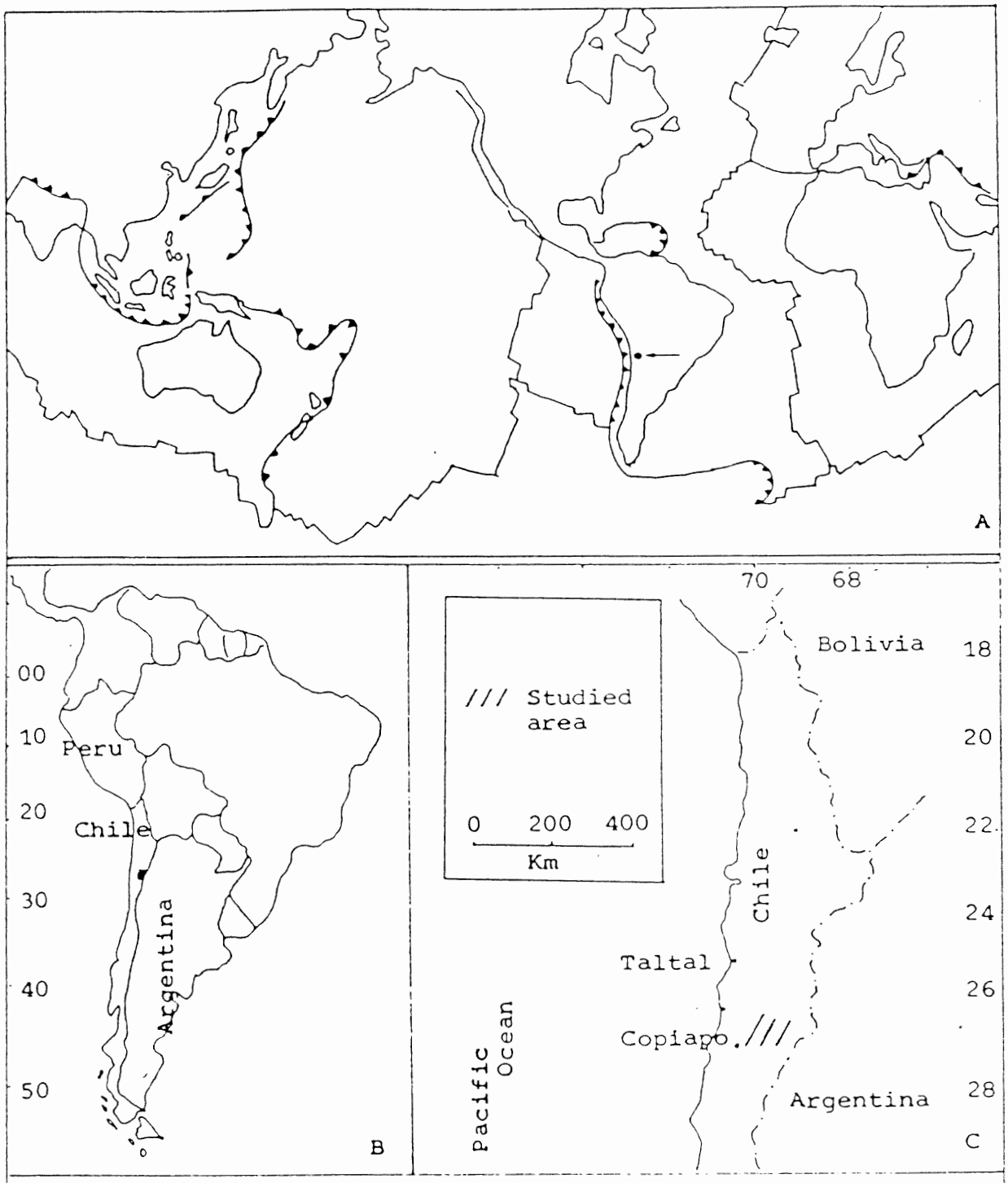

Figure I.1 Setting of Copiapo Volcanic Complex in (A) World Tectonic Map, (B) South America Map and (C) Regional Map.

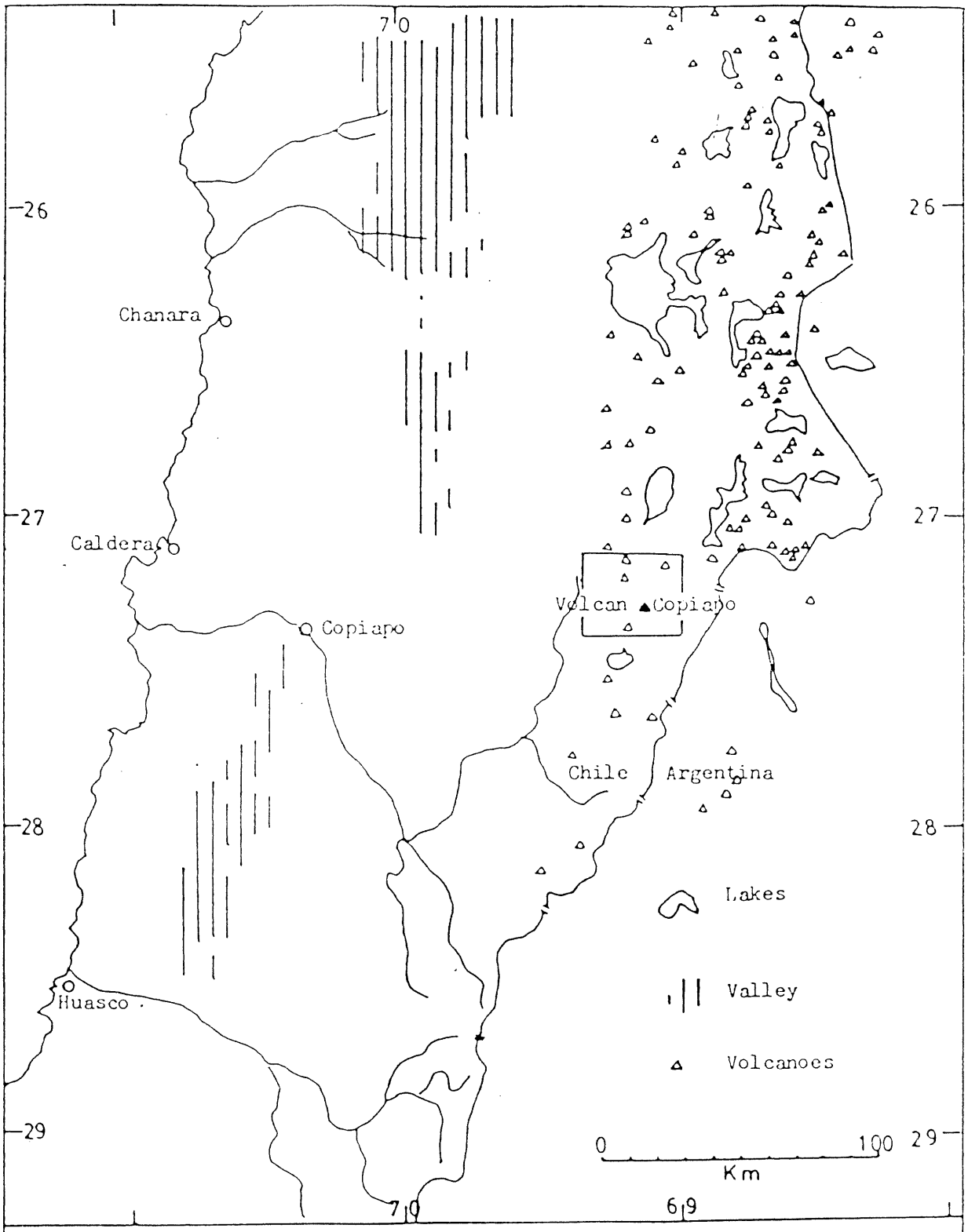

Figure I.2 Location of the study area (map after Zentilli, 1974)

town of Copiapo (Figure I.1). The area is currently under exploration, and accessibility is generally good but unpredictable because of weather. The following geography descriptions draw freely from Zentilli (1974).

Figure I.3 shows the physiographic regions of Northern Chile. Copiapo is located at the boundary between two divisions, Norte Grande (Big North) and Norte Chico (Small North). The boundary lies at about 27° South and coincides roughly with the valley of the Rio Copiapo. The Norte Grande, comprising the Atacama Desert proper, is extensively dry and inhospitable, but to the south of the Rio Copiapo Valley, vegetation is more abundant and the climate less extreme.

Copiapo lies within the Chilean Precordillera physiographic division, one of the Chile's predominant structural lines which run north-south. This region has a mean altitude of about 4000 meters and is covered by the products of intense Tertiary and Quaternary volcanism, forming the high plateau. A large number of strato-volcanoes attain altitude of 6000 meters or higher. In the high Precordillera, rain falls predominantly during the austral summer, and snow storms are frequent in winter and summer. There is no record on the amount of precipitation in this terrain. Vegetation is limited to hard grasses and hard bushes near lakes and seasonal streams.

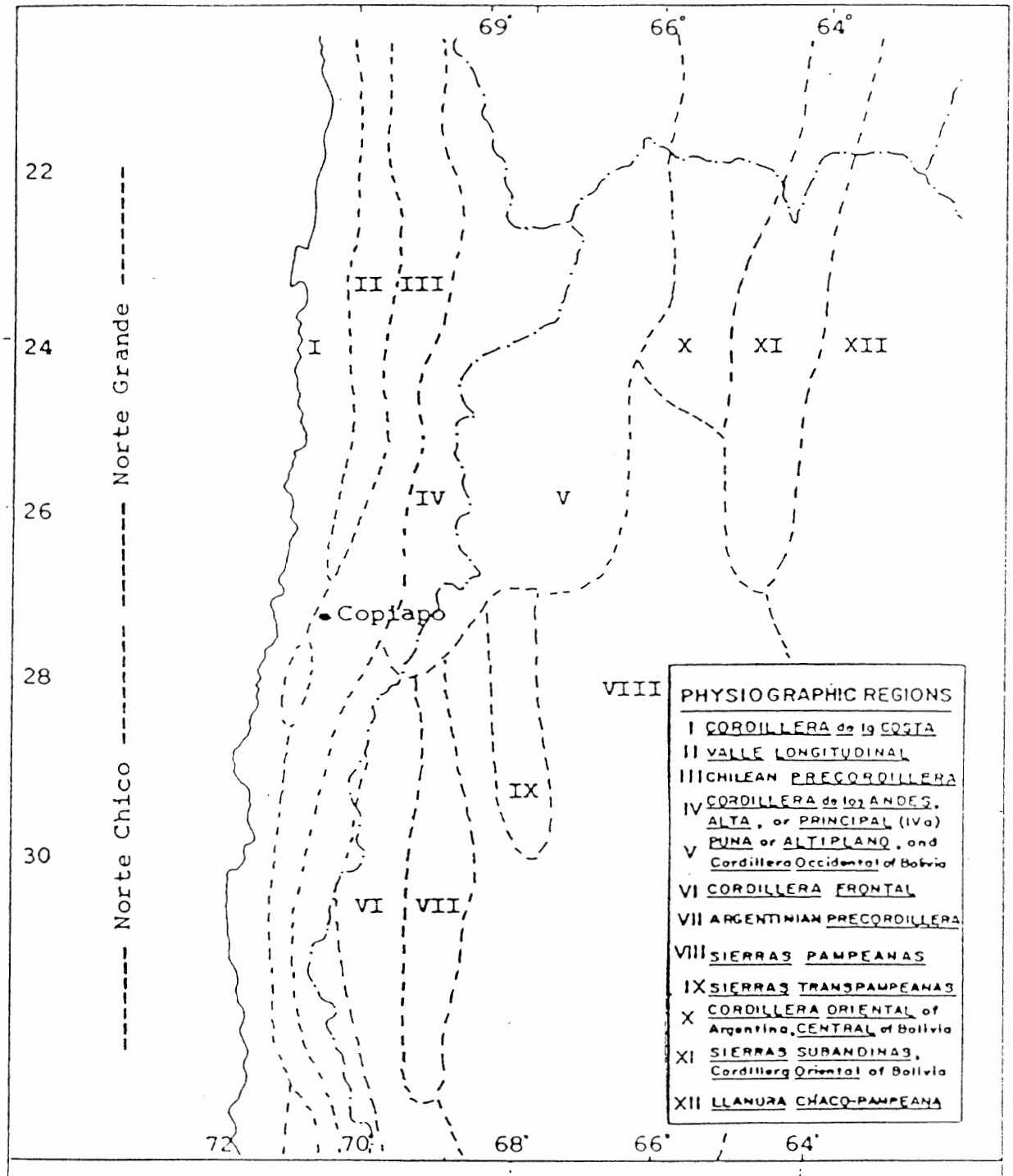

Figure I. 3 Physiographic regions of part of northern Chile and Argentina (after Zentilli, 1974).

1.3 Previous and current work

Numerous works have been carried out at regional scale in the Central Andes between latitudes 26°-29° South (Table I.1). However, only few reports including the geology of Copiapo have been published. Among these are Segerstorm (1968), Mercado (1982) and Gonzalez-Ferran et al.(1985).

A number of honours theses have dealt with particular problems, such as volcanic petrology by Corning (1974), regional geochemical variation by Palma (1976) and opaque mineralogy of lavas by Burke (1978). However, these writers did not include alteration and gold mineralization in their studies. A collaborative research program on magmatism and metallogeny of the Copiapo region was initiated in 1984 between geologists with the Servicio Nacional de Geologia y Mineria (SERNAGEOMIN) of Chile, Dalhousie University (M. Zentilli) and Northern Illinois University (J. Walker). This thesis forms an integral part of this continuing research.

1.4 The present study :

A. Objectives, methods and limitations

This thesis has three fundamental objectives: (i) to document the alteration in mineralogy and geochemistry which the studied rocks have undergone as a result of hydrothermal processes, (ii) to determine the distribution characteristics of gold mineralization in the studied area, and (iii) to place

Prime Study	Author(s)	Year
General Geology	Segerstorm	1959
	Mercado	1982
Tectonics, Stratigraphy,	Clark and Zentilli	1972
Magmatism, Metallogeny	Zentilli	1974
	Lortie and Clark	1975
	Haynes	1975
	Caelles	1979
	Gonzalez-Ferran et al.	1985
	Walker and Zentilli	1985
Strontium isotopes, Trace	McNutt et al.	1975
elements	Dostal et al.	1977
	Zentilli and Dostal	1977
Igneous rocks, Geochronology	Farrar et al.	1970
	Caelles et al.	1971
	Quirt	1972
	McBride	1972
	McBride et al.	1976

Table I.1 Selected publications on Central Andes (26°-29° S). Not all of them are consulted for this thesis.

the hydrothermal event(s) which are responsible for the alteration and gold mineralization, in the context of the geologic history of the area.

Selected rock samples, both fresh and altered, were analyzed petrographically and chemically. X-ray diffraction analyses were carried out for mineral identification. Biotite and hornblende grains were separated by hand-picking from fresh rocks for geochronology. Literature research was also part of this study in order to provide the background understanding of epithermal deposits which in turn provides the basis for comparisons between Copiapo and other mineralized areas. In addition, 17 chemical data of fresh rocks from Zentilli were included.

Since this thesis is a preliminary investigation there are some limitations on every subject to be presented. For example, the petrology and geochemistry of the studied rocks are descriptive; the general characteristics of those rocks are explained through petrography and geochemical data. Petrogenesis is beyond the scope of this thesis as it will be the basis of a study by others. The discussion on chemical changes as a result of hydrothermal processes is limited to the calculations of gains and loosses of major and selected trace elements. Discussion on gold mineralization is limited to its distribution in comparison with other trace elements and in relation to alteration.

B. Sampling and analytical methods

Thirty new samples which represent fresh and altered volcanic rocks, shallow intrusives, veins and silicified caps were analysed. These samples were collected by M. Zentilli and J. Walker in the austral summer of 1984. Figure I.4 is a sample location map.

All samples were crushed and ground to about minus 120 mesh. Random orientation method was used for mounting clay powder for X-ray diffraction. A Phillips X-Ray Diffractometer was used to identify the clays with nickel-filtered, copper alpha radiation at 40 Kv and 20 mA. Major elements were analyzed at Dalhousie Geochemistry Laboratory by the Atomic Absorption Spectrophotometry method, using a Perkin-Elmer 530 AAS. Trace elements were analysed by the X-ray Fluorescence method at St Mary's University. Gold analyses were carried out by Bondar Clegg Company Ltd., of Ottawa, Ontario, Canada. Geochronological samples of biotite and hornblende were irradiated by the McMaster University nuclear reactor, while the $^{40}Ar/^{39}Ar$ dating was carried out at Dalhousie University Geochronology Laboratory. Dating one sample of alunite was done by Krueger Enterprise Inc., of Cambridge, Mass., USA. The analytical data are dependable as the results from rock standards are accurate and from duplicates are consistent (see Appendix I).

All sample preparation, major element analyses, X-ray diffraction analyses and mineral separation were carried out

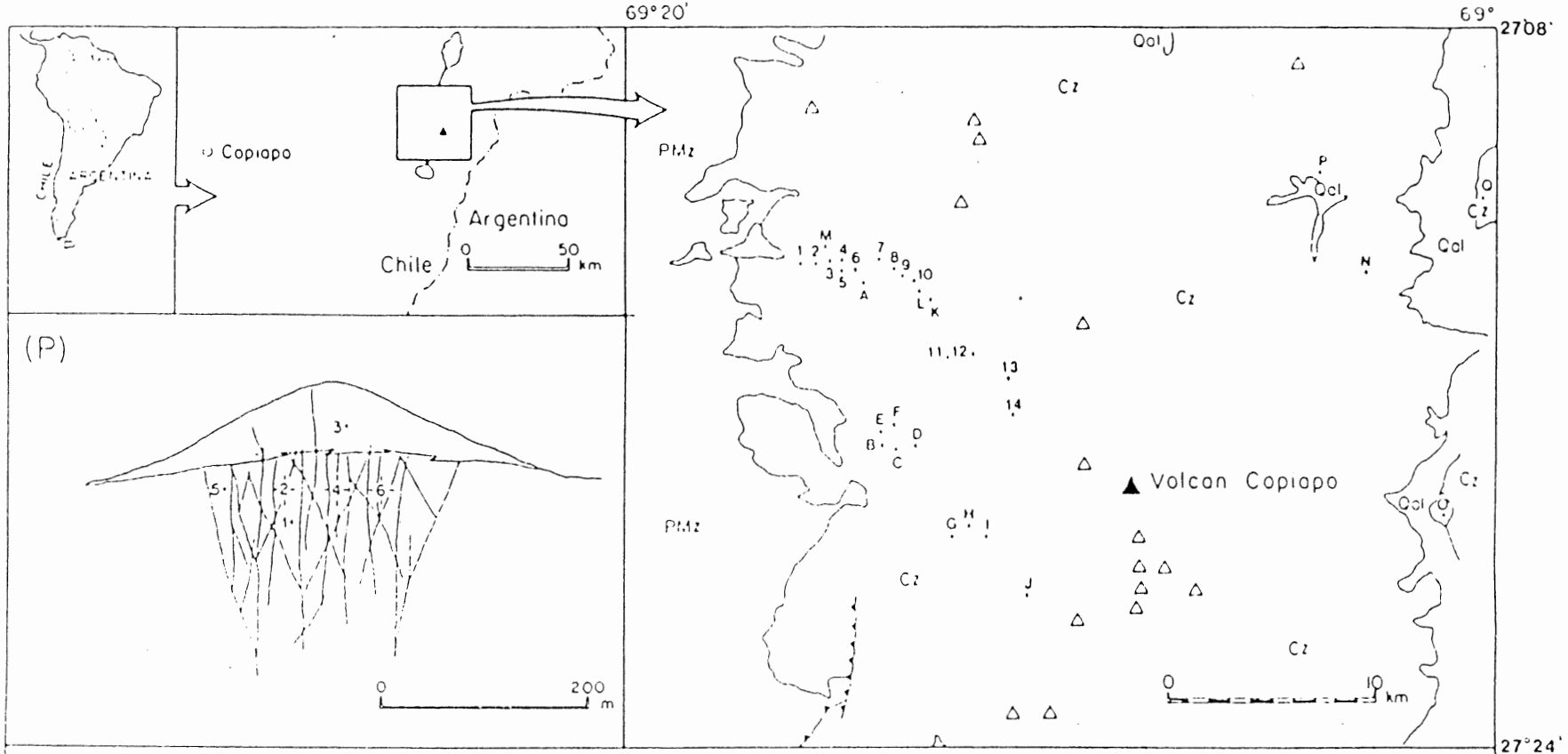

KEY:

Qal	Quaternary sediments
Cz	Cenozoic volcanics
PMz	Paleozoic-Mesozoic rocks
△	Volcano and volcanic center
+	Sample location & number

No.	Field Number
1	Z-50-78
2	Z-51-78
3	Z-52-78
4	Z-53-78
5	Z-55-78
6	Z-56-78
7	Z-58-78
8	Z-59-78
9	Z-60-78
10	Z-61-78
11	Z-62-78
12	Z-63-78
13	Z-64-78
14	Z-65-78
	Z-67-78
	Z-68-78
	Z-69-78
	Z-70-78

No.	Field Number
A	WZ-16-84
B	WZ-18-84
C	WZ-19-84
D	WZ-20-84
E	WZ-21-84
F	WZ-22-84
G	WZ-23-84
H	WZ-24-84
I	WZ-25-84
J	WZ-26-84
K	WZ-29-84

No.	Field Number
K	WZ-30-84
	WZ-31-84
	WZ-31a-84
	WZ-32-84
	WZ-33-84
	WZ-34-84
L	WZ-35-84
	WZ-36-84
M	WZ-39-84
	WZ-40-84
	WZ-41-84

No.	Field Number
N	WZ-107-84
O	WZ-114-84
P	1 WZ-117-84
	2 118
	3 119
	4 120
	5 121
	6 122
Q	WZ-128-84

OCM

by the writer. Appendix I outlines the detailed analytical procedures.

C. Organization of this thesis

Following this introductory chapter, Chapter II reviews the concepts of caldera resurgence and its association with epithermal ore deposits. Chapter III describes the geological setting of Copiapo both in regional (26°-29° S) and local scale. The latter includes the petrology and chemistry of the studied rocks. Chapter IV discusses alteration in terms of physical, mineralogical and chemical changes as a result of hydrothermal activity. Relations between mineralogical and chemical changes are part of this chapter. Chapter V presents the characteristics of gold distribution in the study area. Chapter VI outlines the chronology of volcanic activity of Copiapo and the timing of mineralization in a local scale context. This leads to the final chapter (VII) which presents the general discussion, conclusions, and recommendations for future work.

Chapter II

Caldera Resurgence and Mineralization :
a review of volcanogenic epithermal ore deposits

2.1 Introduction

Although the association of volcanism and epithermal ore deposits was recognized by Lingren as early as 1933, not until a decade ago or so have geologists started to investigate and relate volcanic landforms and ore deposits. Sillitoe and Bonham (1984) describe the ore deposits which are genetically, spatially and temporally related to magmatic systems characterized in the surface by distinct volcanic landforms. One of these landforms which is commonly related to gold mineralization is a caldera, especially one that has undergone resurgence. Figure II.1 illustrates a generalized model of ore deposits associated with a caldera from Sillitoe and Bonham (1984)

2.2 Caldera resurgence

Studies of caldera resurgence range from field investigations (Smith and Bailey, 1968) to a mathematical model approach (Marsh, 1984). Common distinct stages marking the evolution a resurgent caldera can be recognized (Figure II.2). Marsh suggested that the most likely mechanism of caldera resurgence is the coupled effect of regional detumescence and magmatic vesiculation. The former compresses the magma chamber, squeezing magma upward against and through the caldera block. The latter also compresses the chamber but tends to dome the caldera block. The subsidence of the roof along ring fractures, the walls of the caldera block, can be either a cause or an effect of the eruption.

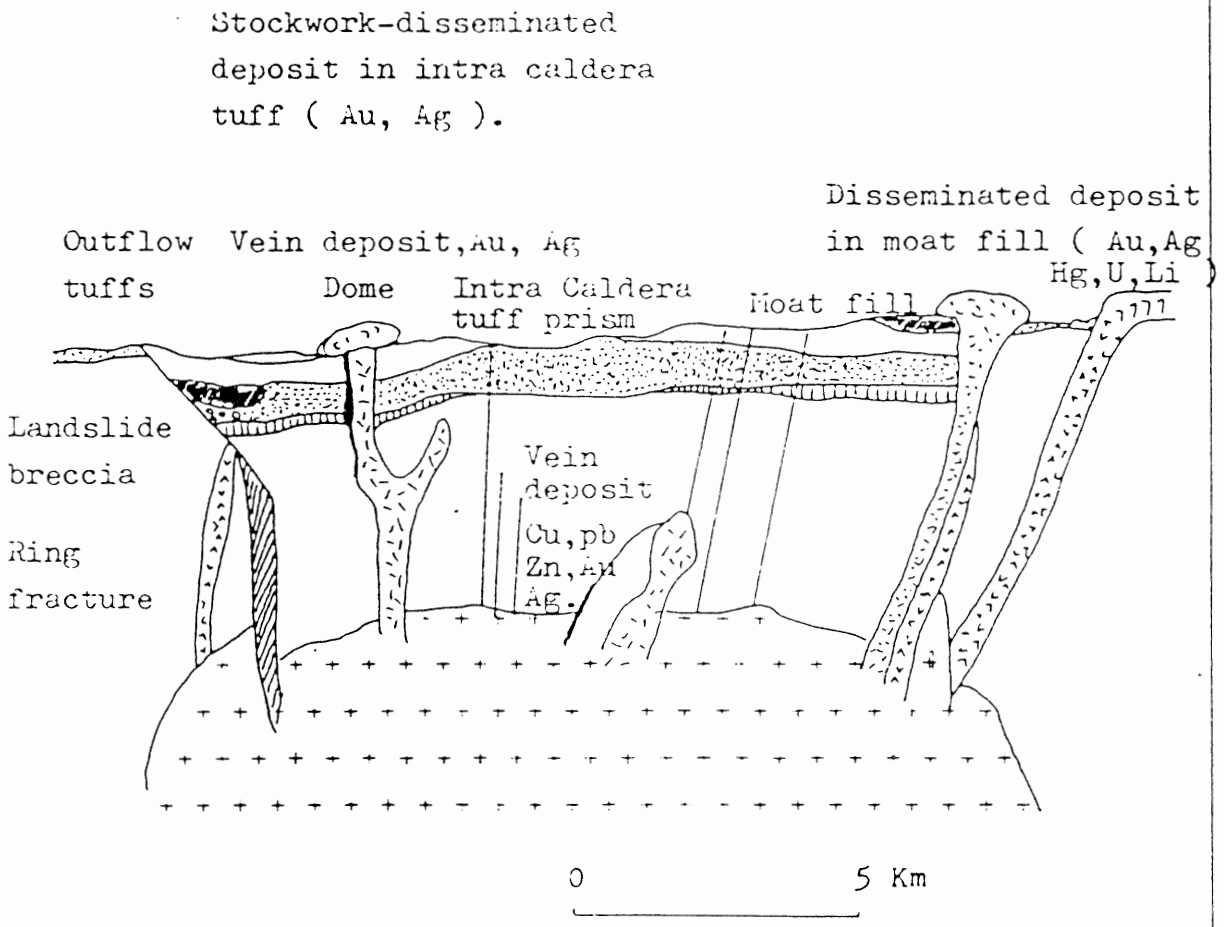

Figure II.1 Typical model of ore deposits associated with a caldera (Sillitoe and Bonham Jr, 1984).

Drawn by T.M.

Events in Figure II.2

Distinct stages mark the evolution of a resurgence caldera.

1. In the first stage, magma at depths (~ 5 Km) below the surface forms a pluton, or magma chamber, which slightly domes the surface.

2. In the pluton there are zones that differ in composition, with viscous magma rich in silica and dissolved gas at the top. Eventually an eruption of tuff and pumice begins. Plinian columns develop above a great ring-shaped fracture.

3. Collapse of the roof of the pluton along the fractures, leaving a caldera, and the plinian columns give way to pyroclastic flows.

4. Minor volcanism and sedimentation fill the caldera with ignimbrite and also blanket the surrounding area. Later, caldera walls begin to erode and a lake may also form.

5. Still later, over a period of a few thousand years, the intrusion of fresh magma into the pluton causes parts of the caldera floor to move upward again. Minor volcanic activity persists along the ring fractures.

6. The heat of the pluton may power convection currents of water rich in minerals and so give rise to hot springs and geysers at the surface for millions of years. This is the hydrothermal stage.

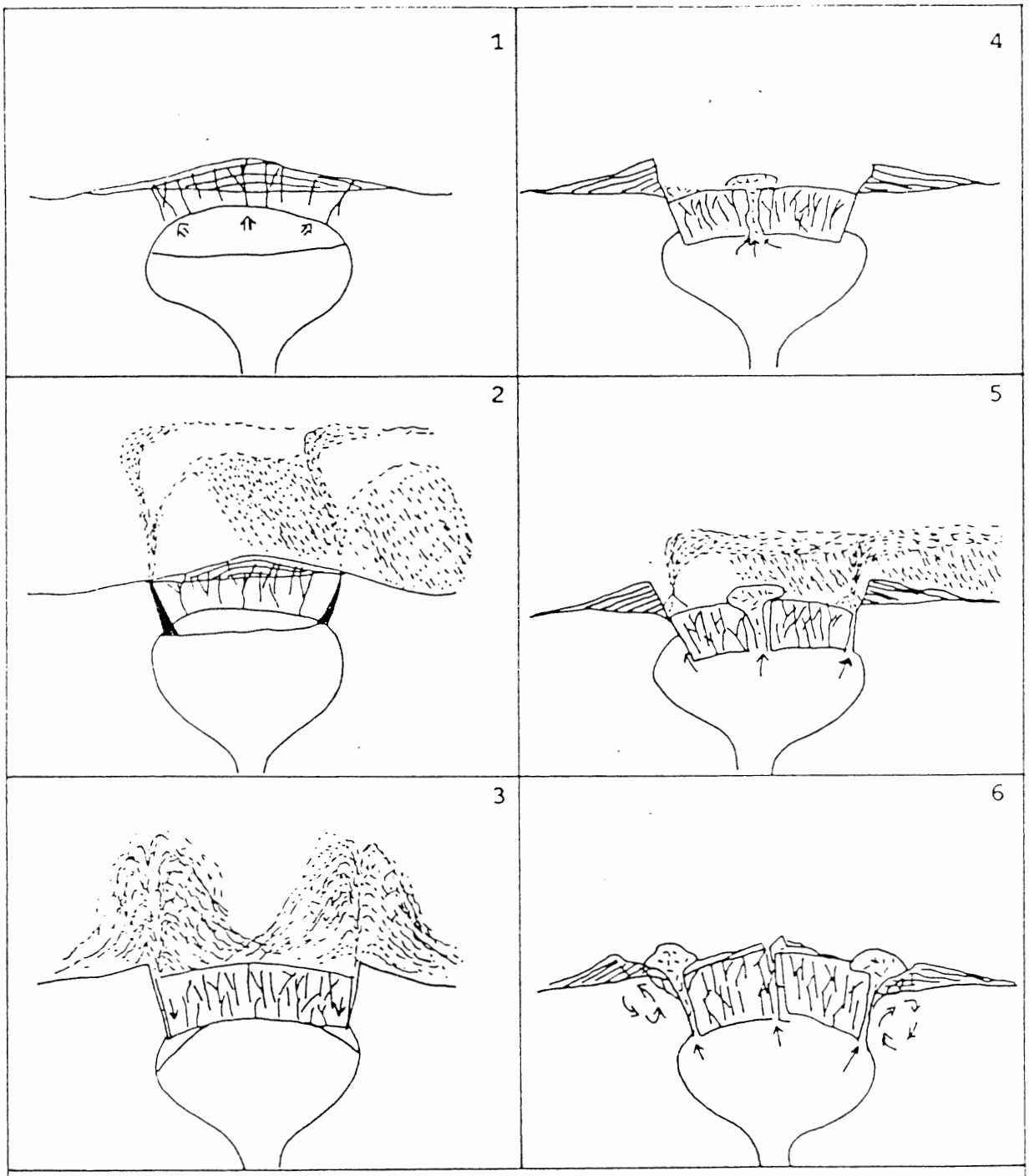

Figure II.2 Evolution of a resurgent caldera (from Francis, (1983 and Smith and Bailey, 1968).

Typical rocks ejected by an erupting caldera are lavas and pyroclastic rocks or flows. The latter when solidified and permanently deposited are termed ignimbrites, whether or not the clasts are welded (Francis, 1983). Compositionally, the lavas and pyroclastics range from andesitic (rarely basaltic) to rhyolitic. Petrologically they generally belong to the calc-alkaline group (Thorpe, 1984). Tectonic setting, nature of the upper mantle, thickness of the lower continental crust which underlies the calderas and processes during magma ascent contribute to the variations of the erupted rocks.

The extent of the erupted pyroclastic rocks can be as far as tens of kilometers from the source, a phenomenon which is rare in an ordinary volcanic eruption. An area extensively covered by ignimbrites is often cited as a guide to discover a caldera (Francis, 1983). If the resurgent processes continue for a long period, then a composite/strato volcano will form at the summit of the caldera.

2.3 Mineralization

Mineralization in a resurgent caldera normally takes place at later stages in the sequential events (Figure II.2F) where meteoric waters percolate through the ground and are heated by the cooling magma at depth. These waters, when ascending, become hydrothermal solutions(Figure II.2F) which may carry metals in diluted form. Hydrothermal activity and mineralization are likely controlled by extensional faults and fractures which developed during subsidence of caldera. The

ore bearing solutions precipitate metals in the fractures, forming mineralized veins and may simultaneously alter the surrounding rocks. Buchanan (1981) suggets the late stage intrusions are heat sources to drive cells of convecting waters.

The resulting mineral deposits in volcanic terrains are frequently referred to as epithermal deposits. Originally, only deposits formed at depths of about 500 m and at temperatures of between 50 and 100 C are qualified as " epithermal " by Lingren (Evans, 1980). However, the word " epithermal " is so widely used and is now generally understood to refer more to a genetic class rather than to a temperature class of deposits (Buchanan, 1981). The present writer is inclined to call these deposits " volcanogenic epithermal deposits " in order to distinguish them from other non-volcano type of epithermal deposits. Buchanan (1981) compiles data on epithermal deposits hosted by volcanic rocks from various known districts and presents a generalized model of the deposits (Figure II.3). Together with the data from Sillitoe (1976), the writer summarizes the characteristics of the deposits in Table II.1. It should be borne in mind that generalization should be taken as a guide only and that each deposit has its own characteristics.

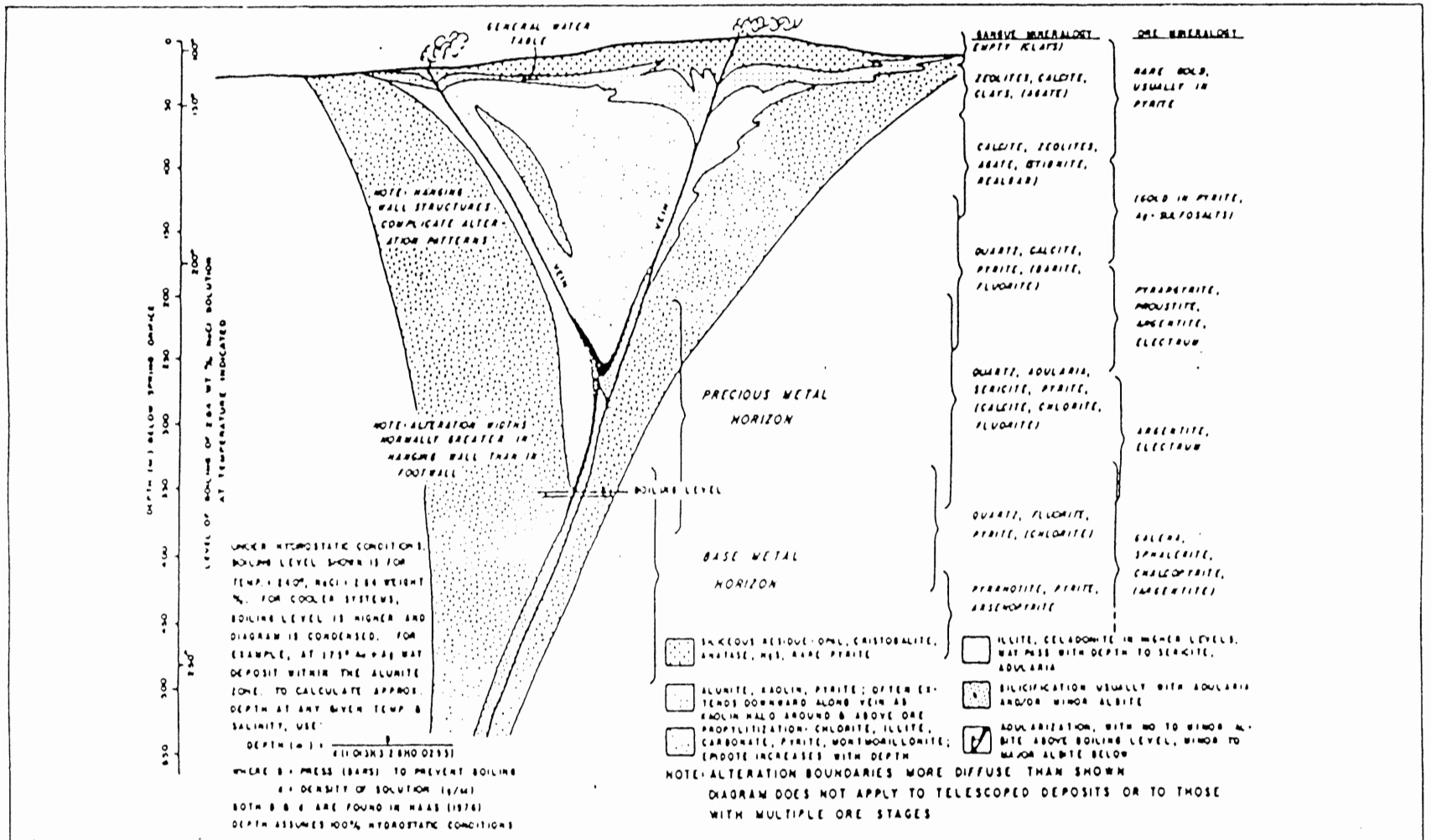

Figure II.3 Generalized model of an epithermal deposit and its alteration patterns (From Buchanan, 1981).

Tectonic setting and host rocks	: Subduction related; Inter-arc trough, volcanic arc underlain by continental crust. Andesitic to rhyolitic lavas and pyro-clastic flows.
Age	: Tertiary, predominantly Oligocene and younger
Type of deposit and ore age	: Vein type; 25 - 0 million years.
Mineralogy of vein*	: Qt, Se, Ka, Rb, Au, Py, Fa, Te, Ba, Ga, Al, Ti, Ad, Ca, Ar, El, Sp, Cp, Gu, Si, Ch, Pl, Rc, Pa, As.
Alteration assemblages	: Propylitic, argillic, phyllic, alunitic and silicic. Not all of them are always present in a deposit. The round mountain deposit in Nevada is the only one known that all of them developed. Propylitic alter-ation effects volcanics in the vicinity of veins, with more restricted alteration haloes of

sericitization and silicification, commonly with adularia, bounding the veins. Propylitization is, however, a commonly regional phenomenon not directly related to vein formation. Alternatively, zones or haloes consist of advanced argillic and argillic alteration, with clays, alunite, pyrophyllite etc, are accompanied by widespread silicification.

Table II.1 Summary of characteristics of volcanogenic epithermal deposits (from Sillitoe, 1976 and Buchanan, 1981).

•Abbreviations are:

Ad	Adularia	Cp	Chalcopyrite	Qt	Quartz
Al	Alunite	El	Electrum	Rc	Rhodochrosite
Ar	Argentite	Fa	Famantite	Rb	"Ruby Silvers"
As	Arsenopyrite	Ga	Galena	Se	Sericite
Au	Gold	Ka	Kaolin, Kaolinite	Si	Siderite
Ba	Barite	Pa	Pyrargyrite	Sp	Sphalerite
Ca	Calcite	Pl	Polybasite	Te	Tetrahedrite
Ch	Chlorite	Py	Pyrite	Ti	"Tellurides"

Chapter III

Geology and Petrology

3.1 Introduction

The Central Andean Cordillera, where Volcan Copiapo is located, is interpreted as the result of collision between the oceanic Nazca plate underneath the South American continental plate. The consequences of having such tectonic setting are characterized by seismicity, tectonism and magmatism in the overlying continental plate margin (Thorpe, 1984).

Seismic studies (Figure III.1)along the length of the Andes indicate an unexplained seismic discontinuity in the central Andes at about latitute 27° South (Barazangi and Isacks, 1976). From 27° to about 33° latitute South, there is a lack of active volcanism, and it has been interpreted by the same authors as a segment of shallow angle subduction of the Nasca plate (Figure III.2).

The regional geology of the Central Andes at latitudes 26-29 South (Figure III.3) has been described by Zentilli (1974). A more general approach was presented by Thorpe (1984). Unless otherwise stated, the following section draws freely from Zentilli (1974).

The oldest rocks in the region are the basement plutons which are overlain by the Paleozoic (Devono-Permian) continental sediments and volcanics. Subsequent geology is dominated by intrusive and extrusive rocks which have been emplaced by tectonic and magmatic events beginning during the earliest Jurassic until the present. The intrusive rocks are

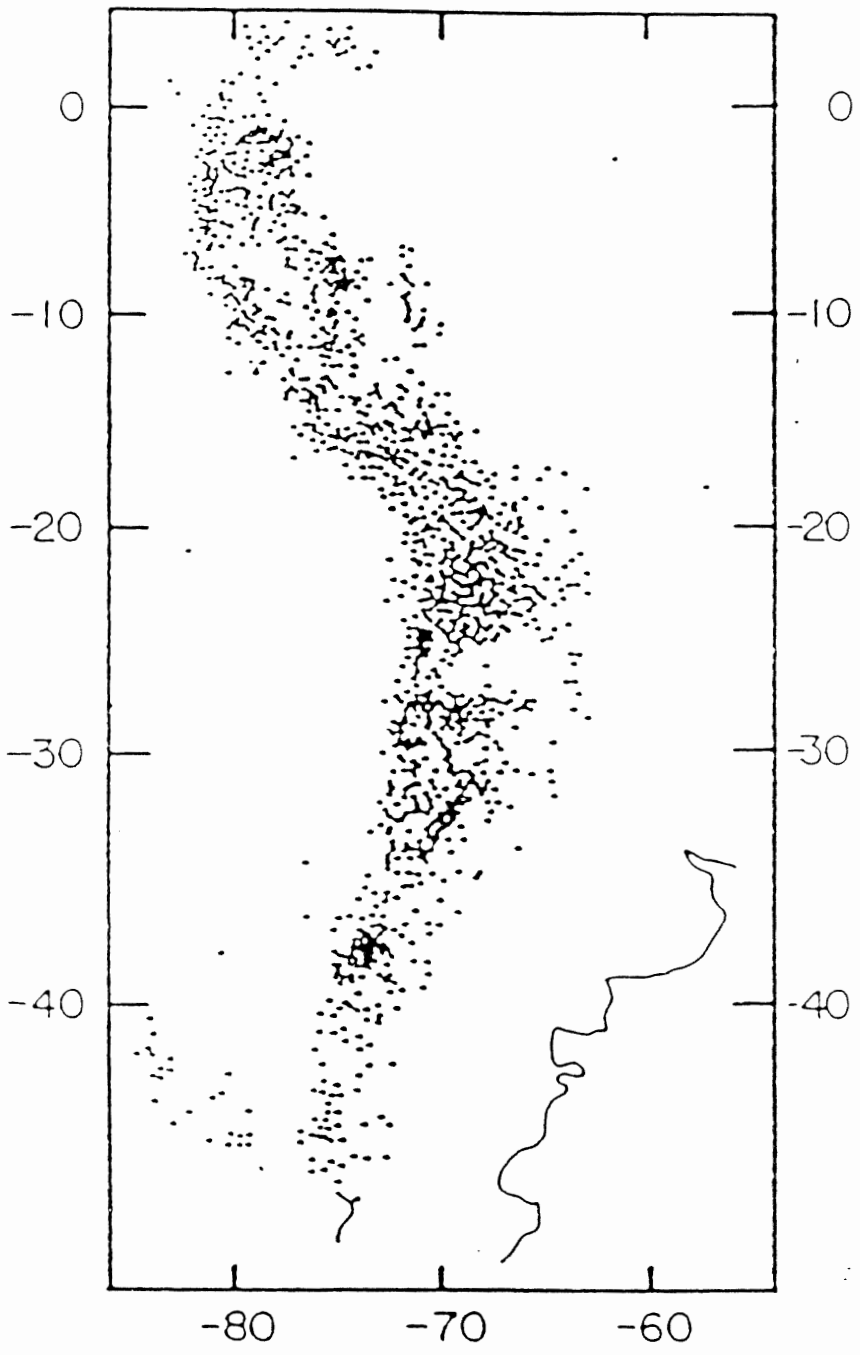

Figure III.1 Distribution of earthquake epicenters with foci up to 700 Km (Barazangi and Isacks, 1969), showing the paucity of seismic activity near 27 S.

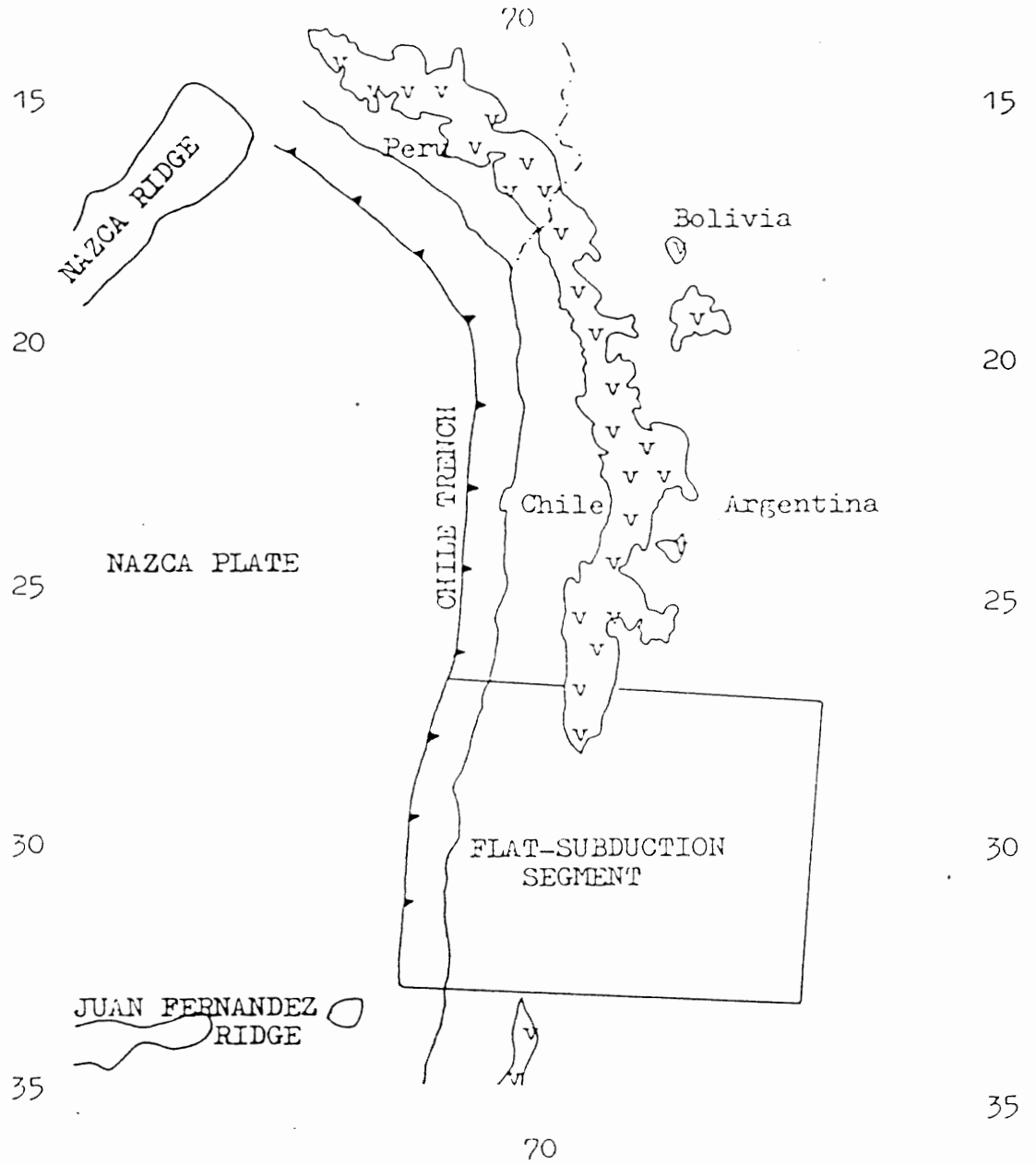

Figure III.2 Distribution of late Cenozoic volcanism in the Central Andes and relationship to the flat-subduction segment (Walker and Zentilli, 1984).

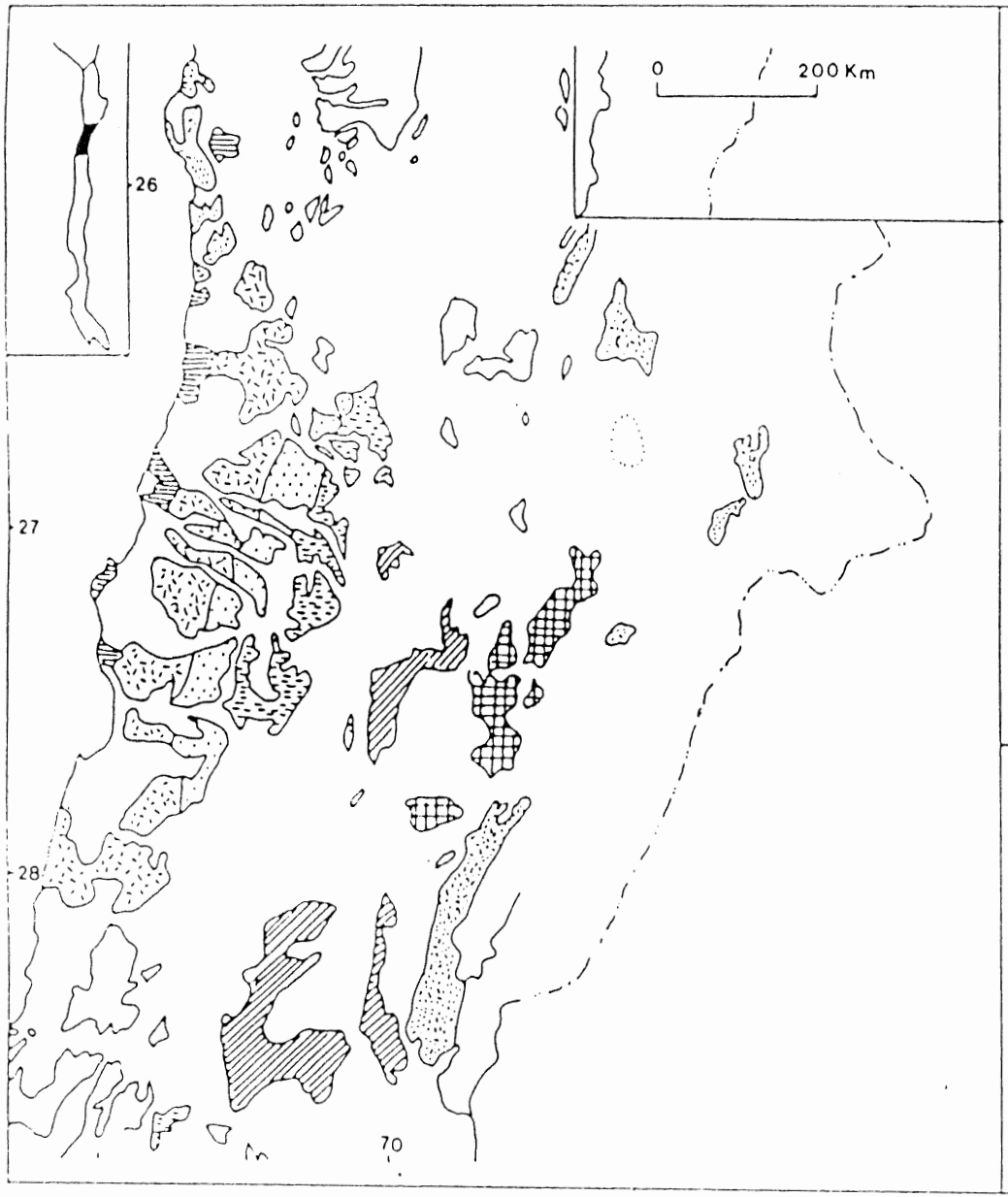

LEGEND

- Oligocene-Miocene
- Late Eocene, Early Oligocene
- Paleocene
- Mid to late Cretaceous
- Early Cretaceous
- Late Jurassic
- Early Jurassic
- Basement plutons

Figure III.3 Simplified geological map of igneous rocks of the Andes at Lat. 26° - 29° south (After McNutt et al, 1979).

generally dioritic to granodioritic and the extrusives are andesitic to rhyolitic.

Geochronological investigations and field relationships suggest that the main magmatic arc migrated with unusual regularity towards the east at a rate of increasing from ca. 0.6 millimetres per year in the early Mesozoic to ca. 1 millimetre per year in the mid-Tertiary. Figure III.4 shows a compilation of the results of K/Ar dating on both intrusive and extrusive rocks in the area under study.

The migration of magmatic arc and volcanic activity towards the interior of the Central Andes has been paralleled by the chemical composition of the volcanic rocks. For example, Dostal et al (1977) show the increase of potassium contents in those rocks with the distance from the trench to the interior (Figure III.5). Citing the data showing higher contents of K, Rb, Sr, Ba, Zr and REE and also higher K/Na and La/Yb ratios in the volcanics rocks of the interior, Dostal et al (1977) suggest that the chemical variations across the volcanic belt reflect systematic changes in the composition of the magmas because of decreasing degree of partial melting with increasing depth, but cannot discount the possibility of them being influenced by the heterogeneity of the source materials.

3.2 Geology of Copiapo volcanic complex

This section describes the geology of Copiapo and its

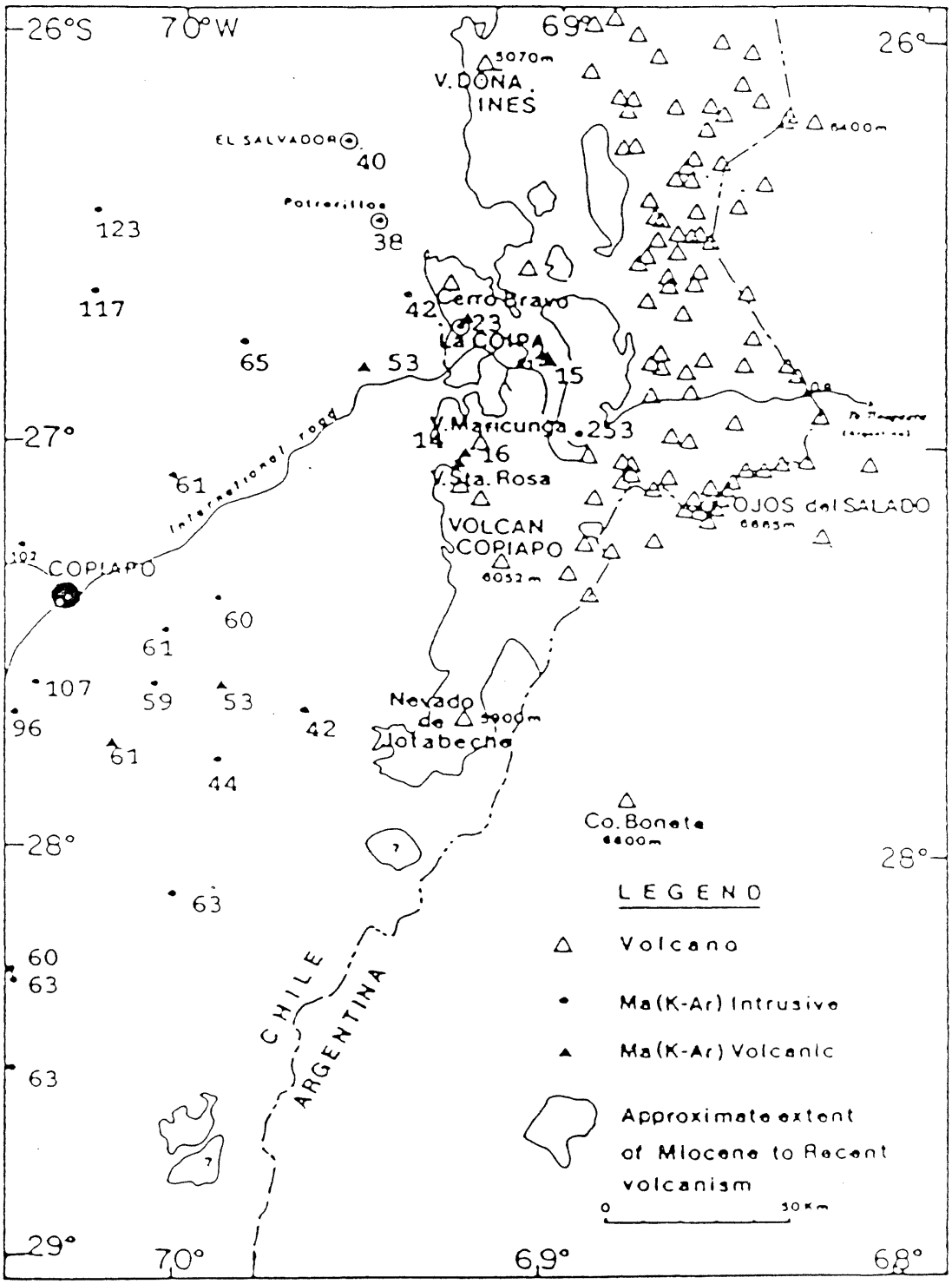

Figure III.4 Geochronology map of the Andes, 26-29° S (From Walker and Zentilli, 1984).

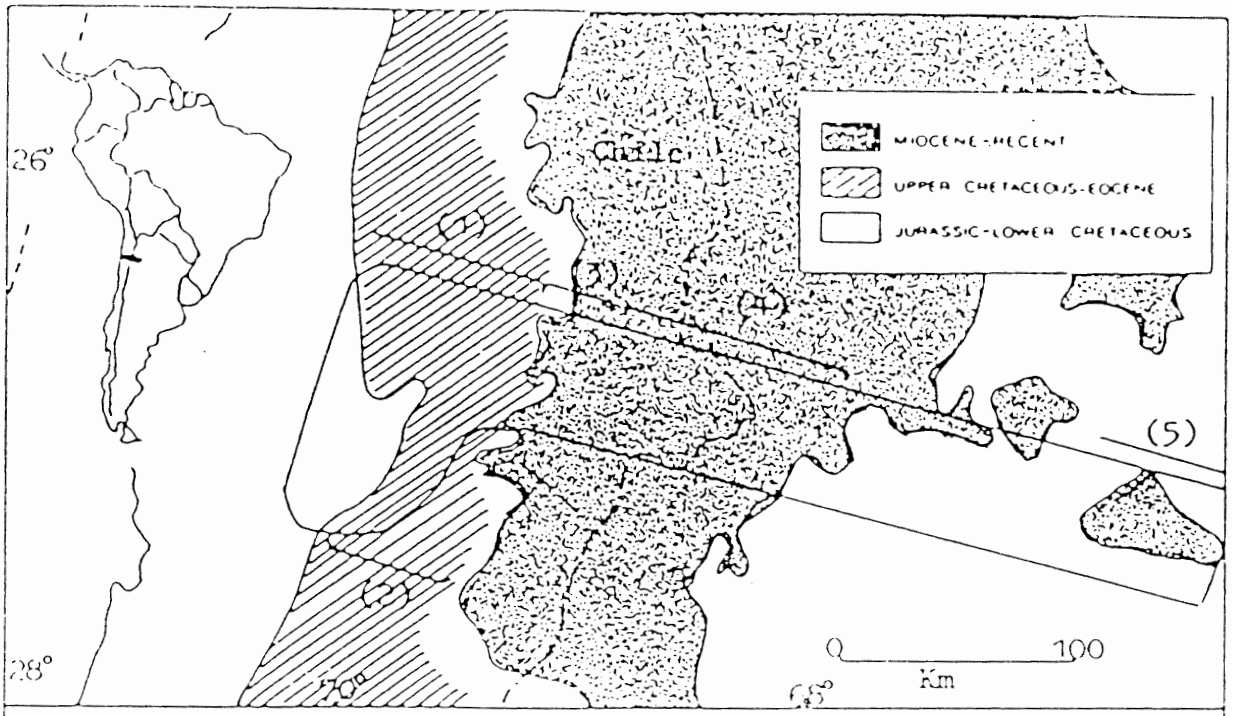

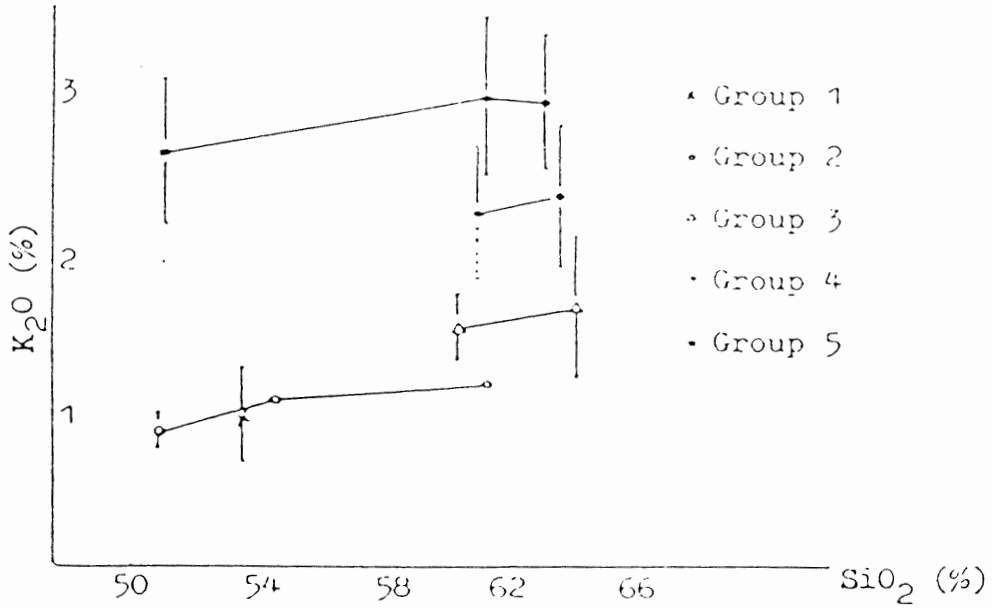

Figure III.5 Chemical variations along the Chilean-Argentinian Transect (After Dostal et al., 1977).

immediate environs within the latitutes 27° 08' - 27° 24' South and longitudes 69° 00' - 69° 20' West (Figure III.6). The study area is underlain by pre-Tertiary lithologies and other Tertiary lithologies. The source of information are the geological map by Mercado (1982) and personal communication with M. Zentilli. For the purpose of this discussion, the lithologies are divided into " pre-Tertiary " and " Tertiary ". Quaternary sediments are also present but there is no information available yet.

A. Pre-Tertiary basement rocks

The Paleozoic-Mesozoic rocks are the oldest and consist of volcanic and sedimentary rocks, bordering with the Tertiary volcanic flows at about 69° 20 west. The lower formation is the Chinches formation, consisting of arenites, pelites and limestones. The upper Pantanoso Formation, which comprises volcanics and conglomerates, marks the boundary between the Paleozoic and Mesozoic rocks.

All these formations were regionally folded and faulted with a NNE-SSW trend. This strike direction is parallel to the overall structural trend in the Central Chilean Andes. The highest regional metamorphic grade, attained by the Tertiary rock, is the lowest greenschist facies (Zentilli, 1974).

B. Tertiary lithologies

Tertiary rocks cover a wide area and are bounded in the

Legend

Q Quaternary continental and marine sediments

Qs Quaternary sediments

Cz Cenozoic volcanic and volcaniclastic rocks

Tm_3 Miocene continental sediments

Tpe Paleocene-Eocene sediments

Tpg Tertiary intrusives

KT Cretaceous sediments

Kg Cretaceous intrusives

Kij Cretaceous marine sediments

J_2 Jurassic volcanics

Jld Jurassic marine and volcanic sediments

TR_2 Triassic volcanic and marine sediments

CTR Carboniferous-Triassic hyperbyssal volcanics

Pzg Paleozoic intrusives

Pz Paleozoic basement complexes

Oa Andesitic composite Volcano

Thrust fault

Ob Andesitic-basaltic Volcano

Antiform

Figure III.6 Geological map of Copiapo volcanic complex (from M.T. Canas P., MAPA GEOLOGICO DE CHILE, Hoja No.2 de 6, 24 - 30 30 Lat. South., escala 1:1,000,000, 1980, 1982.


Qa
Tm3
Cz
Pz
Jld
Qa
Pz
Sta. Rosa
Cº Coplapo
Qa
Cz
CR
Pz
R2
Jld
Laguna del Negro Francisco
Pz
Qa
Pz
27°
t
b
Q
24'
0
10km
30'

west by pre-Tertiary rocks and in the north and south partly by Paleozoic-Mesozoic rocks and Quaternary sediments. The following summarizes the current knowledge of the area.

Walker et al. (1985) state that there are more than a dozen discernable vents in the Copiapo volcanic complex. Volcanism persisted for about 5 Ma. The oldest units (14-12 Ma) outcrop around the margins of the complex. Compared to other volcanoes, Copiapo was probably one of the most active and its flows cover an area of about 300 kilometers square, travelling as far as 21 kilometers from the volcanic center. Final volcanic activity (10-8.6 Ma) was focused near the composite cone Azufre. Azufre fills a pre-existing caldera formed in a moderate eruption during which pyroclastic flows were emplaced to the north-northeast, northwest and southeast. Although the main rock types are volcanic, where Neogene erosion has been deeper, a number of shallow intrusive outcrops were found and sampled by M. Zentilli and J. Walker in 1984. There are no published reports on the detailed geology of this large volcanic complex.

C. Structural geology

The geological map by Mercado (1982) does not show any structural features within Copiapo. However, a 1973 satellite image (Figure III.7) shows several structural lineaments. The most obvious one is the north-south trend, located at the eastern flank of the volcan Copiapo, which is most likely a fault or fracture zone. This lineament is undergoing active

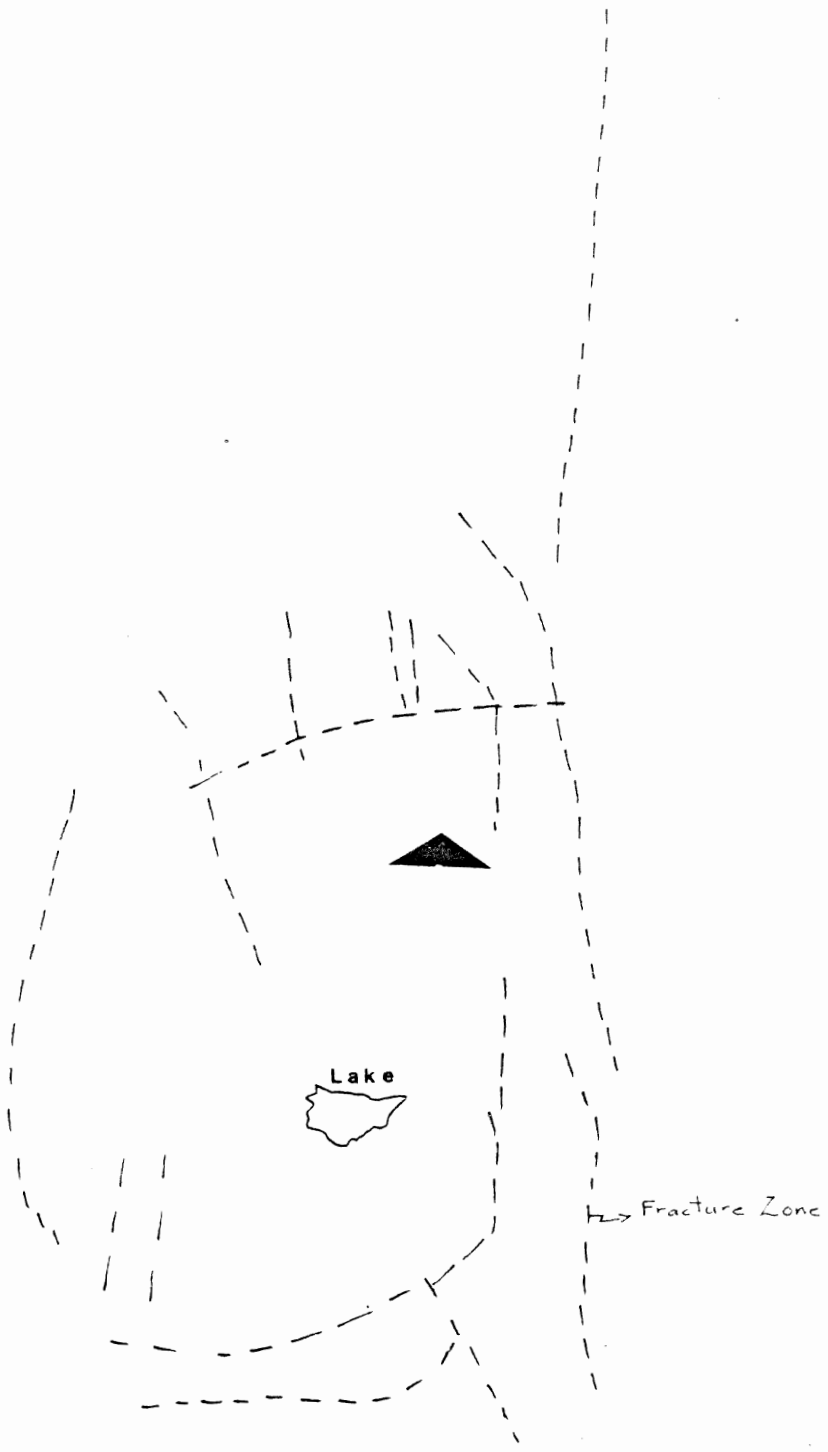
Lake
Fracture Zone
0
10km


FROM NASA ERTS Band 6 23 Mar 73
Volcan
COPIAPO
10 Km

exploration for gold (Zentilli, 1984a). Just along the northern flank of the volcano, a semi-circular east-west fracture is obvious as well. It might represent a ring fault which is normally associated with a caldera. A dome appears to have developed in the northeastern part of the volcano. Veining, hydrothermal alteration, and gold-silver mineralization has been reported in that area.

3.3 Petrology and geochemistry of Tertiary lithologies

In this section, the studied rocks are described in terms of texture, mineralogy, and chemistry. The last part deals with the fresh rocks only, because altered rock geochemistry is presented in the following chapter. The determination of fresh samples was based on hand specimen, petrographic observation and chemical analyses. Any rock containing secondary minerals is considered altered. Rock chemical analyses with more than 3.5 weight percent H_2O+ were excluded.

The separation of the various rock types was based on petrographic studies. The order of description is pyroclastic rocks, lavas, intrusive rocks and vein rocks.

Appendix II describes each of the new samples used in this thesis.

A. Pyroclastic rocks

These rocks constitutes the majority of the samples used in this thesis. For the purpose of the discussion in this

Plate 1. A typical andesitic ignimbrite in which porphyritic plagioclase, biotite and hornblende are set in a matrix of glass (crossed polarizer).

0 1mm

section, the rocks are conveniently divided into unsorted and sorted pyroclastics. The former are composed of angular to rounded clasts or fragments of pumice and other volcanic rocks set in a matrix of very fine crystals and glass. The size of the clasts ranges from few millimetres to five centimeters in diameter, and are generally lighter colored than the groundmass. The color of the groundmass is generally brown, except sample number WZ-30-84 which is pinkish brown. The rocks are generally welded, although vesicles may occupy up to 15 percent of the rock. Alteration and oxidation are moderate and are characterized by the production of fine clay and an iron staining surface, respectively. Alteration caused the development of a banded oxidation pattern in which part of the rock was oxidized more than the other. For example, sample number WZ-36-84 shows a very distinctive boundary between the least and most oxidized part of the rock.

Mineralogically, broken feldspar crystals are the only constituents readily recognized. They are all anhedral to subhedral without any well preserved twinning pattern for the An-content determination. These minerals are lath-shaped and average less than one and half millimetres long and are randomly distributed. Minor and fine grained minerals such as quartz, feldspar and opaque oxides are present. The majority of the rocks show a partially devitrified glassy groundmass.

Sorted pyroclastic rocks are typically poorly welded and fine to medium grained. Mafic minerals such as hornblende and

biotite are visible in hand specimen. Most rocks are andesites in terms of rock chemistry and petrography. Plagioclase phenocrysts are the major crystalline minerals in all rocks and exhibit anhedral and euhedral shape. These grains constitute more than 50 percent of the crystalline minerals. The size of these minerals ranges from less than 0.1 millimetre to 2.0 millimetres long, with an average of 1.25 millimetres long. Some phenocrysts show twinning but were not well developed therefore the An-content cound not be determined. K-feldspars, especially sanidine, are abundant in Z-68-78.

Hornblende is an important mafic mineral besides biotite. The grains are generally subhedral to euhedral, exhibiting a greenish-brown to reddish brown pleochroism. The average size is 1.25 millimetres long. Biotite and pyroxene are also present and occur as individual grains less than one millimetre long. Pyroxenes are important mafic minerals and constitute about 10 percent of the whole mineralogy in samples Z-50, 51, 52, 55-78, WZ-40 and 41-84. But they are rare or absent in the rest of the samples. Opaque minerals such as pyrite are present in hand specimen.

B. Lavas

This group has petrographic and chemical characteristics of andesite and dacite. The fresh andesitic lavas are characterized by a porphyritic texture in which 40 to 50 percent of the rock consists of zoned palgioclase crystals

which average 2 to 5 millimetres long. These phenocrysts are normally enclosed in a groundmass of small plagioclase laths and glass. Subhedral to euhedral hornblendes, of which some are rimmed and pseudomorphed by opaque oxides, occur both as phenocrysts and as individual grains up to 2 millimetres in diameter. Biotite and pyroxene are also present. The remainder of the rock is a fine to very fine-grained matrix of K-feldspar, plagioclase laths, opaque oxides and glass. A typical andesitic lava is sample number WZ-26-84. Dacite is distinguished from andesite by the presence of quartz. Its characteristics are similar to that of andesite.

Mineralogy of lavas

Plagioclse crystals in the andesitic lavas are subhedral to euhedral and average 1.5 to 2 millimetres long. They occur both as aggregate and individual grains. The boundaries of the individual grains are euhedral and irregular. Some show weak reaction rim along the edges. Plagioclase crystals are moderately and strongly zoned from andesine to labradorite (An 36-58). Albite and Carslbad twinnings occur in most well-developed plagioclase phenocrysts. Some also show sieve and mymerkitic textures.

Hornblende occurs as individual prisms up to 2 millimetres long and, in some rocks, as phenocrysts together with plagioclase. Hornblende grains are generally anhedral to euhedral. Some rocks such as WZ-26-84 contain pseudomorphs by opaque oxides after hornblende. Unaltered grains generally

Plate 2. A typical greyish porphyritic andesite which consists of phenocrysts of plagioclase and biotite.

Plate 3. An andesitic lava flow shows porphyritic plagioclase (pl), oxide-rimmed amphiboles (ox) in a matrix of glass and tiny plagioclase laths which show a flowage direction (plane polarizer).

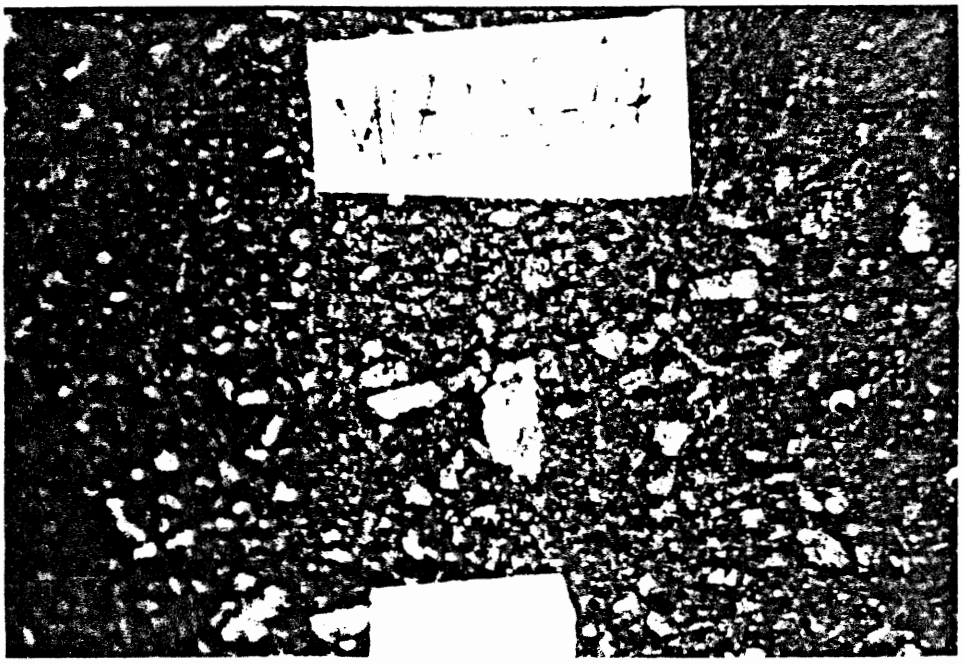

Plate 2 0 2 cm

Plate 3 0 1mm

show a greenish brown to reddish brown or red brown pleochroism.

Biotite is an important mafic mineral. It constitutes about m. percent of the mineralogy. Biotite grains average about 1 millimetre in their longest dimension. The largest single grain measures 3 x 10 millimetres in sample number WZ-107-84. Pleochroism is uniform within grain, light yellow-brown to reddish brown.

Pyroxene is rather rare and constitutes less than 5 percent of the whole rock mineralogy. Both clino- and ortho-pyroxenes occur as fine individual grains up to 1 millimetre and aggregates up to about 3 millimetres in size. Grains are anhedral or euhedral. Hypersthene is colorless or very pale green and has greensih to reddish pleochroism. Augite occurs as fine prismatic and colorless grains and has a weak pleochroism.

Quartz is confined only to dacite and occurs as single grains up to 3 millimetres in diameter and as aggregate in the groundmass. The latter is difficult to analyse with a student microscope. Individual grains, averaging 1.5 millimetres in diameter, show smooth crystal edges which suggest resorption and modification of the margin of the grain.

K-feldspar is rare and occurs as very fine grained crystals in the groundmass. Accessory minerals are opaque oxides. Some rocks contain up to about five percent by replacing mafic

minerals such as hornblede; others contain little or none. No attempt was made to analyse these opaques.

C. Intrusive rocks

Intrusive rocks, described as such in the field, are porphyritic and grey, consisting at least 50 percent zoned plagioclase phenocrysts which average 1 to 2 millimetres long. Other minerals are hornblende, biotite and opaques. The groundmass consists of very fine plagioclase and sericite.

Plagioclase phenocrysts which are subhedral to euhedral show compositional range from An 40-56. Some show partial melt along the crystal boundaries. Alteration includes sericitization and chroritization after plagioclase and biotite, respectively. Pseudomorphs after hornblende by opaque minerals are also present.

Alteration in one intrusive rock sample (WZ-22-84) has been so intense that little original minerals remain. Porphyritic relict texture can be seen by pseudomorphs after plagioclase, amphibole, and biotite which were altered to sericite, opaque minerals and chlorite, respectively. Chlorite was confirmed by X-ray diffraction. Sericite constitutes 30 percent of some rocks, followed by chlorite and others which consist of fine grained minerals forming the groundmass.

D. Veins and siliceous cap

Quartz-alunite veins are the most important lithology in terms of alteration and precious metal mineralization. Although the gold is not visible the grade is as high as 4.6 ppm (Table V.1).

These rocks were collected from a complex of veins which is overlain by aluminous-siliceous capping rocks (Figure I.3). The veins are characterized by microfractures ranging from few millimetres to centimetres which are filled by alunite and silica minerals. The alunite is white and soft while the silica is grey. In thin section, alunite is colorless and forms very fine aggregates which show a moderate birefringence. Alunite was confirmed by X-ray diffraction analyses (Appendix III). Accessory minerals are sericite, rutile, chlorite, carbonate and opaque oxides.

The capping rock is mainly composed of fine grained aggregates of transparent minerals and silica minerals replacing former grains. Chemical composition of this rock (See WZ-119-84 in Table IV.4) shows a high aluminum content, more than 40 weight percent. Those transparent materials are perhaps diaspore. Rutile and opaque minerals are present.

E. Summary

Petrographic characteristics of the Copiapo volcanic rocks, especially the lavas and pyroclastics, indicate a narrow range of mineralogical composition from andesite to dacite, but

Plate 4. A quartz-alunite vein system shows quartz (grey and black) veinlets and tiny fractures filled by yellowish minerals.

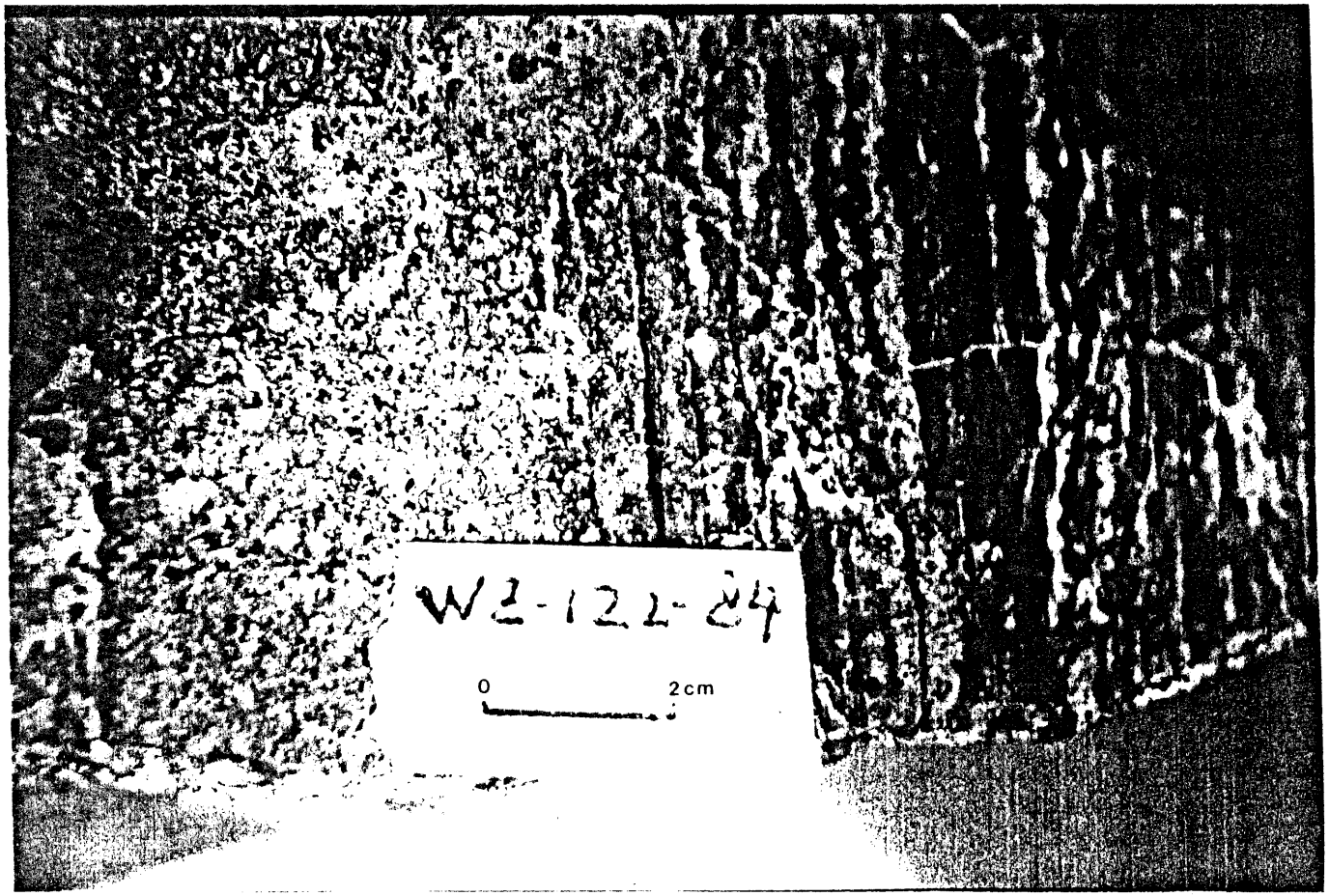
W2-122-24
0
2cm

there exists a clear predominance of hornblende-and biotite bearing andesites. Andesitic lavas and pyroclastics are characterized by phenocrysts of plagioclase, hornblende and biotite. These petrographic characteristics are typical of the calc-alkaline series (Kuno, 1968; Gill, 1981).

The presence of intrusive outcrop, which was not recognized before, is significant. It implies the emplacement of a body or bodies of subvolcanic (shallow) intrusion. This kind of intrusion has frequently been considered to be a heat source for hydrothermal solutions (Buchanan, 1981). Rock samples from this outcrop show alteration, suggesting the existence of past hydrothermal activity.

The field relation between vein and cap rock, in which the former is overlain by the latter (see Figure I.3), is implying a volcanogenic epithermal system (Worthington, 1981 and Buchanan, 1981).

F. Geochemistry

Table III.1 lists the results of chemical analyses of 24 fresh rock samples used in this thesis. All were analysed for major and trace elements. The latter are Rb, Ba, Sr, V, Cr, Ni, Zr and Cu. New samples, except sample numbers WZ-40, 41, 114 and 128-84 were further analysed for gold and its associated elements such as Ag, As and others, which are the main content of the chapter on gold mineralization.

Sample #	Z-50-78	Z-51-78	Z-52-78	Z-53-78	Z-55-78
SiO_2	59.43	59.14	58.91	60.92	56.61
TiO_2	0.68	0.80	0.80	0.71	0.55
Al_2O_3	17.95	17.50	17.67	17.66	19.75
FeO(total)	4.92	5.65	5.41	5.20	4.47
MnO	0.08	0.10	0.08	0.10	0.04
MgO	2.53	3.35	3.01	2.59	1.02
CaO	4.97	6.47	6.45	5.90	2.90
Na_2O	3.47	4.04	4.40	4.07	2.20
K_2O	2.08	1.85	1.82	2.08	2.71
P_2O_5	0.17	0.25	0.25	0.16	0.17
H_2O+	1.87	0.00	0.19	0.16	1.97
H_2O-	0.80	0.57	0.93	0.31	1.43
S	0.10	0.01	0.01	0.05	0.05
Total	99.05	99.63	99.53	99.91	93.89
Rb	69	72	69	68	89
Ba	624	581	577	696	565
Sr	559	685	681	714	571
V	113	158	130	120	89
Cr	15	60	52	16	13
Ni	9	26	20	7	6
Zr	151	150	159	153	102
Cu	19	29	24	26	32

Sample #	Z-56-78	Z-58-78	Z-59-78	Z-63-78	Z-64-78
SiO_2	60.54	61.60	60.54	60.66	63.69
TiO_2	0.70	0.71	0.75	0.50	0.59
Al_2O_3	18.02	17.72	18.44	19.84	16.90
FeO(total)	4.88	5.16	4.94	2.83	3.68
MnO	0.08	0.08	0.04	0.01	0.05
MgO	2.20	2.43	0.54	0.13	0.71
CaO	5.80	5.75	5.43	3.02	5.38
Na_2O	4.14	3.99	4.12	4.24	4.29
K_2O	2.05	2.03	2.11	2.15	2.92
P_2O_5	0.28	0.15	0.07	0.17	0.22
H_2O+	0.24	0.44	1.00	2.50	0.43
H_2O-	0.67	0.50	1.39	0.67	0.78
S	0.01	0.01	0.01	n/a	n/a
Total	99.61	100.33	99.38	96.72	99.72
Rb	64	63	68	76	94
Ba	753	672	766	747	838
Sr	714	701	659	789	680
V	102	113	102	63	88
Cr	10	13	11	15	14
Ni	10	10	8	6	10
Zr	151	149	149	141	144
Cu	49	23	36	33	33

Sample #	Z-65-78	Z-67-78	Z-68-78	Z-69-78	Z-70-78
SiO_2	61.24	64.98	64.82	62.12	62.02
TiO_2	0.98	0.51	0.51	1.00	0.96
Al_2O_3	17.32	17.89	16.91	17.11	17.22
FeO(total)	4.54	2.86	2.84	4.86	4.45
MnO	0.06	0.05	0.05	0.07	0.06
MgO	2.30	1.00	1.07	2.58	1.93
CaO	4.91	3.92	3.94	5.02	4.74
Na_2O	4.92	5.12	4.93	5.00	4.96
K_2O	2.11	2.84	2.82	2.07	2.15
P_2O_5	0.35	0.19	0.20	0.35	0.33
H_2O+	0.00	0.99	0.75	0.00	0.14
H_2O-	0.46	0.11	0.09	0.14	0.50
S	n/a	n/a	n/a	n/a	0.00
Total	99.19	100.46	98.93	100.32	99.46
Rb	55	97	92	50	57
Ba	740	799	805	745	774
Sr	866	748	746	880	870
V	97	49	50	78	128
Cr	26	8	22	33	27
Ni	14	3	12	15	13
Zr	199	161	148	191	198
Cu	23	28	31	36	33

Sample #	WZ-16-84	WZ-23-84	WZ-24-84	WZ-26-84	WZ-40-84
SiO_2	57.85	60.96	64.40	61.37	58.33
TiO_2	0.52	0.52	0.60	0.88	0.79
Al_2O_3	18.33	18.43	18.09	17.03	18.37
FeO(total)	3.05	4.31	4.45	4.09	5.38
MnO	0.05	0.06	0.07	0.07	0.07
MgO	1.45	2.04	1.74	2.28	3.06
CaO	4.90	5.06	4.71	5.14	5.97
Na_2O	6.89	5.60	4.61	4.89	3.71
K_2O	2.00	2.07	2.51	2.60	1.93
P_2O_5	0.25	0.27	0.20	0.27	0.33
H_2O+	3.31	0.00	0.00	0.48	
H_2O-	0.78	0.06	0.09	0.20	1.38
S	0.40	0.00	0.00	0.00	0.00
Total	99.67	99.38	101.47	99.57	99.38
Rb	65	83	81	81	57
Ba	680	736	770	690	575
Sr	888	749	765	608	680
V	48	74	90	108	118
Cr	56	14	9	39	45
Ni	1	5	9	10	18
Zr	152	169	179	195	169
Cu	19	13	33	25	33

Sample #	WZ-41-84	WZ-107-84	WZ-114-84	WZ-128-84
SiO_2	59.35	62.14	62.26	63.65
TiO_2	0.82	0.65	0.62	0.60
Al_2O_3	17.27	17.59	17.44	16.12
FeO(total)	4.95	5.73	4.53	3.35
MnO	0.10	0.08	0.08	0.05
MgO	2.93	2.00	1.69	1.36
CaO	6.48	4.92	4.97	5.22
Na_2O	4.01	3.89	3.45	3.62
K_2O	1.88	2.38	2.95	3.43
P_2O_5	0.28	0.25	0.27	0.24
H_2O+		0.23		
H_2O-	n/a	0.10	1.96	1.54
S		0.02	0.04	0.00
Total	98.05	99.98	100.16	99.18
Rb	57	87	117	148
Ba	587	626	616	712
Sr	696	581	562	488
V	130	108	71	54
Cr	39	13	14	11
Ni	22	13	11	12
Zr	157	155	133	207
Cu	53	20	32	19

Table III.1 Chemical analyses of 24 fresh rocks from Copiapo volcanic complex. Major elements are in weight percent and trace elements are in parts per million.

Major elements

The 24 fresh samples (Table III.1) in this thesis range from 56.61 to 64.98 % SiO_2, a narrow range interval composition.

Using the nomenclature of normal volcanic rocks (Figure III.8), which is the $Na_2O + K_2O$ vs SiO_2 diagram, the majority of the studied rocks fall into the field of andesite, with few to that of dacite. These andesites, according to criteria set by Bailey (1981), belong to orogenic andesitees on the basis of the following characteristics : high Al_2O_3 (generally > 15.5 %, often > 17.0 %) but low total Fe (FeO < 8%); low TiO_2 (0.50 - 1.30 %), Zr (35 - 250 ppm); low Zr/TiO_2 ratio (< 0.3) and mineralogy (phenocryst rich; dominantly labradorite, hornblende + biotite). Furthermore, in the nomenclature of orogenic andesites by Gill (1981) the majority of these rocks are medium-K andesites (Figure III.9).

The major element characteristics of the volcanic rocks comprising the Copiapo volcanic complex are typically calc-alkaline. This is demonstrated by the AFM diagram (Figure III.10), where the plotted data, except Z-58-78, fall in the calc-alkaline field. Plotting the major element data in the Harker variation diagrams (Figure III.11), there are several notable relationships. Besides samples Z-55 and 63-78 and WZ-16-84, FeO, MnO, MgO and CaO in all other rocks shows similar behavior; i.e., their concentrations fall with SiO_2

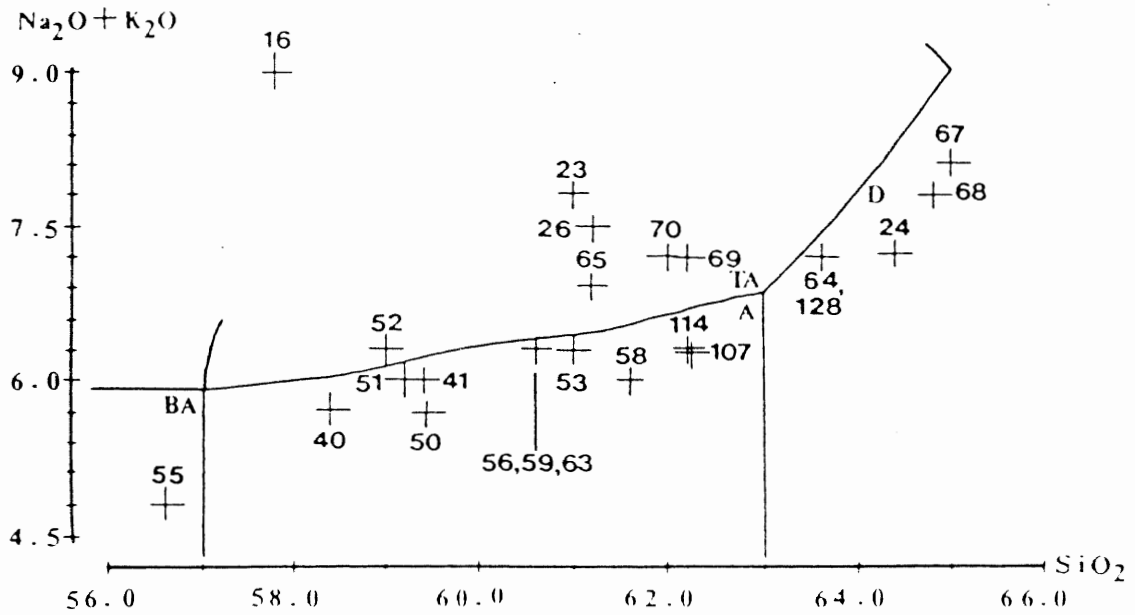

Figure III.8 Classification of Copiapo volcanic rocks based on the $Na_2O + K_2O$ vs. SiO_2 diagram. BA: basaltic andesite, A: andesite, TA: trachytic andesite, D: dacite. The diagram is after that of Cox, Bell and Pankhurst (1979).

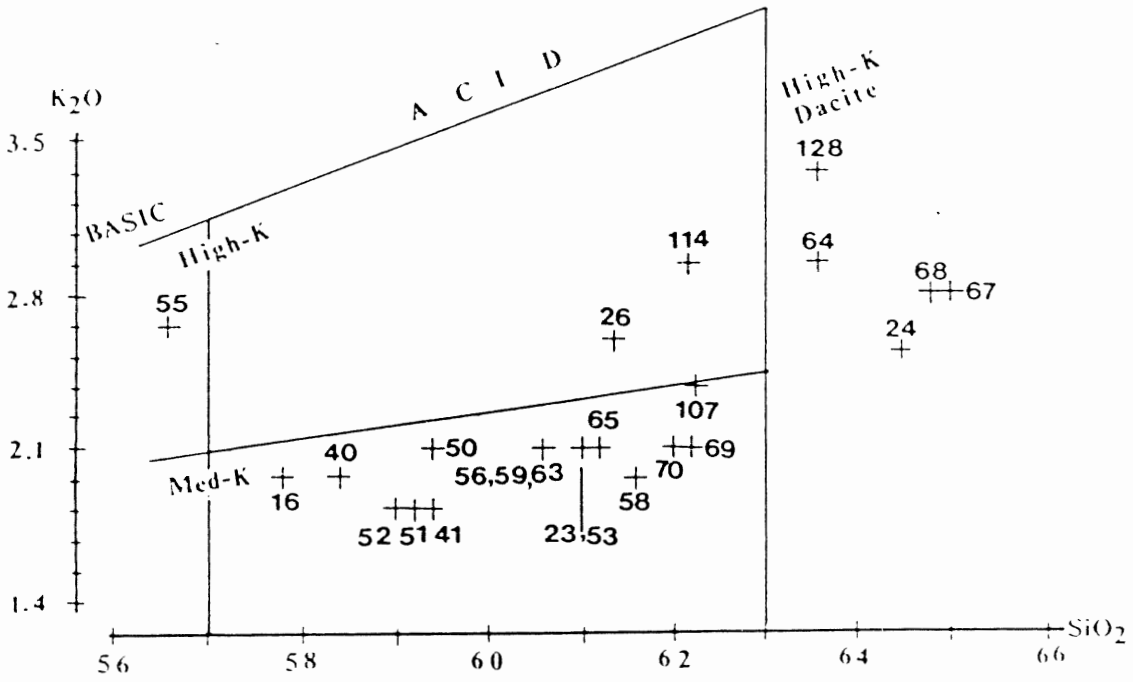

Figure III.9 Nomenclature of orogenic andesites based on K_2O and SiO_2 contents. The boundaries and nomenclatures are from Gill (1981).

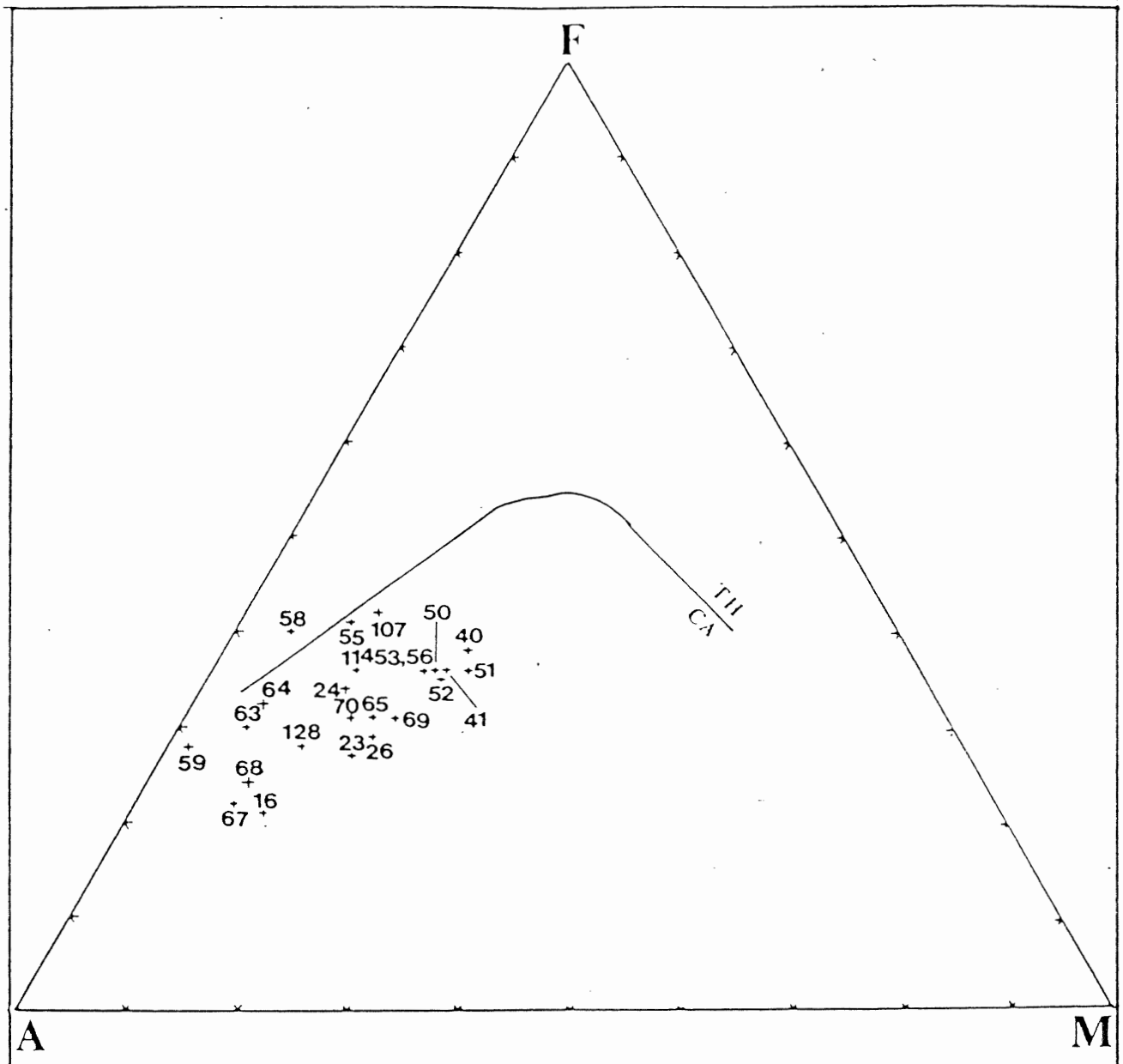

Figure III.10 The AFM diagram for Copiapo volcanic rocks. A: $Na_2O + K_2O$, F: FeO (total) and M: MgO. The boundary between CA (calc-alkaline) and TH (tholeiitic) is from Gill (1981).

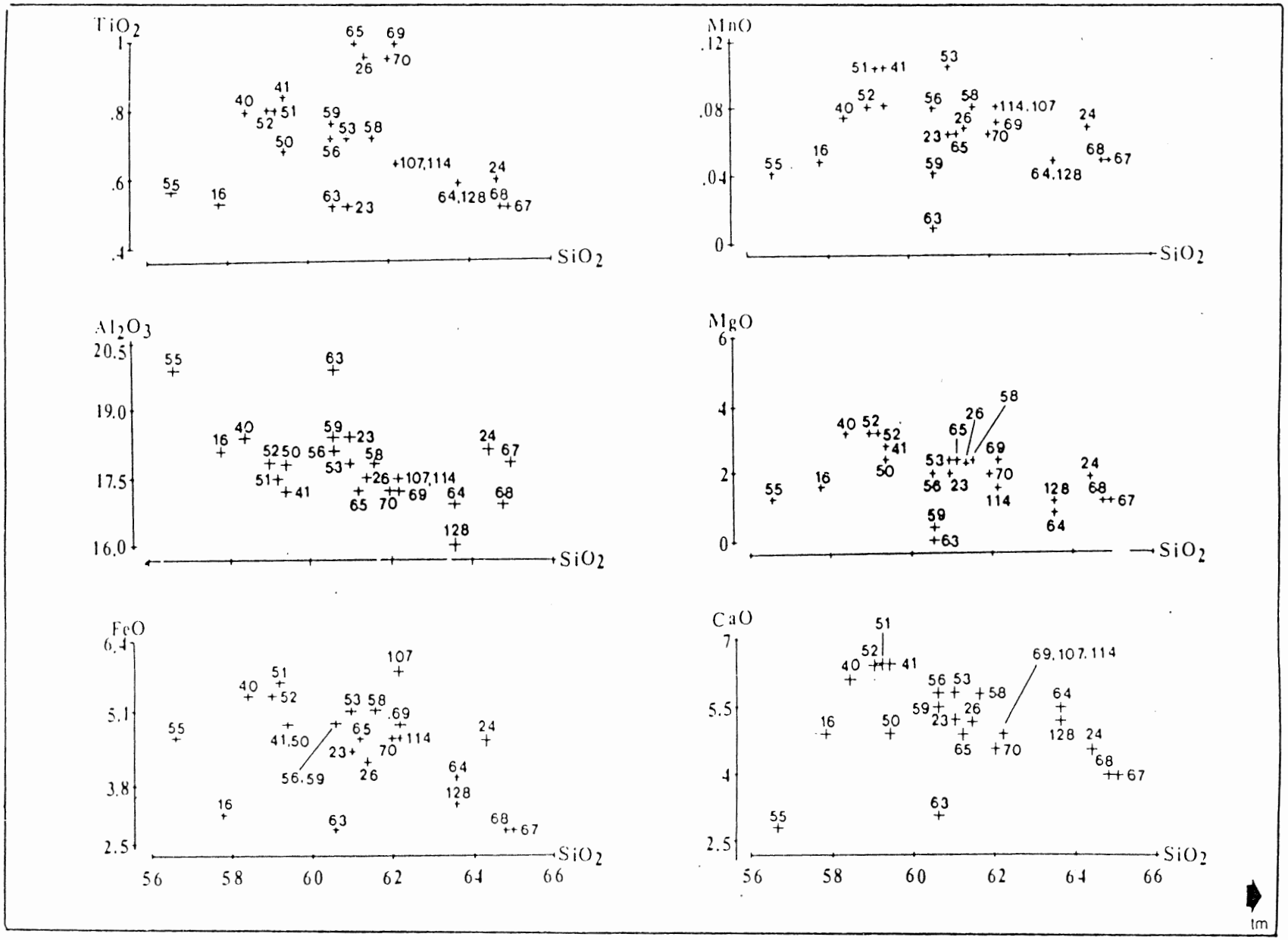
TiO2
1
.8
.6
.4
SiO2
MnO
.12
.08
.04
0
SiO2
Al2O3
20.5
19.0
17.5
16.0
SiO2
MgO
6
4
2
0
SiO2
FeO
6.4
5.1
3.8
2.5
SiO2
56
58
60
62
64
66
CaO
7
5.5
4
2.5
SiO2
56
58
60
62
64
66
tm

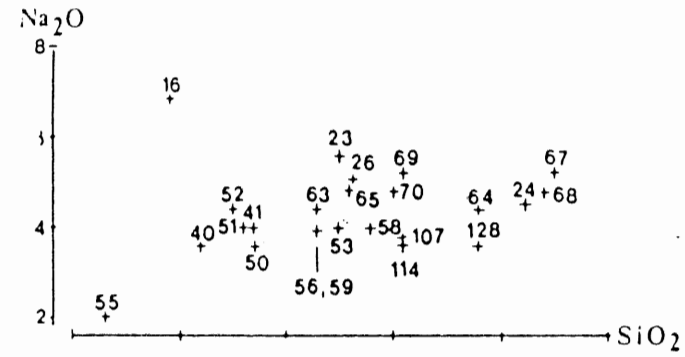

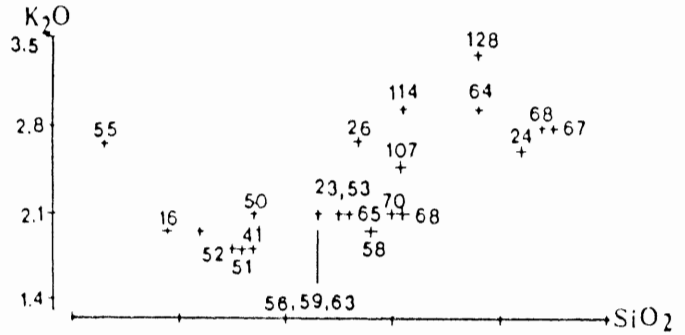

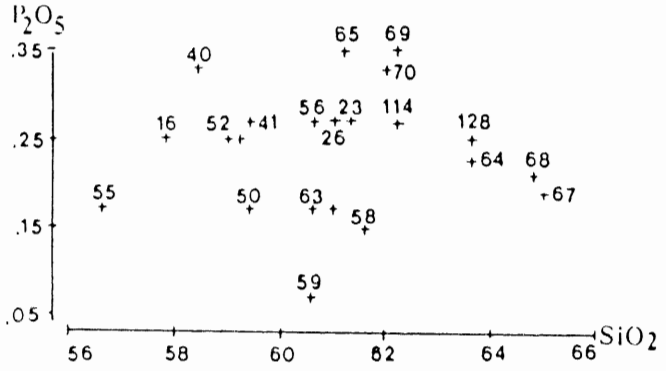

Figure III.11 Variation diagrams of major elements of Copiapo volcanic rocks. Plots are accompanied by the actual field sample numbers. All oxide values are in weight percent.

lm

increases. K_2O and Na_2O increase with silica. Al_2O_3 shows a slight increase but then decreases with SiO_2. TiO_2 and P_2O_5 show erraric distribution.

Krauskopf (1979) states that the rise and fall of major elements with respect to increasing silica can be explained by the evolution of magmatic crystallization. CaO, MgO and FeO decline because these oxides are concentrated in the low silica minerals (olivine, pyroxene, calcic plagioclase) that make up the earlier rocks of the sequence. The alkali metals increase across the diagram is due to abundance of alkali feldspar and micas in the later stages of differentiation.

Petrographic observations of the studied rocks indicate that there are mineralogical changes from lower to higher silica rocks. Samples with 57 to 60 % silica (e.g. Z-50, 51, 52-78, WZ-40, 41-84) are dominated by pyroxene, amphibole and plagioclase. Porphyritic plagioclase crystals are less than 50 %. K-feldspar is minor. Mafic mineral abundance becomes less in samples with silica contents from 60 to 63 weight percent. Minor biotite is present. Plagioclase phenocrysts are more than 50 % of the total crystals. Samples with silica contents from 63 to 65 % (Z-64, 67, 68-78, WZ-24, 128-84) are dominated by plagioclse and K-feldspar phenocrysts. Biotite is the predominant mafic mineral. Pyroxene and amphibole are minor or absent. Thus, there is a clear relationship between chemical and mineralogical variations in the studied rocks.

As for samples Z-55 and 63-78 and WZ-16-84 which appear to be unrelated to the majority of the rocks, there are some possible explanations for their behavior. One of the possibilities is that those rocks are representative of a different magma from the one which produced the majority of the studied rocks. This is more apparent when the trace element Zr is plotted against Ti (Figure III.12). A straight linear line connecting all the points indicates that the rocks were produced from differentiation of a single magma, because Zr and Ti behave similarly during magmatic evolution (Personal communication with Dr. G.K. Muecke, 1985). Thus, Figure III.12 suggests that, together with samples Z-55 and 63-78 and WZ-16-84, samples Z-67 and 68-78 and WZ-23, 24 and 128-84 were produced by a separate magma.

On the contrary, all the samples might indicate origin from a single source of magma if the behavior of Ti during crystallization is examined. Introduction of variable amounts of fraction of mafic minerals during early crystallization have been suggested to contribute in part to the poor correlation of TiO_2 with SiO_2 within low siliica range (Giles and Hallberg, 1982). This may be the reason for the erratic distribution for Ti in the lowest silica value in studied rocks (Figure III. 11). The Early fractionation of ilmenite could also lead to the clustering of those " erratic " samples (Personal communication with Dr. G.K. Muecke, 1985). This is supported by the low FeO concentrations in those sample as well.

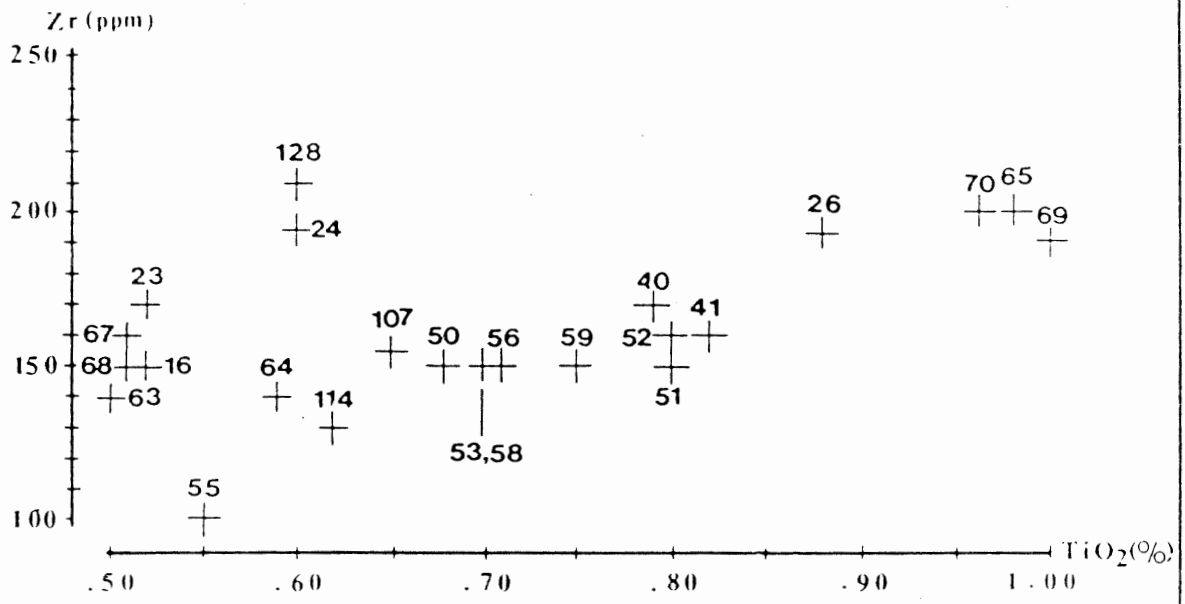

Figure III.12 $Zr-TiO_2$ plot, showing the general linear relationship of the majority of the rock. The clustering of several samples can be explained by ilmenite fractionation during the early magmatic differentia tion (see text).

At this stage, there can be no any satisfactory answer to that problem because of limited data in this thesis. A combination of various sufficient inputs from petrography, field, geochemistry and geochronology will give a better answer.

Trace elements

These elements are discussed in groups of those known to be of close associations. The order of discussions is Rb, Ba, Sr, Zr, Ni, Cr, V and Cu.

The K-group : Rb, Ba and Sr.

Rb and Ba contents in Copiapo volcanic rocks range from 55 to 148 ppm, and from 565 to 838 ppm, respectively. Both elements increase from low to high SiO_2 (Figure III. 13a). Rb and Ba form no minerals of their own, being always incorporated in potassium minerals; in igneous rocks they are present in biotite and potash feldspar (Mason, 1966). Thus, the same author suggested that these two elements increase with differentiation.

Samples Z-55-78, WZ-16-84 and WZ-128-84 tend to have a separate trend from majority of the samples. The explanation is thus similar to those already pointed out in the discussion of the major element geochemistry.

The relationship between Rb and Ba and K_2O is shown in Figure III.13b. As predicted, rubidium increase with

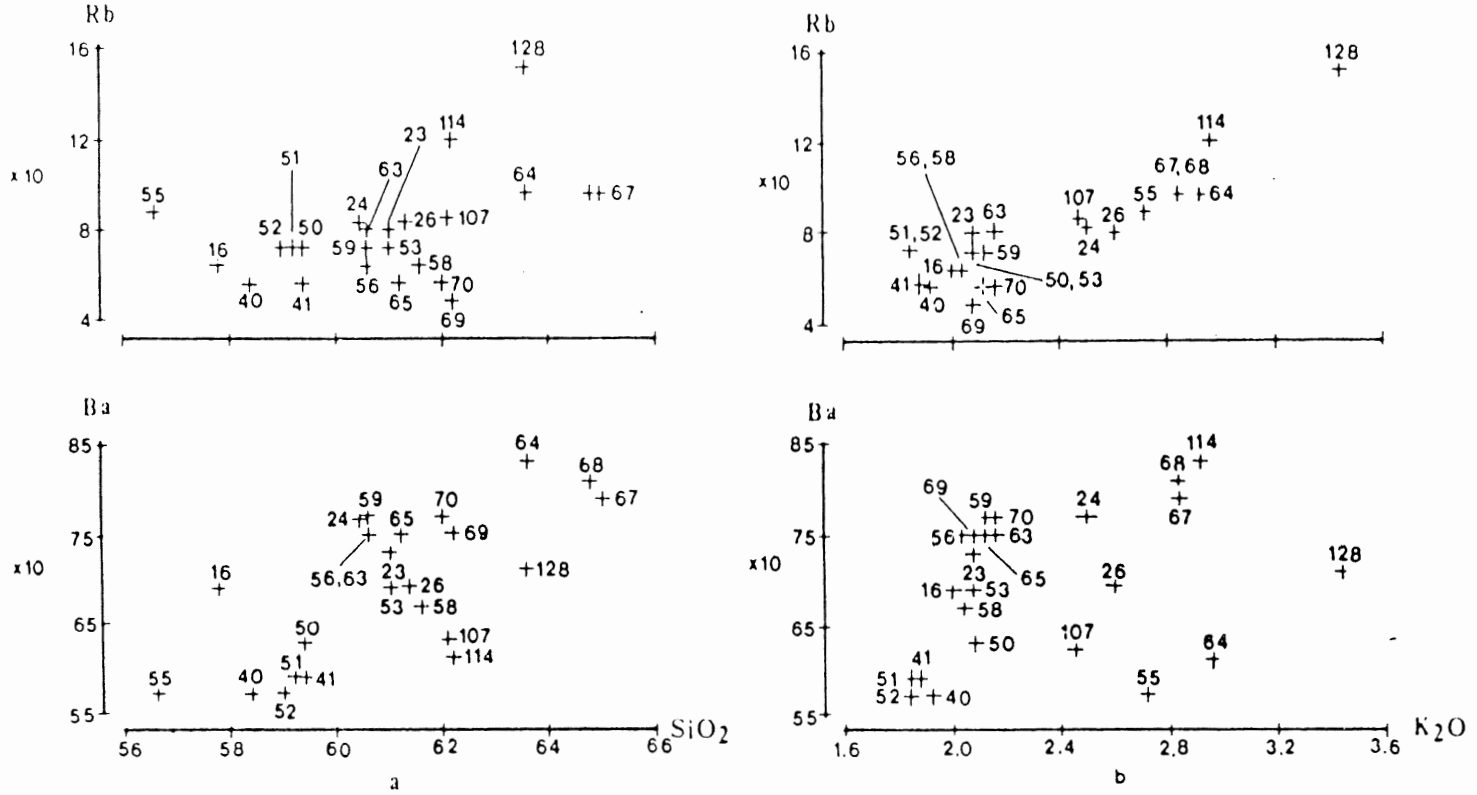

Figure III.13a Rubidium and Barium versus SiO_2.

13b Rubidium and Barium versus SiO_2.

The trace elements are in parts per million, while the major elements (SiO_2 and K_2O) are in weight percent.

tm

incresing potassium. However, barium does not seem to have any relationship with potassium.

The Ti-group : Zr.

Titanium characteristics have been discussed in the previous section. Owing to high field strength (charge/ionic radius), Zr and other Ti-group elements (not analyzed) are not incorporated appreciably in common minerals (Gill, 1980).

Zr in the study rocks range from 102 to 207 ppm, with a majority of 14 out of 21 samples below 153 ppm. Gill (1981) states that most orogenic andesites contain Zr in between 50-150 ppm. The higher Zr concentrations in the study rocks are not unusual. Taylor (1962) states that the range of Zr values varies from region to region.

The compatible group : Ni, Cr and V

The abundance and behaviour of Ni, Cr and V in the studied rocks are given in Figure III.14. Each of these elements shows an overlapping range between rock types. The few numbers of observations of dacite limit further tangible comparisons between andesite and dacite. Plotted in the Harker diagrams, these elements, except V, show erratic correlation with silica. For vanadium, Samples Z-55-78 and WZ-16-78 do not follow the general trend of differentiation of the majority samples. This behavior has been encountered in the major elements and in some of the trace elements as well.

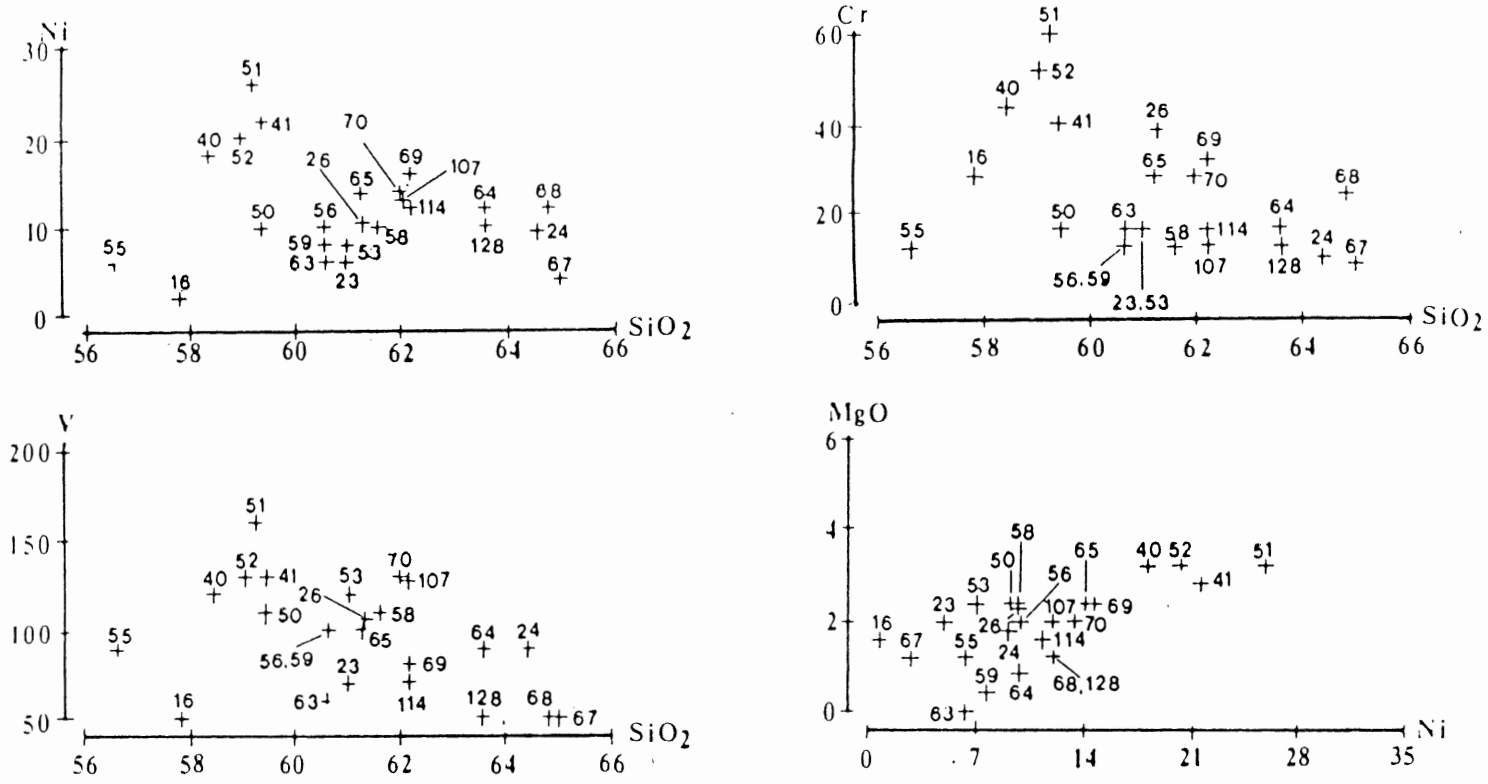

Figure III.14 Variation diagrams of Ni, V and Cr versus SiO_2, and MgO versus Ni. Trace elements are in parts per million, while major elements (SiO_2 and MgO) are in weight percent.

MgO and Ni correlate positively, a common case for these two elements.

Ni, Cr and V are known to be highest in early formed crystals and show a steady decline in the later formed rocks and minerals (Mason, 1966, Taylor, 1962). Consequently, these elements are expected to correlate negatively with silica. Ni and Cr concentrations in andesites can either correlate positively with MgO or remain remarkably constant or vary randomly over a constant range with decreasing MgO or increasing SiO_2 (Gill, 1981). This behaviour, according to the same author, reflects significant differences in source compositions versus differentiation processes.

The Calcophile group : Cu

Copper is the only chalcophile element analysed in all studied rocks. Figure III.15 illustrates the relationship between Cu and silica in the studied rocks. No correlation appears between the two elements. Table III.4 summarizes the statistical data of Cu in all the studied rocks (fresh, altered and vein).

Rock type	Range (ppm)	Mean	St.Div
Andesite (19)	13-53	30	6
Dacite (5)	19-33	29	6
Altered (17)	0-273	47	63
Vein (4)	35-80	60	16

Table III.2 Simple statistical data of Cu in the studied rock Numbers in brackets indicate the number of observations.

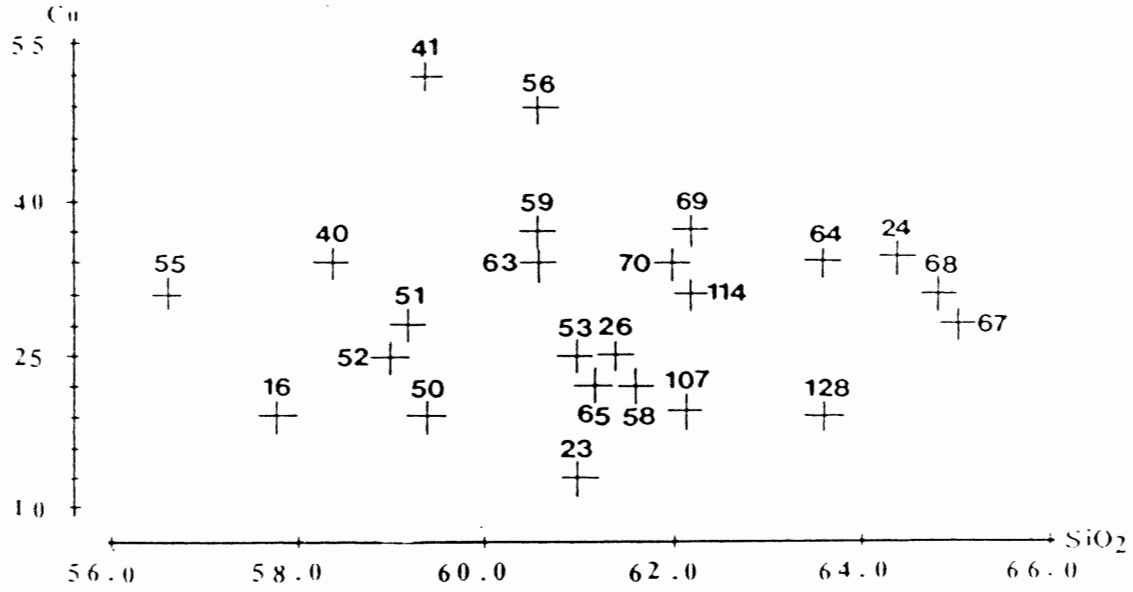

Figure III.15 Contents of copper (ppm) versus SiO_2 (weight percent) in fresh volcanic rocks. Plots are accompanied by their actual field sample numbers.

There is no distinction of Cu contents in andesite and dacite. Cu is generally higher in altered rocks than in fresh rocks. The mean and the standard deviation would have been higher and lower respectively if the zero Cu in two highly silicified rocks were excluded. Cu is generally expected to be higher in hydrothermally altered rocks. The absence of Cu in silicified rocks can be explained because Cu is diluted by silica.

The geochemical behaviour of Cu has been extensively studied because of its economic importance. The geochemistry of Cu is dominated by its strong chalcophile character (Mason, 1966; Taylor, 1962). This, as suggested by Lacy (1974), contributes to the erratic behaviour of Cu in igneous rocks. It has a tendency to form tiny grains of sulphide minerals in igneous rocks rather than substituting in the silicates. Lacy (1974) reports that Cu can partition to rock-forming minerals such as biotites and hornblendes. He showed that Cu content in biotite varies from 15 to 3658 ppm and suggested that there are no meaningful correlations found between Cu and any major elements.

Cu in andesites has frequently been associated with porphyry copper ore deposits (Gill, 1981), although people have different ideas of its role. The range of Cu content in andesitic rocks is variable, depending on whose data are used. It can range from 10 to 150 ppm. The high Cu concentration in any rocks should not be regarded as potensial source of ore.

Baldwin and Pearce (1982) prove that rocks with high Cu content can also be actually barren (non-productive) in an economic sense.

G. Summary

Petrographic studies show that the sequence of rocks from pyroxene-amphibole to amphibole-biotite dominated andesites to biotite-feldspar dacites are present in Copiapo. Chemically the rocks appear to represent medium-K calc-alkaline to high-K dacite sequences. The former, which constitutes the majority rocks, are low in Ti (< 1.00 %), high in alumina (> 15.00 %) and medium in potassium (1.50 to 2.10 %). To a large extent, the results from petrographic and chemical studies of the rocks are relatively consistent.

Chapter IV

Hydrothermal Alteration

4.1 Introduction

An important knowledge acquired from the study of hydrothermally altered rocks is to know the association of metal concentration with a certain kind of alteration mineral assemblage(s). This in turn provides a useful guide for mineral exploration in such environments. This chapter describes the mineralogical and chemical changes that had taken place in the studied altered rocks. Their relation to gold mineralization is described in the following chapter.

4.2 Physical changes

The physical changes in rocks as a result of hydrothermal alteration are readily apparent in hand specimen in terms of color and texture. The Copiapo suite used in this thesis consists of altered rocks which are excellent examples of how alteration changes the color of the fresh rocks into lighter or darker. In the andesitic and related rocks, because of the abundance of secondary (alteration product) lighter colored minerals such as alunite, kaolinite and other clays, the altered rocks are generally pale as compared with the unaltered equivalents. Chemical analyses (dealt with in the next part) indicate the loss of iron and other components which colored the fresh rocks. Pyroclastic rocks are generally oxidized, leaving an iron-staining color on the rock surface. The pink color (sample no. WZ-35-84) is an example of " red coloration ". It is developed by the formation of red feldspar and the removal of biotite which

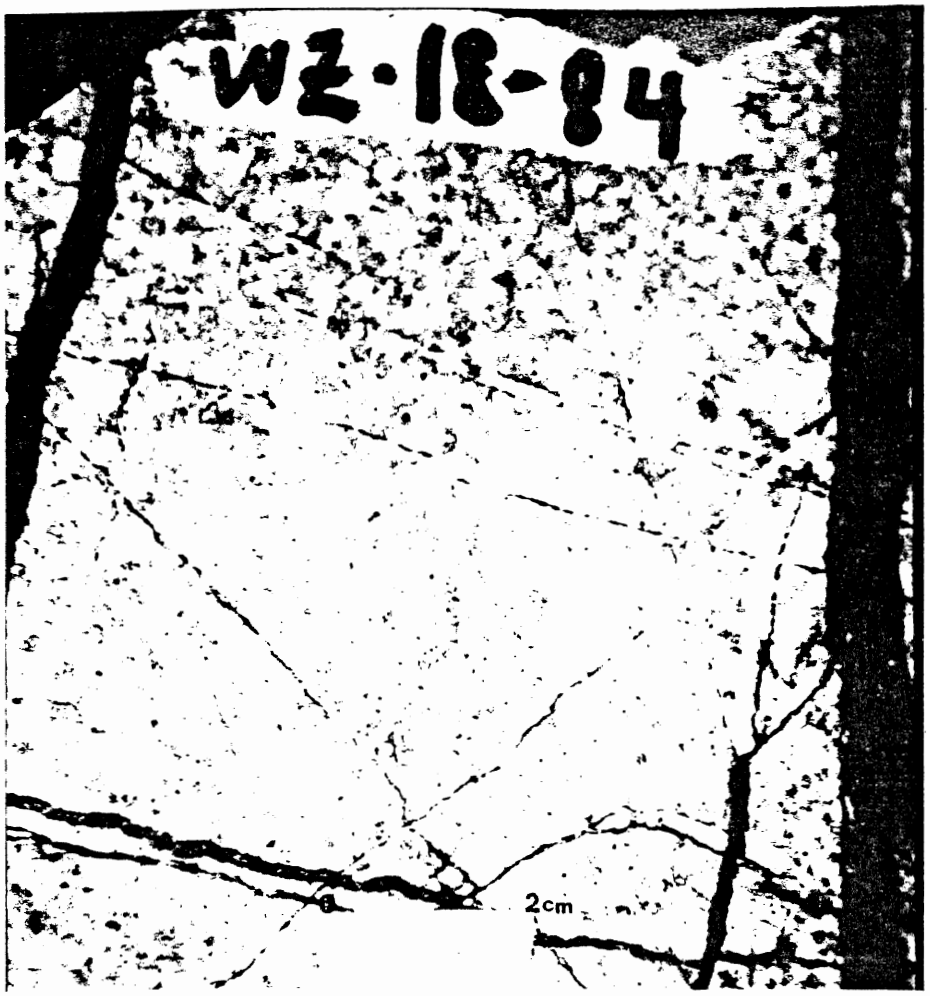

Plate 5. A pale altered rock which shows relicts of former phenocrysts and cross-cutting veinlets.

presumably furnished the iron to form hematite that colors the feldspar (Schwartz, 1959). Thus, changes of color can be both ways, lightening or darkening the color of the rocks.

Hydrothermal alteration has resulted in the decrease of grain size in the rocks. Replacement of feldspar phenocrysts by clay minerals, sericite, alunite and others result in a significant change in grain size. For example, feldspar phenocrysts ranging from few up to five millimetres long are replaced by sericite flakes averaging about 0.01 millimeters in diameter. Even though fine grained aggregates replace large crystals it is rare to have the original texture completely destroyed. Relicts of phenocrysts remains and the distribution of various mineral species often gives clues to the original texture.

4.3 Mineralogical changes

Petrographic descriptions of " alteration mineralogy ". include all minerals which might have formed because of hydrothermal activity. The identification of some clay minerals which are difficult to be identified in a petrographic microscope was confirmed by X-ray diffraction (Appendix III). Table IV.1 lists the altered minerals. Secondary quartz, which is not listed in Table IV.1, occurs in sericite-bearing rocks and in Samples WZ-117- and 121-84.

Sample No.	Al.Gls	Chlo	Kaol	Dick	Ser	Jar	Alu	Mont	Preh
WZ-18-84			x		x				
19	x								
20		x			x				
21		x			x				
22			x		x				
25 (silicified)									
29	x								
30	x			x			x		
31a	x								
32	x		x					x	
33	x					x		x	
34	x					x			
35	x					x		x	
36	x					x		x	
117				x			x		
121							x		x

Table IV.1 Alteration mineralogy of the studied rocks.
Al.Gls=Altered glass,Chlo=Chlorite,Kaol=Kaolinite,
Dick=Dickite,Ser=Sericite,Jar=Jarosite,Alu=Alunite,
Mont=Montmorillonite, Preh=Prehnite.

Alteration type

There are many ways to classify the altered rocks on the basis of a single or combination of the following criteria:

Plate 6. Tiny, high birefringence (green, pink, yellow) materials in altered glass (cp).

Plate 7. Welded ignimbrite with K-feldspar in a matrix of welded glass shards. Note the presence of high birefringence materials (pp).

Plate 6

Plate 7

Plate 8a. Relicts of former feldspar phenocrysts in a silicified rock (pp).

Plate 8b. Replacement of former phenocrysts (8b) by silica minerals (cp).

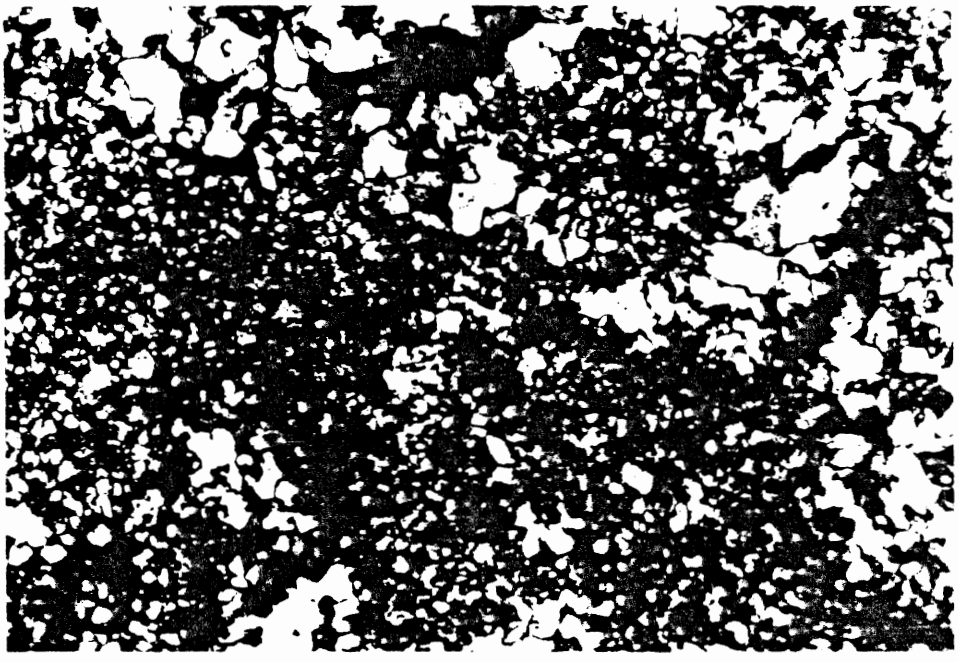

0 1 mm

Plate 9. Fine aggregates of sericite replace feldspar phenocrysts in a matrix of fine quartz and sericite grains (cp).

Plate 10. Coarse aggregates of prehnite replace feldspar phenocrysts in an altered andesite (cp).

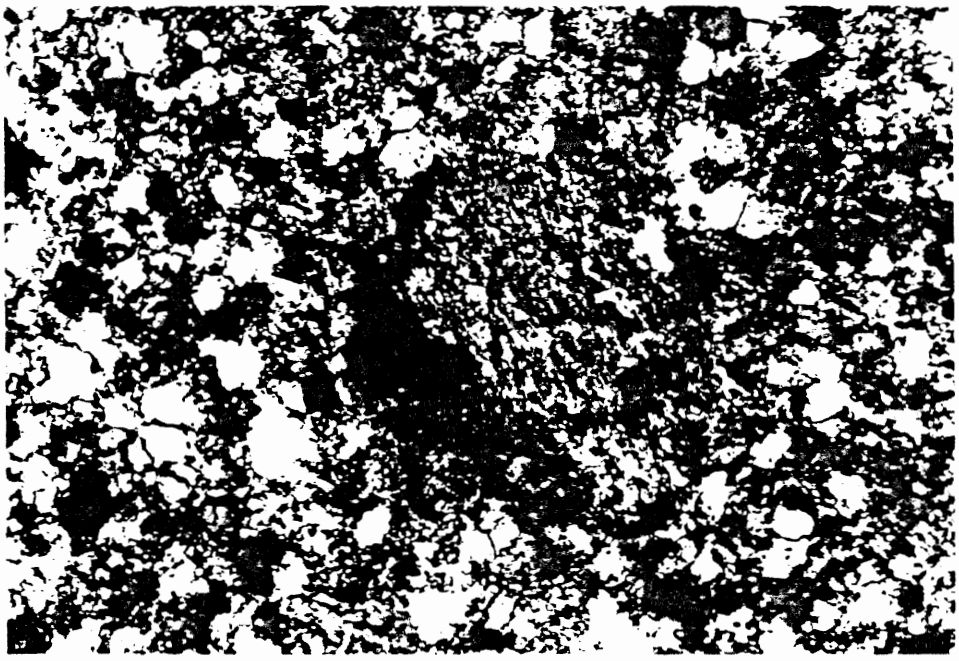

0 0.4mm

0 0.5mm

mineral abundances, texture, parent rocks, chemical change and others. However, no authors have yet combined all those criteria to describe altered rocks. This is the means which Rose and Burt (1979) have suggested to be the best way of describing altered rocks. They also indicated that current terms for alteration types are not clearly defined, are not uniformly used by different authors, or do not completely describe the rocks. Therefore, it appears to the writer that the appropriate way in this thesis to describe alteration types is in terms of mineral assemblages. It is based on the alteration mineralogy already presented earlier and on field relations.

Hydrothermal alteration in the present study area produced three types of mineral assemblages (hereafter are refered to as alteration type, or A.T. I, II and III). Their distributions are shown in Figure IV.1.

A.T. I. Montmorillonite $\pm$ jarosite $\pm$ kaolinite : This assemblage comprises rocks which are characterized by broken plagioclase, montmorillonite and oxidized and altered glass. Color of the rocks ranges from light yellow/brown to pink. In thin section, dark grey and sharded texture are indicative of montmorillonite. All minerals are confirmed by X-ray diffraction. Their optical properties are difficult to determine by a simple petrographic microscope.

Glass is a major constituent of most of the altered rocks. It is the groundmass of the rocks. All samples show that

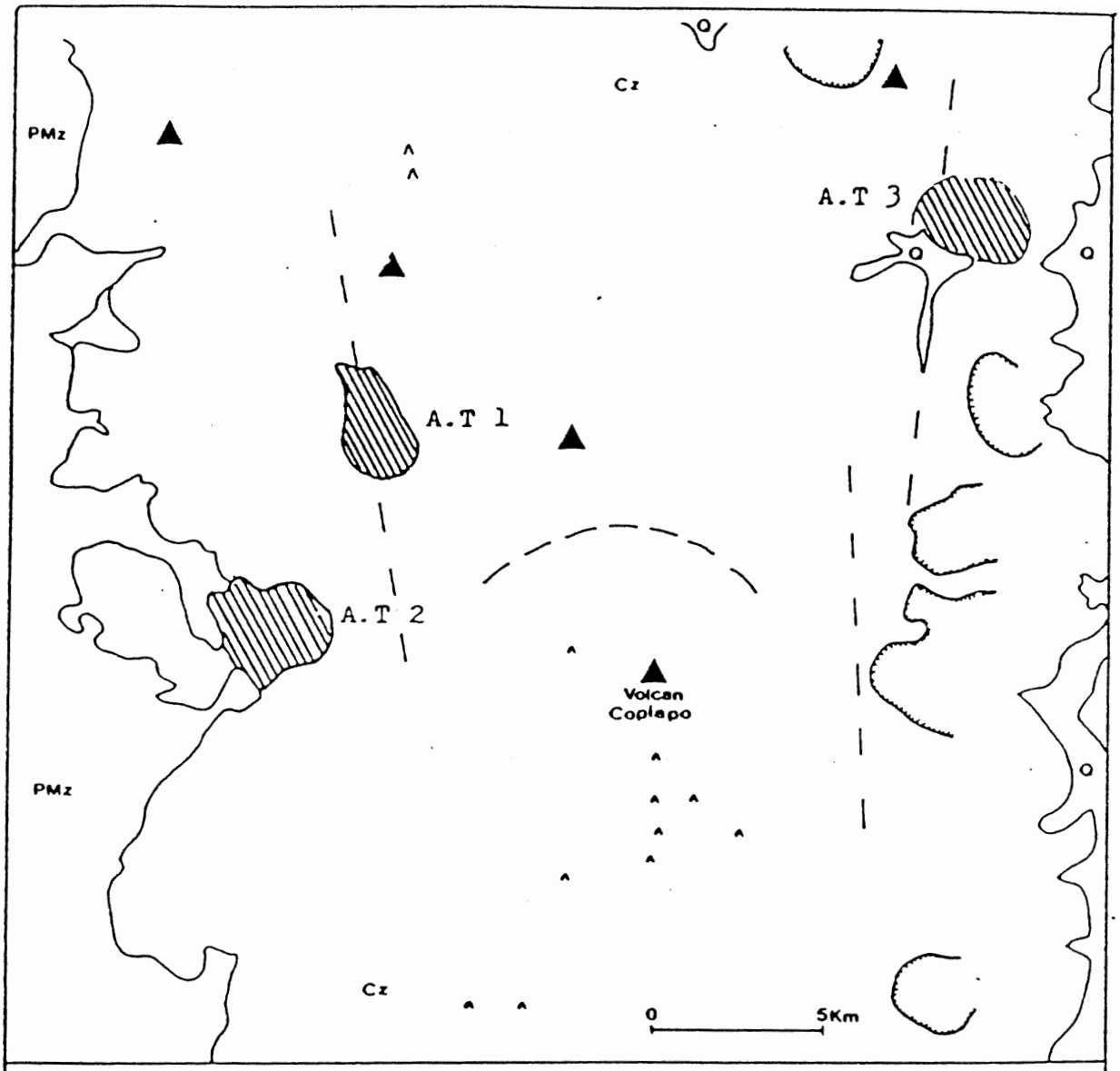

Explanation

PMZ: Paleozoic-Mesozoic rocks

Cz: Cenozoic volcanic rocks

Q: Quaternary sediments

A.T: Alteration type

1. Montmorillonite ± jarosite ± kaolinite
2. Quartz + sericite ± kaolinite ± chlorite
3. Alunite + quartz ± dickite ± prehnite

▲ Volcanic center/volcano

^ Volcanic vent

Caldera

---- Fracture zone

Figure IV.1 Distribution of alteration assemblages (types). The extent of the alteration is approximate.

alteration almost completely transformed the whole glassy groundmass. Two petrographic groups of glass alteration were identified. The first is stained glass. This is characterized by yellow, red or brown colors, which may be due to iron oxidation. The other group shows that the glass was devitrified to a clear, yellow-green material which is very fine grained. It has a high birefringence and shows normal extinction under crossed nicols.

Alteration of plagioclase is characterized by optical isotropy which is typically grey under crossed nicols. Under plane polalizer, its relict clearly remains.

A.T. II. Sericite + quartz $\pm$ Kaolinite $\pm$ chlorite : There is a clear progressive alteration within this assemblage. Chlorite diminishes as sericite + quartz $\pm$ kaolinite dominated assmblage merges. The altered rocks are white to green and show relicts of phenocrysts in both hand specimen and thin section. They have a lighter color than that of the matrix and are assumed to be former plagioclase phenocrysts. The pseudomorphs of those phenocrysts by sericite attest to the assumption. Tiny veinlets also cut two of the samples.

Sericite is the most abundant altered mineral in this assemblage. It occurs in two modes: very fine, randomly and/or partially oriented grains in a quartz-sericite groundmass, and fine to coarse aggregates which formed in rocks adjacent to the quartz-alunite veins. In some samples fine sericite aggregates pseudomorph after the altered

phenocrysts.

Chlorite forms medium to coarse grained felted aggregates, exhibiting green birefringence. These aggregates seem to have replaced mafic minerals. The X-ray characteristics of chlorite is given in Appendix III. Quartz is fine grained and together with sericite forms the major mineralogy. In the altered phenocrysts, quartz grains are surrounded by sericite flakes.

A.T. III. Alunite + quartz $\pm$ dickite $\pm$ prehnite : These minerals (except quartz) completely replaced former porphyritic rocks which left their relicts. These rocks were collected adjancent to quartz-alunite veins where gold mineralization has recently been discovered. The rocks are light grey to yellowish grey. The porphyritic texture is visible in both hand specimen and thin section.

Alunite is present in Samples WZ-117- and 121-84 which are the altered volcanics adjacent to the quartz-alunite vein system. Appropriately, it is natroalunite. Alunitization appears to be co-genetic with gold mineralization; hydrothermal activity transformed k-feldspar minerals into alunite and precipitated gold (discussed in gold mineralization and geochronology). Fine grains of dickite are present, replacing phenocrysts (Wz-117-84). Coarse aggregates of prehnite completely altered feldspar phenocrysts (WZ-121-84). The average grain size is 3 x 2 millimetres.

The matrix is a microcrystalline mosaic of quartz, fine prehnite and feldspar which are fine grained and interlocked. Adularia is present and together with quartz forms veinlets.

4.4 Chemical changes

Table IV.2 lists the results of chemical analyses of the altered rocks used in this thesis. To quantify the gains and losses of elemental abundances during hydrothermal alteration, it is necessary to know the original types of the altered rocks and to apply the appropriate calculation method.

The original type of each altered rocks can be deduced by comparing its Ti/Zr ratio to that of the the fresh equivalent. Those two elements are known to be immobile during hydrothermal alteration (Finlow-Bates and Stumpfl, 1981 ; Floyd and Winchester 1978 and many others). Therefore their ratio is expected to be consistent in both fresh and altered rocks. The strongest support for their immobility in the present altered rocks is their almost linear relationship (Figure IV.2). The ratio of those elements has been used by many investigators such as Floyd and Winchester (1978) and Hallberg (1984) to identify rock types. The last author suggested that for volcanic rocks Ti/Zr ratios are

rhyolite < 4 < dacite < 12 < andesite < 60 < basalt

Table IV.3 lists the Ti/Zr ratios of the altered rocks used in this thesis.

Sample No.	WZ-18-84	WZ-19-84	WZ-20-84	WZ-21-84	WZ-22-84
SiO_2	74.93	46.63	58.80	63.95	70.25
TiO_2	1.00	0.99	0.83	1.01	1.06
Al_2O_3	15.76	1.09	17.44	16.80	18.66
FeO (Total)	0.78	29.37	5.86	4.95	0.68
MnO	0.01	0.01	0.16	0.12	0.01
MgO	0.15	0.00	3.20	1.81	0.17
CaO	0.09	0.09	4.40	0.13	0.08
Na_2O	1.05	0.26	3.50	2.98	0.17
K_2O	1.57	0.05	1.33	0.61	0.80
P_2O_5	0.04	2.36	0.22	0.09	0.11
H_2O+	3.33	12.31	3.66	3.72	5.23
H_2O-	1.16	2.09	1.26	4.01	2.40
S	0.04	0.12	0.00	0.38	0.32
Total	99.91	95.37	100.67	100.56	99.94
Rb	61	7	33	27	40
Ba	332	784	684	363	258
Sr	72	40	456	184	245
V	128	0	119	127	102
Cr	6	25	6	10	9
Ni	1	0	3	2	2
Zr	160	170	155	175	153
Cu	29	36	1	237	8

Sample No.	WZ-25-84	WZ-29-84	WZ-30-84	WZ-31-84	WZ-31a-84
SiO_2	99.00	42.51	47.75	71.02	45.68
TiO_2	0.71	0.86	0.59	0.72	0.39
Al_2O_3	0.35	0.95	22.26	3.11	24.47
FeO (Total)	0.00	32.58	4.72	12.47	7.09
MnO	0.01	0.01	0.01	0.01	0.01
MgO	0.01	0.00	0.00	0.00	0.00
CaO	0.00	0.05	0.40	0.08	0.70
Na_2O	0.05	0.05	2.40	0.20	2.60
K_2O	0.00	0.04	3.54	3.02	6.71
P_2O_5	0.00	2.51	0.20	0.81	0.54
H_2O+	0.32	12.21	15.67	5.78	8.44
H_2O-	0.36	2.61	1.32	1.78	1.08
S	0.17	0.02	0.46	0.51	0.53
Total	100.96	94.40	99.32	99.51	98.18
Rb	1	6	82	17	82
Ba	913	769	528	792	456
Sr	23	38	708	806	1063
V	0	0	126	64	0
Cr	30	16	22	23	318
Ni	0	0	0	0	0
Zr	142	179	117	158	97
Cu	0	42	17	13	36

Sample No.	WZ-32-84	WZ-33-84	WZ-34-84	WZ-35-84	WZ-36-84
SiO_2	61.35	48.66	43.32	54.15	54.33
TiO_2	0.55	0.51	0.56	0.50	0.82
Al_2O_3	19.11	17.89	21.64	22.52	16.97
FeO (Total)	2.52	13.12	13.63	4.99	15.66
MnO	0.01	0.01	0.01	0.01	0.01
MgO	0.74	0.00	0.01	0.19	0.01
CaO	0.16	0.46	0.56	0.95	0.23
Na_2O	3.44	1.51	2.39	3.52	2.96
K_2O	2.82	7.08	5.89	3.70	4.85
P_2O_5	0.04	1.20	0.31	0.23	0.00
H_2O+	5.33	8.88	8.84	6.35	7.98
H_2O-	4.37	0.72	2.47	1.91	1.88
S	0.19	0.58	0.57	0.55	0.55
Total	99.63	100.56	100.34	99.57	98.15
Rb	88	61	66	63	55
Ba	506	493	506	569	536
Sr	463	2262	1040	1034	1614
V	53	526	699	160	714
Cr	8	54	51	36	53
Ni	0	0	0	1	5
Zr	154	120	112	127	118
Cu	2	40	46	24	59

Sample No.	WZ-117-84	WZ-121-84
SiO_2	86.46	73.51
TiO_2	0.75	0.96
Al_2O_3	8.28	16.51
FeO (Total)	0.05	0.00
MnO	0.00	0.00
MgO	0.00	0.00
CaO	0.16	0.48
Na_2O	1.03	1.80
K_2O	0.91	2.43
P_2O_5	0.07	0.35
H_2O+	1.93	3.77
H_2O-	0.30	0.52
S	0.36	0.54
Total	100.31	100.51
Rb	25	1
Ba	114	748
Sr	125	170
V	97	88
Cr	19	32
Ni	1	0
Zr	176	159
Cu	172	34

Table IV.2 Chemical analyses of altered rocks.

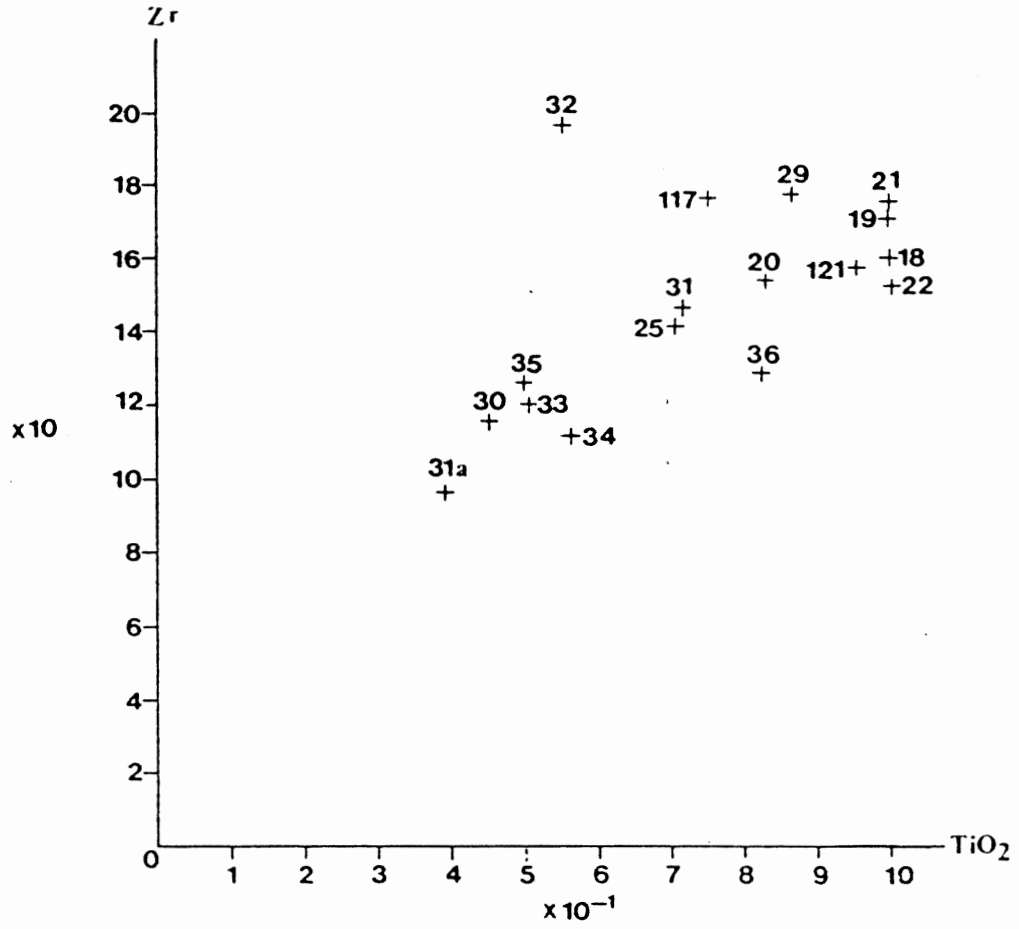

Figure IV.2 Relationship between Zr and TiO_2 in the altered rocks. Zr is in parts per million, while TiO_2 is in weight percent. There is a linear relationship between the two elements, except sample number WZ-32-84. The linear relationship suggests the relative immobility of Zr and Ti during alteration.

tm

Sample No.	Ti/Zr	Rock type	Sample No.	Ti/Zr	rock type
WZ-18-84	62.5	Basalt	WZ-31a-84	40	Andesite
WZ-19-84	58	Andesite	WZ-32-84	36	-
WZ-22-84	69	Basalt	WZ-33-84	43	-
WZ-25-84	50	Andesite	WZ-34-84	50	-
WZ-29-84	48	-	WZ-35-84	39	-
WZ-30-84	50	-	WZ-36-84	69	Basalt
WZ-31-84	46	-	WZ-117-84	43	Andesite
			WZ-121-84	60	basalt/ andesite

Table IV.3. Original lithology of the altered rocks based on Ti/Zr ratio.

From Table IV.4 it is apparent that the majority of the rocks have andesite as their original lithology. As to three samples which are designated as basalts by the Ti/Zr method, their petrographic characteristics suggest otherwise. Those altered rocks retained their porphyritic texture which is typically andesitic. Those phenocrysts which were altered to sericite are therefore believed to be former plagioclase phenocrysts. Basalts are rarely porphyritic. In addition, each of those " basalts " has Ti/Zr ratio close to that of andesite.

Having known the original lithology of each altered rock,

it is now required to use one of the calculation methods for determination of the geochemical transfer. Grensens (1967) suggests a method which requires volume changes associated with alteration, specific gravity of fresh rock and its altered equivalent and/or the absolute variation of one chemical constituent. A number of factors make that method impractical to evaluate density-volume relationships in the present altered rocks. For example, the high initial porosity of the rocks could lead to inconsistent density values. Assuming a constant volume is not reasonable, because there is no evidence for this assumption, even preservation of pseudomorphed phenocrysts in altered rocks is not proof of maintainance of constant volume (Roberts and Reardon, 1978).

An alternative method which does not depend on the volume factor is the Ti-constant method suggested by Colman (1982). The method is simple: an element is chosen and can reasonable be assumed to have been immobile during alteration. In this thesis, Ti appears to have been immobile. The support for that assumption has been shown in Figure IV.2 . The weight of each elemental oxide in the altered rocks is calculated by multiplying its weight percentage by the ratio of the weight percentage of TiO_2 in the fresh rock to that in the altered sample. The calculated values are equivalent to the amount remaining after the alteration of 100 gr of fresh rock. Appendix III describes in detail the calculation method and lists the gain or loss of individual samples.

The gains and losses of major elements and two selected trace elements (rubidium and barium) that had occurred during hydrothermal alteration are graphed in Figure IV.3. These data were obtained from Appendix IV. Each graph in Figure IV.3, which shows the chemical changes of an element, consists of three separate groups of columns corresponding to the three alteration types already described. It must be borne in mind that since a systematic rock sampling from unaltered to altered zones was not possible at this stage, it can not be assumed that there is any necessary spatial relationship between the groups. Therefore, each group is separately discussed with constraints from petrographic observation and elemental behaviors.

A.T. I. Montmorillonite $\pm$ jarosite $\pm$ kaolinite: This alteration resulted in large gain in silicon, aluminum, potassium and water, but there are some local losses in these elements as well, except water. All rocks in this assemblage lost, to a large extent, their mangnanese, magnesium and calcium constituents. The gains and losses of sodium and phosporous tend to be equally numbered. The latter, which shows small increase and decrease in abundance, might suggest that there had been little movement during alteration.

The gain of silicon and aluminum might be due to devitrification of glass to tiny bright green materials. Coleman (1982) carries out analyses of these grains and discovers that silicon is the main constituent, followed by

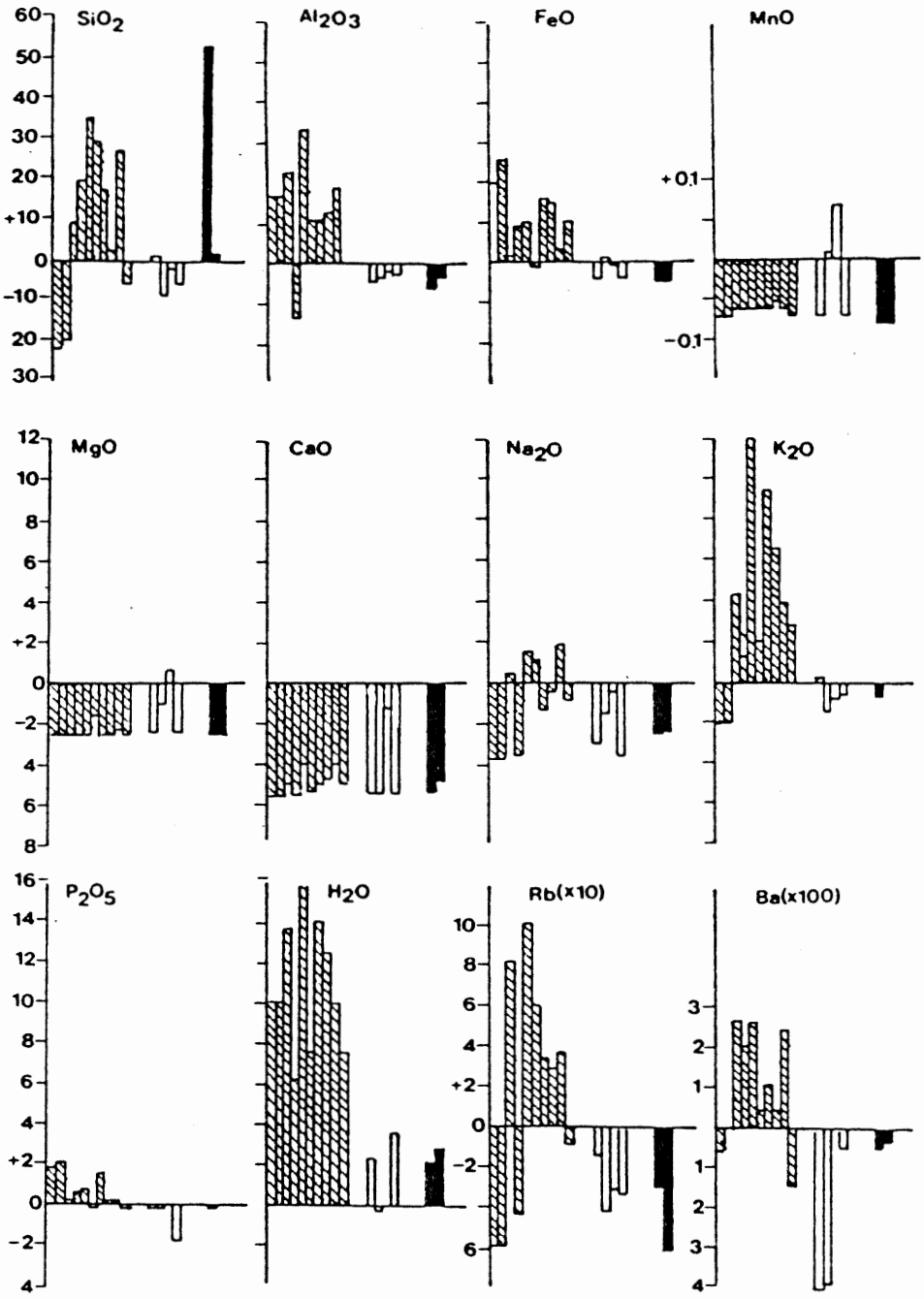

Figure IV.3 Gains and losses of major elements (in g/100g) and trace elements (Rb and Ba, in parts per million). Shaded columns are A.T I, blank columns are A.T II and filled columns are A.T III.

aluminum, iron and calcium. The increase in aluminum can also be explained, together with potassium, by the presence of clay minerals such as kaolinite (Al-rich) and jarosite (K- and Fe-rich). The gains and local losses of potassium are simultaneously accompanied by rubidium, an element whose atoms are known to be similar in size, electronegativity and ionization potential to potassium (Taylor, 1965). Barium shows an almost similar pattern with potassium, because it frequently substitutes for K among the common cations (Taylor, 1962).

The gain in iron resulted from the staining and devitrification of glass. It is also reflected in the presence of jarosite. The removal of manganese and magnesium is due to the fact that they are rather soluble. In fact, in some hydrothermal ore deposits, manganese forms haloes surrounding the ore zones. The loss of calcium is due to the transformation of plagioclase phenocrysts into isotopic materials. It can also be due to a base exchange.

A.T. II. Sericite + quartz $\pm$ kaolinite $\pm$ chlorite : In this assemblage, small gains in silicon, iron, magnesium, manganese, potassium, phosporous and moderate gain in water occurred together with losses in aluminum, calcium and sodium. The gaining elements are also accompanied by local losses. The gain in silica can be explained by the presence of tiny quartz veinlets and perhaps by the precipitation of silicon in cavities. The increase of iron, manganese and magnesium is

reflected in the formation of chlorite. The gain of potassium is a consequence of the formation of sericite and adularia from plagioclase. The loss of silicon might be due to its migration towards silicic zone which is adjacent to the rocks which make up this assemblage. The loss of calcium might be due to the breakdown of plagioclase. The loss of potassium is due to the formation of kaolinite from feldspar. It is also accompanied by a decreasing of rubidium and barium. The loss of aluminum cannot be explained petrographically.

A.T. III. Alunite + quartz $\pm$ dickite $\pm$ prehnite : There are only two samples making up this assemblage and they flank the quartz-alunite vein system. Silicon and potassium gained, but the latter also shows some losses. When one examines and compares the geochemistry between this assemblage and the vein rocks (Table IV.4), it becomes apparent that apparent that the chemical exchange between the host rock (A.T. III) and the vein, including the capping rock, is responsible for the elemental gains and losses in the host rock. For example, the loss of aluminum is reflected in the formation of diaspore cap (WZ-119-84). Potassium and sodium formed alunite in the vein. The other elements which are absent in both altered rocks and veins might have migrated towards adjacent rocks. The loss of calcium in WZ-121-84 is minimal because this element is partly retained to form prehnite.

	Altered rocks		Veins and siliceous rocks				
Sample	WZ-117	121-84	WZ-118	119	120Q	120A	122-84
SiO_2	86.46	73.51	57.44	8.77	49.81	7.85	80.08
TiO_2	0.75	0.96	0.82	0.04	0.51	0.57	0.10
Al_2O_3	8.28	16.51	24.39	40.16	20.81	37.64	8.55
FeO (Total)	0.05	0.00	0.16	1.00	1.84	3.32	4.11
MnO	0.00	0.00	0.00	0.01	0.01	0.01	0.00
MgO	0.00	0.00	0.00	0.17	0.15	0.15	0.00
CaO	0.16	0.48	0.22	0.25	0.17	0.88	0.04
Na_2O	1.03	1.80	2.09	4.41	1.95	3.80	1.08
K_2O	0.91	2.43	1.91	5.45	3.01	6.10	2.07
P_2O_5	0.07	0.35	0.23	0.59	0.24	0.54	0.14
H_2O+	1.93	3.77	5.41				2.82
H_2O-	0.30	0.52	0.34	42.10	23.40	39.50	0.38
S	0.36	0.54				2.00	0.53
Total	100.23	100.51	99.02	102.35	102.44	102.96	99.90
Rb	25	1	63	35	22	34	7
Ba	114	748	507	103	80	87	123
Sr	125	170	563	944	373	702	152
V	97	88	146	187	124	229	120
Cr	19	32	26	42	27	21	28
Ni	1	0	0	0	0	0	0
Zr	176	159	95	96	1075	827	89
Cu	172	34	64	79	96	35	52

Table IV.4 Comparison of major and trace elements between alteration type III and veins.

The gain of water in all assemblages can be explained by the statement from Hemley and Jones (1964) who emphasize its role and hydrogen ion in wall-rock alteration. They suggest that the hydrolytic decomposition of many components is a significant process involved in hydrothermal alteration. Calcium, magnesium, sodium and potassium ions are removed and are replced by an equivalent amount of hydrogen ions.

4.5 Discussion

Many authors such as Harvey and Vitaliano (1964), Sillitoe (1976), Buchanan (1981) and Vikre (1985)

indicate that there is normally a progress of alteration characterizing epithermal deposits. The sequence of alteration zones toward the mineralized veins is generally from propylitization to alunitization accompanied by wide spread silicification.

From the distribution of alteration zones in Figure IV.1, it is clear that there are not sufficient data to construct a complete pattern of continueos progression of alteration from the host rock to the altered and mineralized rocks and veins in the study area. However, there are four important phenomena that can be brought in here. Firstly, alterations are localized in the major fracture systems or zones in the study area. This suggests a spatial relationship between structure and alteration. Fractures are known to control the migration or circulation of alteration and possibly mineralizing fluids. The discovery of gold mineralization in these fractures (see Chapter V and Personal communication with Dr. M. Zentilli, 1984) attest to the above statement.

Secondly, the proximity between alteration types I and II (about 3 kilometres apart) gives an indication that they are spatially related. They are also more or less equivalent in mineral assemblages to propylitic and argillic alteration, respectively. The presence of nearby silicified rocks frequently indicates that there are vein systems in the area. Future investigation into the area of alteration type II will verify this hypothesis.

Thirdly, alteration type III flanks the quartz-alunite vein. This style of alteration and vein system is known to occur in many epithermal precious metal deposits where the highest ore grade is located. There is a significant enrichment of gold in alteration type III and in the veins. Thus, this assemblage is equivalent to the so called alunite zone which is known to contain gold and other metals described by many authors, such as Harvey and Viatliano (1963). Consequently, the recognition of this kind of alteration mineral assemblage might lead to reveal the hidden ore zones or deposits. The coexistence between gold (together with other metals) and the minerals which constitute the assemblage may help to determine the physico-chemical condition of mineralization and the nature of the mineralizing fluid.

Fourthly, there is a remarkable similar pattern of the overall geochemical transfer from unaltered to altered rocks both in Copiapo and in the Wairakei geothermal system. The latter, which is a modern system, has been suggested to be analogous to the Tertiary hydrothermal deposits in terms of physical and chemical environment (Hemley and Ellis, 1983). In the Wairakei system, the transfer is characterized by loss of sodium and calcium, gain of potassium and silica in all zones, and loss of aluminum, iron, manganese and magnesium in highest-ranked alteration zones. These characteristics are also observed in the studied rocks (see Figure IV.3), although there are few local variations, for example, in

sodium and potassium.

Despite limited data available to the writer, some significant results which are already described are useful and informative for future studies.

Conclusions

1. Three types of alteration based on hydrothermal mineral assemblages have been recognized and defined as follow:

I. Montmorillonite ± jarosite ± kaolinite,

II. Sericite + quartz ± kaolinite ± chlorite and

III. Alunite + quartz ± dickite ± prehnite.

2. The alteration processes are controlled by the long linear fracture zones.

2. There is no clear spatial and/or temporal relationship among the three assemblages because they do not develope any zoning.

3. The characteristics of alteration type III is similar to those known to be ore-bearing in many epithermal deposits. This provides a useful guide for exploration in epithermal gold.

4. Geochemical transfers are fairly consistent with petrographic observations and X-ray diffraction. This indicates that the Ti-constant method can be applied in order

to determine the gains and losses of elements in the present rocks.

5. Ti and Zr appear to be relatively immobile during hydrothermal alteration.

Chapter V

Gold distribution

5.1 Introduction

It has been well known that in epithermal gold deposits, the richest ore is frequently concentrated in veins, called " bonanza ore bodies ". Nevertheless, altered rocks, which flank the veins and frequently form zonal patterns, are also associated with the mineralization. In fact, many hidden ores were discovered by studying the alteration/mineralization association. In this chapter, the writer attempts to characterize gold mineralization in the studied rocks and to examine the kinds of gold pathfinders which are useful guides in searching for ores in undeformed and young volcanogenic epithermal systems.

5.2 Results and discussion

Analytical results of Au and other selected elements are shown in Table V.1. A limited number of samples prevented employing statistical analyses. Thus, a direct comparison between Au and other elements is made (Figure V.1).

A. Gold

The Au contents in fresh samples range from 2 to 32 ppb and average 12 ppb. Both the range and mean are higher than the average values used by Lacy (1974), whose Au data for calc-alkaline andesites are: 0.05 to 12.00 ppb and 4.5 ppb for range and mean, respectively. Most samples contain anomalous amounts of gold. Significant enrichment is clearly seen in altered rocks and in vein rocks, in which the average values

Fresh

	Au	Ag	As	K	Mo	Pb	S	Sb	Se
WZ-16-84	32	4	4.6	2.00	<1	10	0.40	0.4	5
23	4	<2	17.0	2.07	<1	13	0.00	0.4	5
24	20	<2	21.0	2.51	<1	9	0.00	1.3	5
26	3	<2	4.4	2.60	<1	13	0.00	0.5	6
107	2	<2	8.3	2.38	<1	12	0.02	0.8	5
Average	12	<2.4	14.6	2.31	<1	11.4	0.08	0.68	5.2

Alteration type I

WZ-19-84	25	<7	>3000	0.05	7	51 4	0.12	12.9	16
29	27	<8	>3000	0.04	8	413	0.02	12.8	17
30	3	<8	78	3.54	<1	18	0.46	0.8	5
31	6	<2	1480	3.02	<1	30	0.51	0.7	8
31a	<3	<2	141	6.71	<2	8	0.53	0.6	5
32	16	<2	13	2.82	<1	12	0.19	0.9	5
33	24	<2	426	7.08	<1	0	0.58	0.7	5
34	7	<2	41	5.89	6	14	0.57	1.2	5
35	<2	<2	19	3.70	<1	8	0.55	0.8	5
36	54	<3	111	4.85	9	7	0.55	0.7	5
Average	17	<3.77	831	3.77	3.7	99	0.41	3.21	7.6

Alteration type II

WZ-18-84	200	2	14	1.57	3	25	0.04	2.3	7
20	4	<2	37	1.33	<1	12	0.00	0.4	6
21	237	<2	43	0.61	4	28	0.38	0.7	5
22	26	<2	12	0.80	<1	31	0.32	0.6	5
Average	117	<2	26.5	1.08	2.3	24	0.28	1.0	5.8

Alteration type III

WZ-117-84	1560	<2	108	0.91	33	122	0.36	2.4	8
121	130	<2	23	2.43	22	210	0.54	1.2	5
Average	845	<2	65.5	1.67	27.5	166	0.45	1.8	6.5

Vein and cap rock (119)

WZ-118-84	170	<2	217	1.91	59	187	0.53	4.3	24
119	35	<2	290	5.45	68	307	0.53	3.8	5
120	571	<2	212	6.10	87	469	2.00	6.3	10
122	4670	<2	449	2.07	58	73	0.54	4.6	8
Average	1362	<2	292	3.71	68	268	0.90	4.8	11.8

Table V.1 Analytical results of gold and other elements for the studied rocks. All values are in ppm, except Au in ppb, K and S in weight percentage.

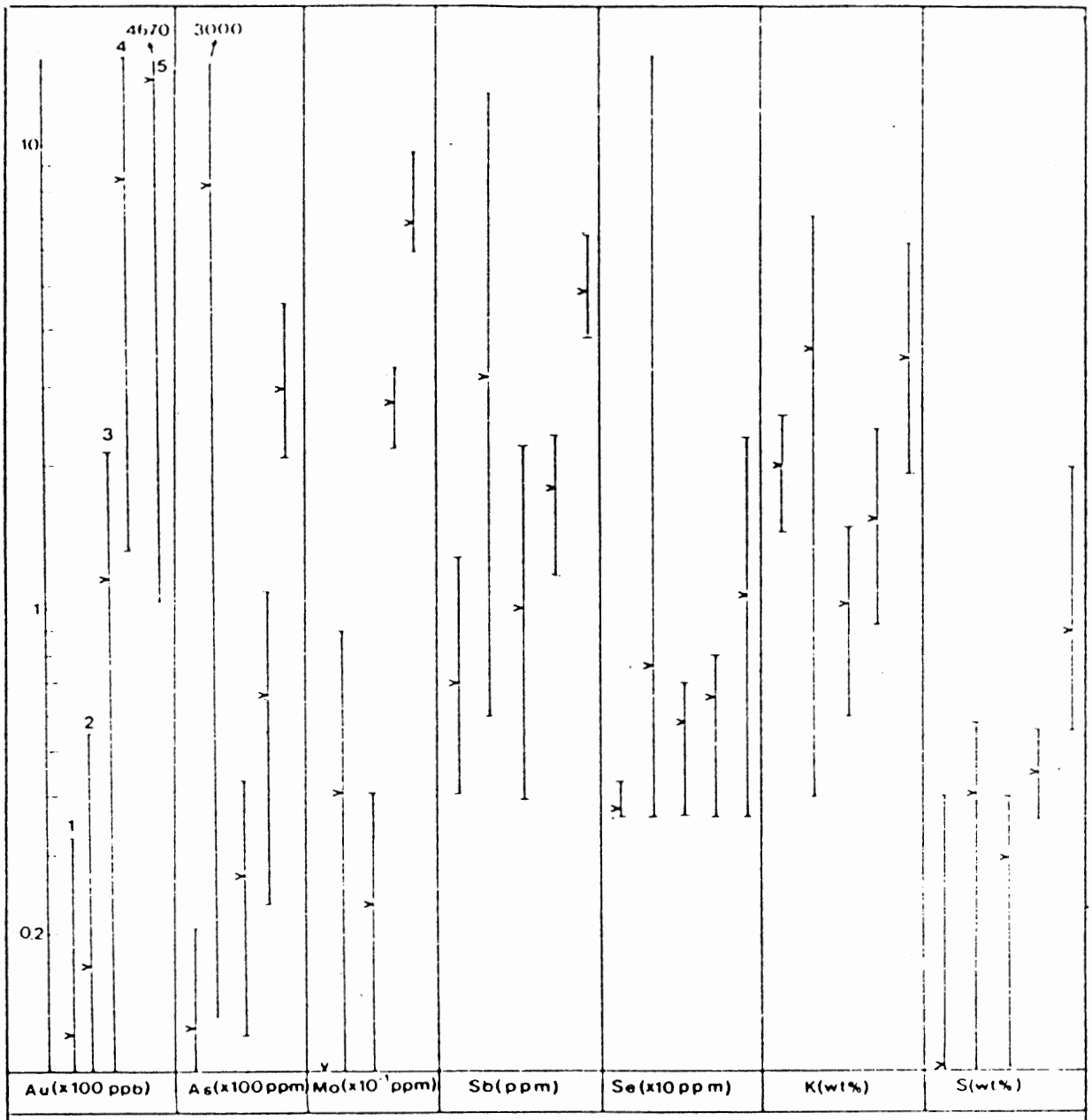

Figure V.1 Comparison of gold and other elements. Each bar represents the range of the element (in a log scale) within a rock group: 1. fresh, 2. alteration type I, 3. alteration type II, 4. alteration type III and 5. vein. The mean is indicated by the arrow.

of gold increase from 12 ppb in fresh rocks to 17, 117, 845 and 1362 ppb in the veins. Although there is no clear spatial relationship among the alteration types, it is apparent that gold concentration is higher in more altered rocks.

Veins, in which gold contents are highest, are characterized by simple mineralogy and texture. the former comprises quartz, alunite, adularia, chlorite, sericite, rutile, carbonate and opaque minerals. The latter shows a repetitively banded fillings. This characteristics is considered to be a diagnostic feature of epithermal veins (Buchanan, 1981). The sealing of these veins by aluminus/siliceous cap rocks is also a characteristic of epithermal deposits (Chapter III.3.3E).

B. Arsenic and antimony

The average and most of the individual contents of these elements in fresh rocks are higher than the values given by many authors such as Boyle and Jonasson (1973) and Levinson (1974). The characteristics of these elements from fresh to vein rocks is marked by an initial increase of concentration, followed by a decrease, then a continuous increase to vein. There are two samples containing more than 3000 ppm As and the rest is in hundreds. This is not unusual as Boyle and Jonasson (1973) point out that arsenic contents range from a few ppm to percentages in the ore shoots and their associated wall rock alteration zones. Although antimony content is somewhat higher than the normal value, its enrichment in

Plates 11 and 12. Quartz veinlets show crustified texture. Browish grains are rutile (cp).

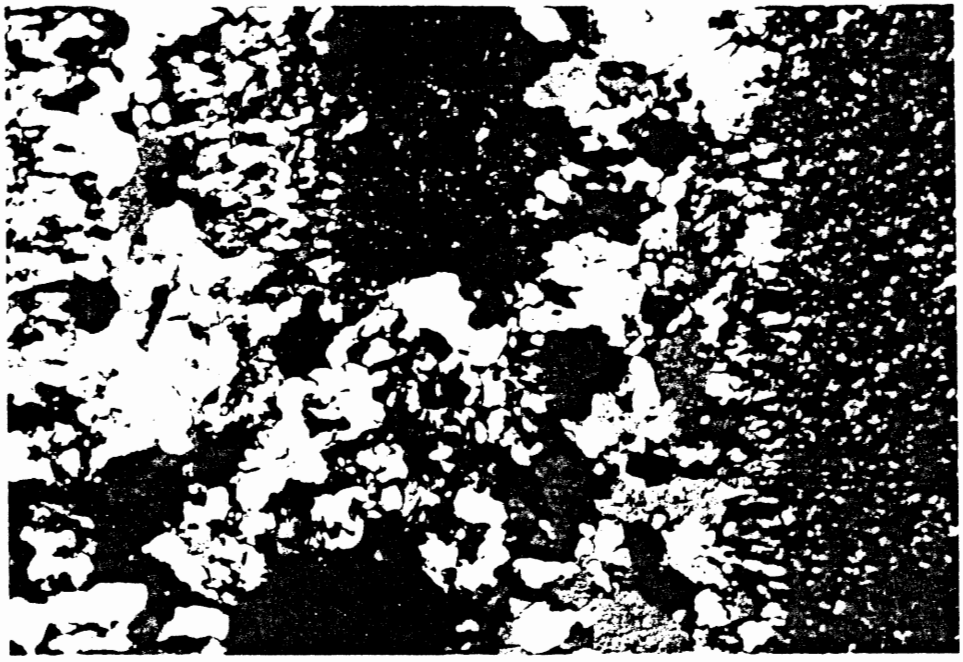

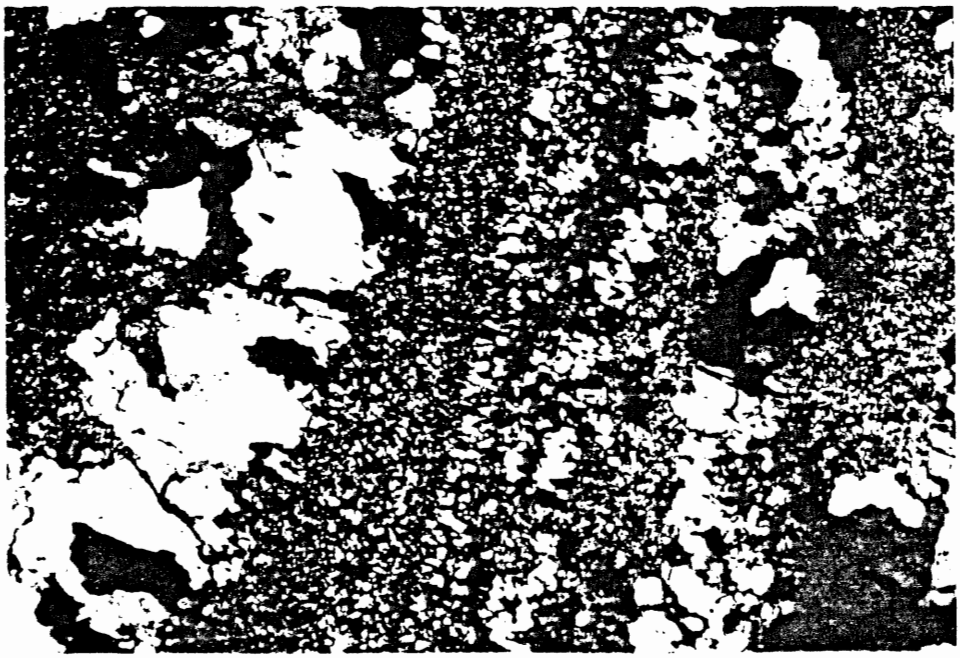

0 2mm

altered rocks is not spectacular. There are no data available yet as to the antimony contents in epithermal gold deposits.

C. Molybdenum, lead and selenium

The trend of contents of these elements in the studied rocks is similar to those of arsenic and antimony. Their average contents are 1, 11.4 and 5.2 ppm, respectively. Molybdenum value is normal, lead is somewhat lower, but selenium is much higher than the average value by a factor of 100. Levinson (1974) gives 0.05 ppm as the average selenium value in intermediate rocks. The average value in the fresh rocks in this thesis is 5.2 ppm. Molybdenum and lead contents are significantly enriched in veins.

D. Potassium and sulfur

Potassium and sulfur are characteristically similar to the other elements, except gold. Their high contents in vein rocks are necessary to form alunite, which, together with quartz, constitutes the quartz-alunite veins. The average contents of both potassium and sulfur in the veins are 3.71 and 0.54 weight percent, respectively.

5.3 Discussion.

Data on contents of gold and other elements clearly show a close association of alteration and mineralization. All element concentrations are enriched towards the more altered rocks. Studies made at various epithermal gold deposits by

many investigators indicated that, beside veins, gold concentrations of economic interest occur where the rocks have undergone appreciable alteration. Any alteration of the host rocks that would weaken or otherwise make them more porous would obviously enhance the potential of such a host for disseminated mineralization (Worthington, 1981).

Highest gold concentrations occurred in veins, suggesting that high grade mineralization is fracture-controlled in the study area. These fractures could have been a wide permeable zone through which mineralizing fluids passed unobstructed. Fracturing events must have some effects on the surrounding host rocks by causing fractures, thus making them more porous. This explains the higher gold contents and alteration intensity in rocks of alteration type III which flank the veins. Thus, the primary function of these fractures in mineralization appears to be the preparation of zones of weakness.

The formation of those fractures may be related to the volcano-tectonic events. It is generally accepted that fracturing in and around a caldera occurs during the subsidence which is due to the withdrawal of magma as a result of eruption (Williams and McBirney, 1979). Alternatively, fracturing can also occur because of resurgence, in which magmatic pressure is against the uplifting caldera floor.

Among the geochemical associations suggested by Boyle (1979), As, Pb, Mo, Sb, S and Se have significant

relationships with gold in the studied rocks. K, which is not suggested, also shows similar behaviour in this study. Silver does not appear to correlate with gold. Most epithermal gold deposits are accompanied by substantial amounts of silver. Its analytical results in the present study are suspect. A reinvestigation into the concentration of silver in the studied rocks is essential.

The association of gold with As, Sb and especially S is related to the mechanism of gold transport and deposition. Seward (1984) recogzines, besides P, T, Eh and Ph, the importance of those elements to form components which would act as ligands in complexing and transporting gold at elevated temperature and pressure. Experimental studies on thermodynamics and stability of gold indicate that sulfur-donor ligands such as HS^-, S^{--} and possibly thioarsenite ligands such as AsS^{--} (or As_2S_4) form some of the most stable complexes with gold and are effective to transport gold in hydrothermal ore solutions. Deposition of gold is related to a decrease in the solubility of the ligands. This may be accomplished by boiling, precipitation of metal sulphides, dilution and oxidation, with the latter processes being most effective (Seward, 1984). In addition, extraction of gold from aqueous solutions need amorphous arsenic and antimony sulphide sols both at high and low temperatures.

5.4 Conclusions

1. Gold mineralization in the Copiapo volcanic complex occurs in two modes: in veins and in altered rocks. Gold content is highest in veins and its concentration in altered rocks appears to be controlled by the intensity of alteration.

2. The mineralization is structurally controlled by long linear fracture systems, which may be related to volcano-tectonic events.

3. The average and range of gold content in Copiapo fresh pyroclastic rocks and lavas are higher by a factor of three than the values given for calc-alkaline andesites.

4. The style of the mineralized veins, which is banded or crustified texture and structurally sealed by cap rocks, is typically characteristic of epithermal vein.

5. Gold is associated with the following elements: As, K, Mo, Pb, S, Sb and Se, each of which can be a useful pathfinder.

6. Silver is not associated with gold in the mineralized rocks.

Chapter VI

Geochronology

6.1 Introduction

Any study on volcanogenic ore deposits is not complete without a discussion on the relationship between timing of mineralization and volcanism. The previous chapter has clearly indicated that gold mineralization in Copiapo volcanic complex is associated with hydrothermal activity. In this chapter, the writer attempts to place the events of volcanism, alteration and mineralization in a local geological context mainly on the basis of new geochronological data on five samples and of a data from Gonzalez-Ferran et al.(1985). The methods of dating are briefly outlined first, followed by results and discussions.

6.2 The K/Ar and $^{40}Ar/^{39}Ar$ dating methods

The five samples selected for this thesis were dated by the K/Ar and $^{40}Ar/^{39}Ar$ method. The following are the brief principles of those methods.

The K/Ar method of dating is one of the most important and most widely used methods of measuring the ages of K-bearing rocks and minerals such as K-feldspar, biotite, hornblende etc (Faure, 1977). This method is based upon the decay of naturally occurring ^{40}K to stable ^{40}Ar. Essentially, this involves the determination of the amounts of ^{40}K and ^{40}Ar in the rock at the present time. Given that information, the age of the mineral is given by solving the following K-Ar age equation;

$t = 1/l * \ln \{ {}^{40}Ar/{}^{40}K (l/le) + 1 \}$

where $l = le + lb$, which is the sum of the decay constants for the decay of ^{40}K to ^{40}Ar and to ^{40}Ca respectively. The $^{40}Ar/^{40}K$ ratio is calculated as follows:

$^{40}Ar/^{40}K$= Conc. K x W x A/ Conc.K x aK x WK x A,

where Conc. is the concentration of the respective elements (in ppm),

WAr, WK, is the atomic weight of Ar and K, respectively,

A is the Avogadro number, and aK is the abundance of K expressed as a decimal fraction.

There are seven assumptions in this method which must be satisfied in order that the resulting age is geologically significant. These can be found in Faure (1977).

The $^{40}Ar/^{39}Ar$ method of dating is based on the formation of ^{39}Ar by the irradiation of K-bearing samples with thermal and fast neutrons in a nuclear reactor (Faure, 1977). When a K-bearing sample is irradiated some of the K atoms are transmutted to Ar atoms by an (n, p) reaction { K (n, p) Ar }. The age of the sample is calculated from the ^{40}Ar (radiogenic)/ ^{39}Ar ratio. The age equation is given by

$t = 1/l * ({}^{40}Ar/{}^{39}Ar * J + 1)$,

where l is the total decay constant of K, and J is obtained from the following equation:

$J = e^{ltm} - 1/({}^{40}Ar/{}^{39}Ar)$, where tm is the known age of the flux monitor. Some of the advantages of this method over the K/Ar method are the elimination of the problem of inhomogeneity of samples and the need to measure the absolute concentrations of K and Ar. Details are given by Faure (1977).

6.3 Results and Discussions

The results of the radiometric dating are given in Table VI.1, including the stepwise degassing of release curves for the four samples dated by the $^{40}Ar/^{39}Ar$ dating method. Dated sample localities are shown in Figure VI.1. It is convenient to discuss the radiometric dates in two groups: biotite and alunite with ages of 13.29 $\pm$ 0.05 and 12.0 $\pm$ 0.6 Ma., respectively, and biotite and hornblende with ages ranging from 10.29 $\pm$ 0.28 to 8.59 $\pm$ 0.09 Ma.

Group 1. Biotite was extracted from an andesitic lava flow (Sample No. WZ-107-84) and yielded an Ar/Ar age of 13.29 $\pm$ 0.05 Ma. This sample is located in the north-eastern corner of the study area, which is partly bounded by the Quaternary sediments. The locality of this sample is within the Villalobos caldera in the Mercado map (1982). Thus, this lava flow is most likely an extrusion from the caldera through a volcanic vent or fracture. Alunite from the gold mineralized vein was dated in order to determine the timing of alteration and possibly gold mineralization. The K/Ar age of the alunite is 12.0 $\pm$ 0.6 Ma. Its proximal locality with the

Sample number	Rock type	Material analyzed	Temp. (°C)	mV ^{39}Ar	% ^{39}Ar	Age ± 1@(MY)		% Atmos.	% Int. Iso.
Z-68-78	D	B	150-650	20.94	3.22	17.34	1.54	93.41	0.14
			650-750	5.18	0.79	17.79	7.52	96.48	0.66
			750-850	25.77	3.96	8.21	2.29	95.14	0.10
			850-950	62.60	9.63	9.22	0.72	88.86	0.52
			950-1050	179.09	27.55	9.07	0.22	74.06	0.13
			1050-1150	356.44	54.83	8.61	0.11	69.48	0.14
Total gas age : 9.14 3.89 MY.									
WZ-16-84	A	H	200-950	69.14	14.02	2.99	0.46	98.25	4.82
			950-1050	42.12	8.54	5.47	1.00	95.12	14.71
			1050-1180	381.66	77.42	8.59	0.09	78.31	28.66
Total gas age : 7.54 4.58 MY.									
WZ-23-84	A	H	200-900	22.99	4.78	6.08	2.99	101.03	0.07
			900-1050	92.41	19.23	9.12	0.42	86.31	0.40
			1050-1100	313.00	65.14	10.09	0.23	80.81	0.45
			1100-1150	45.00	9.36	11.10	1.50	87.66	0.46
			1150-1170	7.05	1.46	20.45	7.94	96.04	0.50
Total gas age : 9.38 6.58 MY.									
WZ-107-84	A	B	200-650	29.04	2.39	5.82	1.09	97.21	0.02
			650-750	24.15	1.98	13.37	1.74	88.13	0.01
			750-850	63.77	5.24	9.70	1.06	82.15	0.00
			850-950	142.41	11.71	12.35	0.22	66.14	0.00
			950-1050	178.38	14.67	12.98	0.16	56.91	0.00
			1050-1150	777.40	63.97	13.29	0.05	47.00	0.00
Total gas age : 12.77 1.95 MY.									

Table VI.1 Radiometric data for the Copiapo volcanic rocks. Rock type, A: andesite D: dacite. Material analyzed, B: biotite, H: hornblende.

Argon analyses:

^{40*}Ar, ppm	^{40*}Ar/Total ^{40}Ar	Ave. ^{40*}Ar, ppm
.003935	.501	.004029
.004122	.289	

Potassium analyses:

% K	Ave. % K	^{40}K, ppm
4.826	4.838	5.771
4.849		

$^{40*}Ar/^{40}K = .000698$

Age = 12.0 ± 0.6 M.Y.

Table VI.1 Potassium-Argon determination of alunite, extracted from Sample number WZ-120-84 which is a quartz-alunite vein.
^{40*}Ar refers to radiogenic ^{40}Ar.
M.Y. refers to millions of years. Analytical work was carried out by Krueger Enterprises, Inc., of Cambridge, Massachusetts, USA.

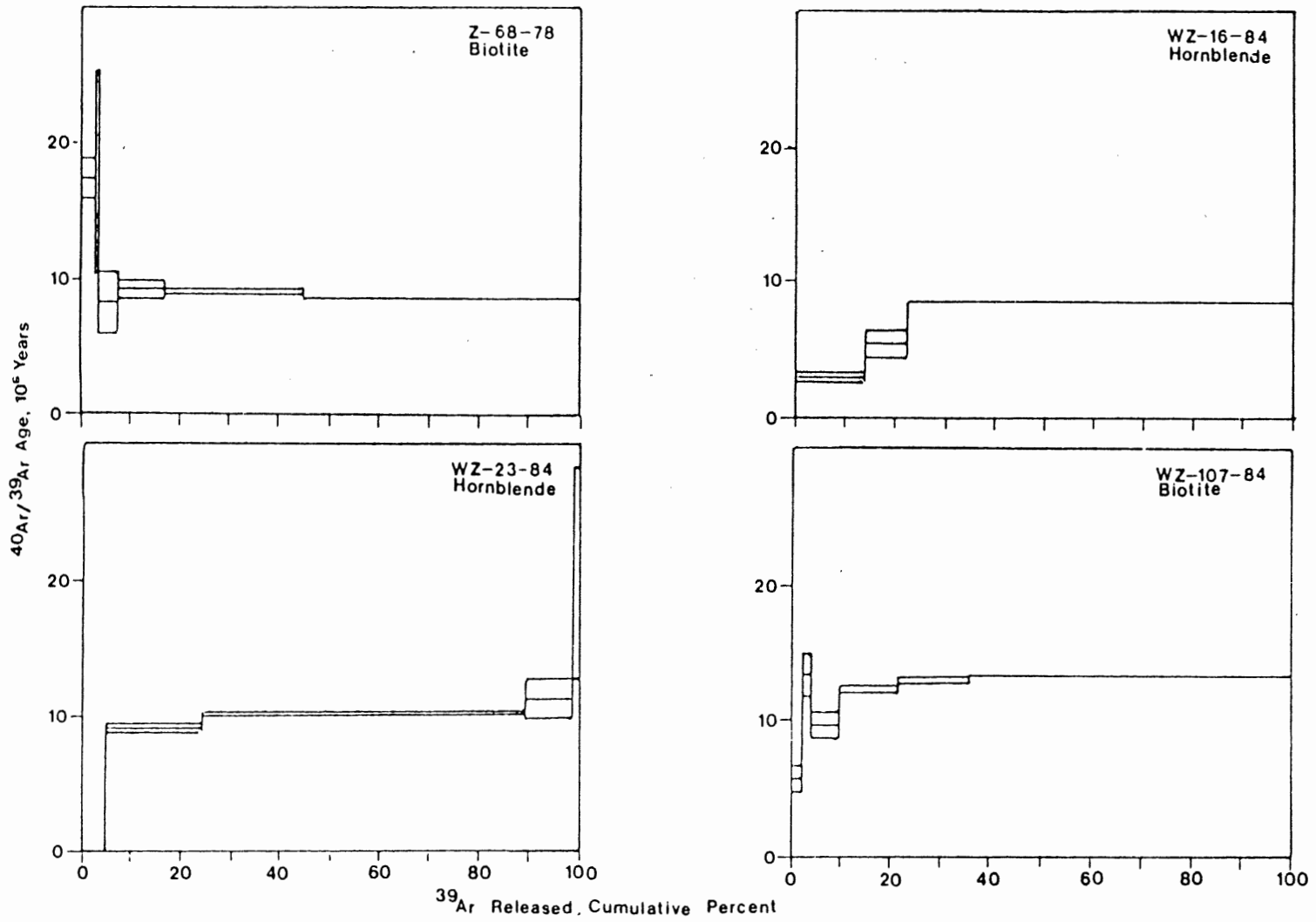

Stepwise degassing of release curves for the $^{40}Ar/^{39}Ar$ dated materials.

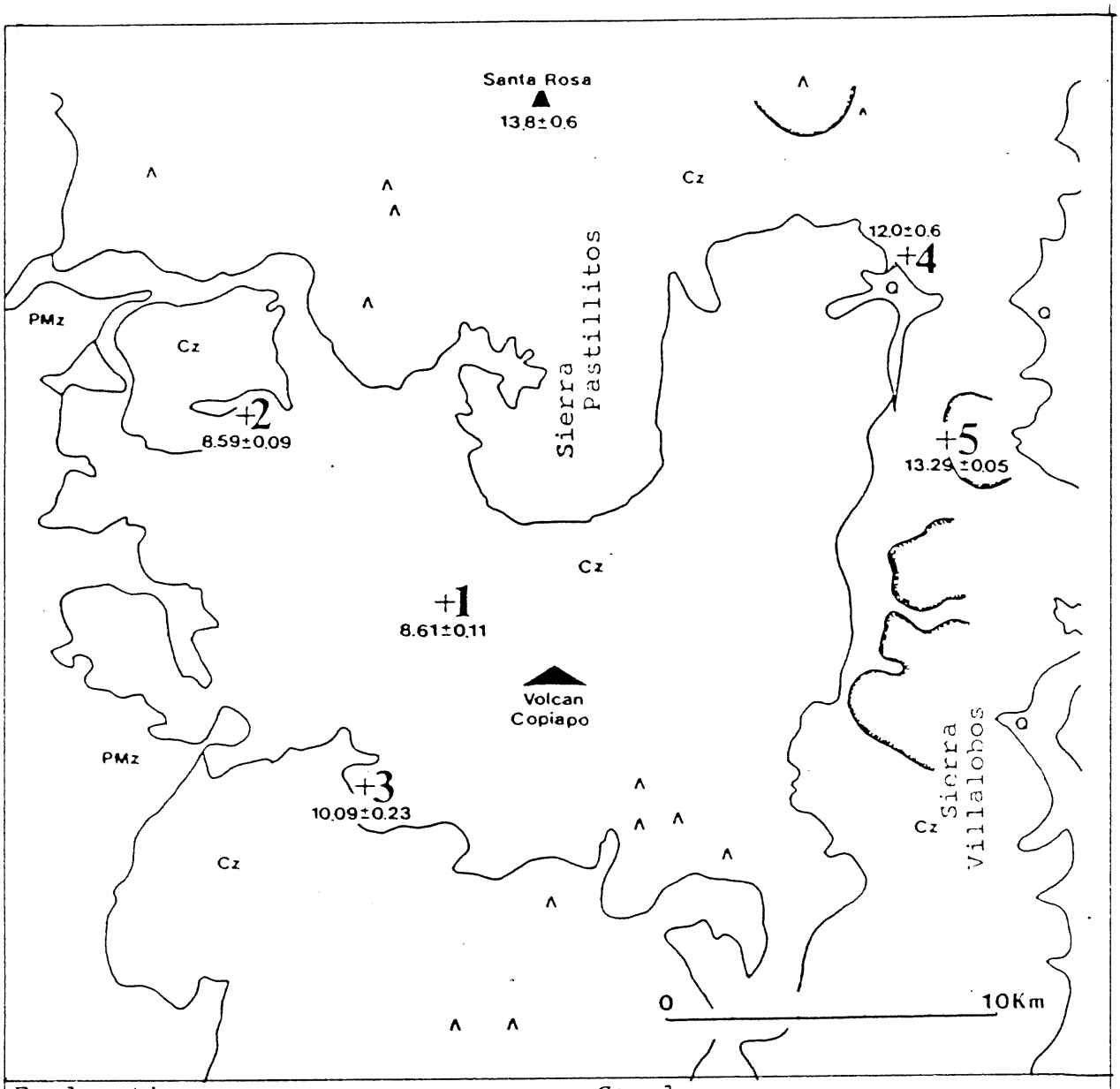

Explanation

Q : Quaternary sediments
Cz : Cenozoic volcanic rocks
PMz : Paleozoic-Mesozoic rocks
: Volcano and volcanic center
: Caldera

Sample

1.	Z-68-78	Dacite
2.	WZ-16-84	Andesite
3.	WZ-23-84	Andesite
4.	WZ-120-84	Qt-Al vein
5.	WZ-107-84	Andesite

Figure VI.1 Location map of radiometrically dated samples. Santa Rosa date is from Gonzalez-Ferran et al, 1985. Three domains of Cenozoic volcanic rocks: Volcan Copiapo, Sierra Villalobos and Sierra Pastillitos.

Pastillos caldera may be indicative of a relationship between magmatism and alteration/mineralization.

Group 2. This comprises biotite and hornblende with ages ranging from 10.09 ± 0.28 to 8.59 ± 0.09 Ma. These minerals were taken from three pyroclastic rocks adjacent to Volcan copiapo. In fact, Mercado (1982) assigns them as Volcan copiapo pyroclastic rocks. Radiometric dates from Z-68-78 (dacite) and WZ-16-84 (andesite) yield ages of 8.61 ± 0.11 and 8.59 ± 0.09 Ma., respectively. The age of the pyroclastic andesite is 10.09 ± 0.23 Ma. Thus, it is apparent that volcanism was active during the 10 to 8 Ma interval. An alteration zone (alteration type II) developed about 5 km west of the Azufre cone of the Volcan copiapo.

A relevant radiometric date is 13.8 ± 0.6 Ma which is the age of a lava flow from Volcan Santa Rosa (Gonzalez-Ferran et al., 1985).

From the data already described, a summary of the volcanic evolution, alteration and gold mineralization is summarized in Figure VI.2., and is outlined as follows.

During the pre-middle Miocene times, Copiapo volcanic complex was dominated by explosive volcanism and caldera formation. This is supported by the extensive pyroclastic deposits and by the existance of calderas, including Villalobos and possibly Volcan Copiapo. Magmatic activity was reinitiated at about 13 - 14 Ma and resulted in the

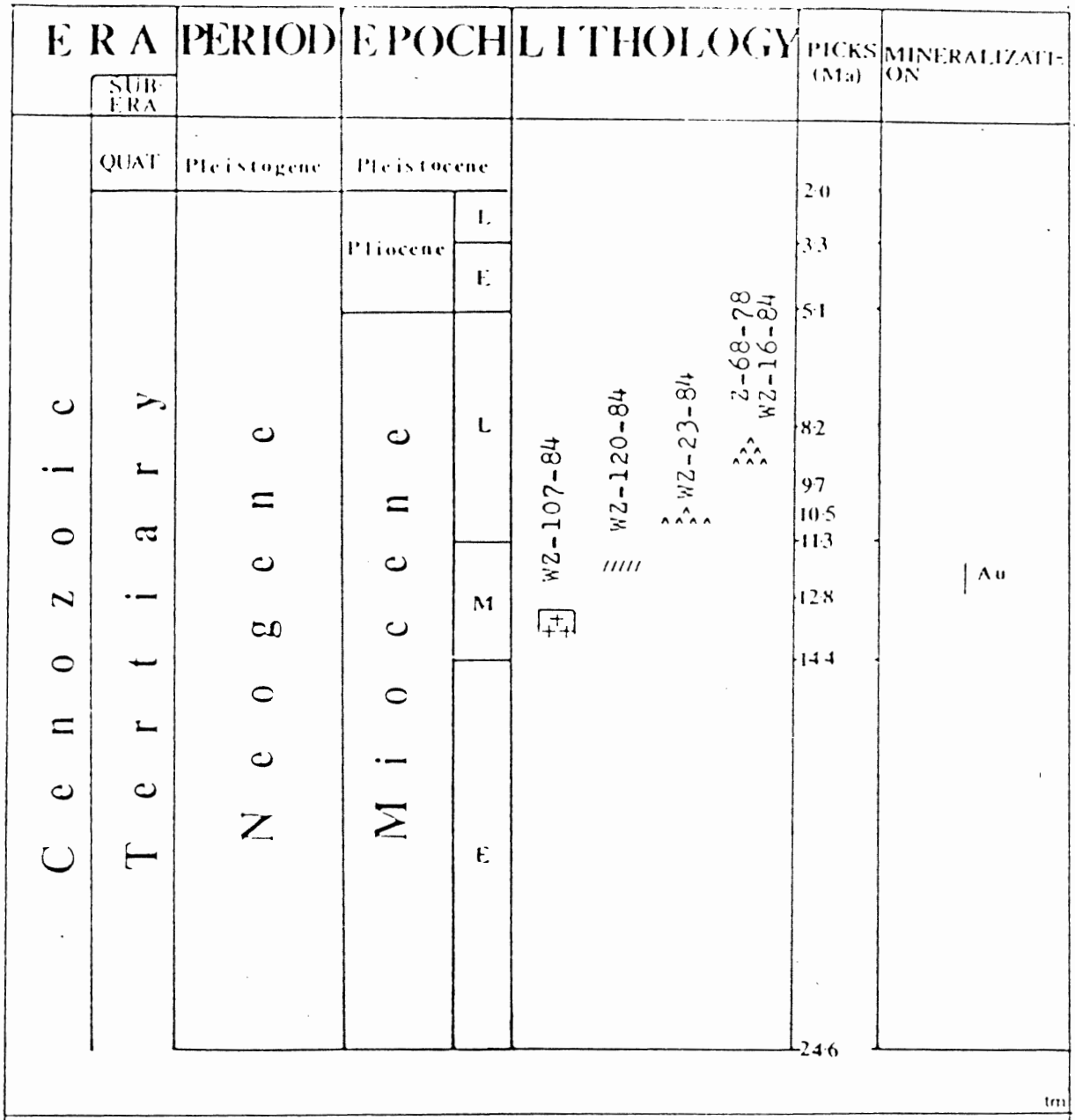

Explanation

^^^^ Pyroclastic rocks

///// Quartz-alunite vein (gold-bearing)

+ + Andesitic lava

WZ-16-84	8.59 · 0.09 Ma
Z-68-78	8.61 · 0.11 Ma
WZ-23-84	10.09 · 0.23 Ma
WZ-120-84	12.0 · 0.6 Ma
WZ-107-84	13.29 · 0.05 Ma

Figure VI.2 Proposed volcanic evolution and mineralization in the Copiapo volcanic complex.

emplacement of lava flows in Volcan Santa Rosa and in Villalobos caldera. The proximity of the location between alteration type III and Villalobos caldera suggests a possible association between the two events. The magma responsible for the eruption of the lava might also have provided heat for the convecting of water cells of meteoric origin. This could have caused hydrothermal activity around the caldera at about 12 Ma. During that event, alteration, and later gold mineralization, occurred.

To date, there is no record of volcanic or related activity having taken place in the study area between 12 or 11 Ma. Volcan Copiapo resumed its activity at 10.09 $\pm$ 0.23 Ma and continued until 8.59 $\pm$ 0.11 Ma. During those times, a powerful explosion must have taken place from Volcan Copiapo. This is evident by the extensive ignimbrites, which travelled as far as 21 kilometres from the volcanic center. This is the ignimbrite in which radiometric date yields 8.61 $\pm$ 0.11 Ma. This event can be supporting evidence as to the resurgence of Copiapo, besides the mounting of the composite Azufre cone. Alteration, which occurred in the west corner of the volcano, may be related to the final volcanic activity. It has been suggested by many authors such as Smith and Bailey (1968) who state that one of the possible final events in a resurgent caldera is the hydrothermal event. Future dating on hydrothermally altered minerals will indicate whether or not there is a relation between resurgence and alteration/mineralization. So far, there is no rock in the

complex known to be younger than 8 Ma. Walker et al. (1985) suggest that final activity in the complex was focused on Azufre cone and occurred at about 10 - 8 Ma. However, there is at least a lava flow, which seems to be recent, emplaced on the slope of Azufre cone which has not been dated yet (Zentilli, 1984).

6.4 Conclusions

The following conclusions were drawn on the basis of the already presented data in the previous sections of this Chapter.

1. Radiometric dates suggest that several events have taken place in the Copiapo volcanic complex during the last 14 Ma.: explosive volcanism, caldera formation and resurgence, alteration and mineralization. The first type of event dominated the activity.

2. Gold mineralization occurred at 12.00 $\pm$ 0.6 Ma which is about one million year after the emplacement of shallow intrusive stocks which acted as a heat source for hydrothermal solutions.

3. Copiapo volcanic complex was reactivated two million years after the mineralization. The results are the pyroclastic rocks dated 10.09 $\pm$ 0.23 Ma., 8.61 $\pm$ 0.09 Ma. and 8.59 $\pm$ 0.09 Ma.

Chapter VII

General discussion, conclusions and recommendations

7.1 General discussion

Many investigators such as Sillitoe (1977, 1983), Buchanan (1981) and others have proposed a number of geological models of epithermal precious metal deposits and alteration systems on the basis of well known deposits. This has been summarized in Chapter II. Although the present study is preliminary, however, the data presented in the previous chapters should reflect characteristics of epithermal systems. The following discussion emphasizes those characteristic features that the writer believes are of interest, and which can be considered in a generalized model.

Geologic setting and age--The Copiapo volcanic complex is situated in a Tertiary volcanic terrain.

Geologic association--Copiapo alteration/mineralization systems appear to be related to volcanism and intrusion. Host rocks are dominated by andesites.

Structural association--The alteration/mineralization systems are spatially related to the major north-south trend fracture zones, which may temporally related with caldera forming and resurgence.

Alteration patterns--Although the three alteration patterns are not yet proved to relate in time and space, their mineralogic assemblages resemble in many well known epithermal systems.

Vein system and gold--Veins flanked by alunitized rocks are an integral part of the alteration-mineralization system and also exhibit gold enrichment outward from the vein to the altered rocks. The sealed caps and crustified texture of the veins are typical features of epithermal.

Alteration-mineralization age--There seems to be a relationship between the emplacement of lava and the timing of alteration/mineralization The proximity of the latter and its younger age may be related to the latter event. Magma which emplaced the lava provided the heat source for hydrothermal activity. The ascent of this magma can be considered to be part of a resurgent event.

Gold-metal association--The association of gold with antimony and arsenic is well known in many epithermal systems.

Thus, those characteristics, which were found in the studied rocks, should in the future, shed some light on the determination of the alteration-mineralization systems in the study area.

7.2 Conclusions

The present study has given an insight into the evolution of the Copiapo volcanic complex in a broad geological scale during the last 14-15 M.a., which involved volcanism and its resulting structures, alteration and mineralization. Among the significant conclusions are as follows:

1. Three hydrothermal alteration patterns have been recognized. Each is based on the alteration mineral assemblages:

I. Montmorillonite ± jarosite ± kaolinite, II. Sericte + quartz ± kaolinite ± chlorite and III. Alunite + quartz ± dickite ± prehnite.

These alteration assemblages are restricted along the north-south trend fracture zones, but exhibit no direct relationship in space and time.

2. The presence of fine grained intrusive outcrops indicates the existence of shallow (subvolcanic) intrusives in the study area.

3. A limited number of radiometric dates on volacnic rocks and on a gold-bearing rock indicates that there are at least four major episodes of volcanic activities which led to extensive deposition of pyroclastic rocks, caldera forming and resurgence, alteration and gold mineralization. The events span 14-15 M.a.

4. Based on geologic setting and alteration/mineralization style, gold mineralization in the Copiapo volcanic complex resembles epithermal.

5. Trace elements such as arsenic, antimony, molybdenum, lead and selenium, which show positive correlations, can be pathfinders for exploration in epithermal gold.

7.3 Recommendations

Since this is a preliminary study of the current investigation into the gold metallogeny in the complex, and the results are informative and encouraging, the following work is recommended:

1. Detailed mapping of the area is a priority in order to better understand the volcanic stratigraphy and other field relations.

2. Convincing the current operating companies to support this research and to allow systematic rock sampling programs from fresh to altered/mineralized zones. This will provide detailed zonal alteration patterns and gold mineralization in the area which in turn can be guides for discovering more potential deposits in the area.

3. Radiometric dating on different lavas, altered rocks, gold-bearing rocks and shallow intrusives is necessary to understand the interactions among the many parameters.

4. Investigating the rare earth element geochemistry of the rocks will gain better understanding of the compositional variations in the volcanic rocks produced by the flatly subducted oceanic plate.

References

Abbey, S., 1983, Studies in " Standard Samples " of silicate rocks and minerals 1969-1982: Geological Survey of Canada, Paper 83-15, 30p.

Bailey, J.C., 1981, Geochemical criteria for a refined tectonic discrimination of orogenic andesites: Chemical Geology, Vol. 32, p 139-154.

Baldwin, J.A., and Pearce, J.A, 1982, Discrimination of productive and non-productive porphyritic intrusions in the Chilean Andes: Economic Geology, Vol. 77, No.3, p 664-675.

Barazangi, M., and Isacks, B.L., 1976, Spatial distribution of earthquakes and subduction of the Nazca plate beneath South America: Geology, Vol. 32, p 139-154.

Boyle, R.W., 1982, Gold deposits: a review of their geological and geochemical setting, in Geology of Canadian gold deposits, CIM special volume 24, p 1-8.

Boyle, R.W., and Jonasson, I.R., 1973, The geochemistry of arsenic and its use as an indicator element in geochemical prospecting: Journal of geochemical exploration, Vol. 2, p 251-296.

Buchanan, L.J., 1981, Precious metal deposits associated with volcanic environments in the Southwest, in Relations of tectonics to ore deposits in the Southern Cordillera, Edited by W.R. Dickenson and W.D. Payne, Arizona geological society digest, Vol. XIV, p 237-255.

Burke, P., 1978, Opaque mineralogy of a suite of Cenozoic volcanic rocks from the Andes at lat. 27 S, unpublished BSc Honours thesis, Dalhousie University, halifax, N.S., Canada, 51p.

Caelles, J. C., 1979, The geological evolution of the Sierras Pampeanas, La Rioja and Catamarca provinces, Argentina: Ph.D. thesis, Queen's University, Kingston, Ontario.

Caelles, J. C., Clark, A.H., Farrar, E., McBride, S. L., and Quirt, G. S., 1971, Potassium-argon agesof porphyry copper deposits and associated rocks in the Farallon Negro-Capillatas district, Catamarca, Argentina: Econ. Geol., v.66, p 961-964.

Canas, P.M.T., 1982, Mapa geologica de Chile, Hoja No.2 de 6, 24 00-30 30 Lat. S., escala 1:1,000,000., Servicio Nacional de Geologica y Mineria.

Clark, A. H., and Zentilli, M., 1972, The evolution of a metallogenic province at a consuming plate margin : the Andes between 26 and 29 south [abs.]: Canadian Mining Metal Bull.,v.65, p 37.

Colman, S.M., 1982, Chemical weathering of basalts and andesites: evidence from weathering rinds: USGS Prof. paper 1246, 44p.

Corning, J., 1974, Chilean calc-alkaline rocks from 27 south lat., unpublished BSc Honours thesis, Dalhousie University, Halifax, N.S., Canada, 50p.

Cox, K.G., Bell, J. D., and Pankhurst, R. J., 1979, The interpretation of igneous rocks, George Allen & Unwin ltd., London, 450p.

Dostal, J., Zentilli, M., Caelles, J. C., and Clark, A. H., 1977, Geochemistry and origin of volcanic rocks of the Andes (26 - 28 S): Contrib. Mineral. Petrol., Vol. 63, p 113-128.

Evans, A.M., 1980, An introduction to ore geology: geoscience text Vol.2, Elsiever, N.Y., 227p.

Farrar, E., Clark, A. H., Haynes, S. J., Quirt, G. S., Conn, H., and Zentilli, M., 1970, K-Ar evidence for the post Paleozoic migration of granitic intrusive foci in the Andes of northern Chile: Earth Planet. Sci. Letters, Vol. 10, p 60-66.

Faure, G., 1977, Principles of isotope geology, John Wiley and sons, Inc, Chapters 9 and 10.

Finlow-Batesand, T., and Stumpfl, E.F., 1981, The behaviour of so-called immobile elements in hydrothermally altered rocks associated with volcanogenic submarine exhalative ore deposits: Mineralium deposita, Vol. 16, No.2, p 319-328.

Floyd, P.A., and Winchester, J.A., 1978, Identification and discrimination of altered and metamorphosed volcanic rocks using immobile elements: Chemical Geology, 21, p 291-306.

Francis, P.W., 1983, Giant volcanic calderas: Scientific American, 248(6), p 46-56.

Giles, W., and Hallberg, J.A., 1982, The genesis of the archean welcome volcanic complex, western Australia: Contributions to mineralogy and petrology, Vol. 80, p 307-318.

Gill, J.B., 1981, Orogenic andesites and plate tectonics, springer Verlag, Berlin, 387p.

Gonzalex-Ferran, O., Baker, P.E and Rex, D.C., 1985, Tectonic-volcanic discontinuity at latitude 27 south Andean range, associated with Nazca plate subduction: Tectonophysics, Vol. 112, p 423-441.

Grensens, R.L., 1967, Composition-volume relationships of metasomatism: Chemical Geology, 2, p 47-65.

Hallberg, J.A., 1984, A geochemical aid to igneous rock type identification in deeply weathered terrain: Journal of geochemical exploration, 20, p 1-8.

Haynes, S. J., 1975, Granitoid petrochemistry, metallogeny, and lithospheric plate tectonics, Atacama Province, Chile: Ph.D. thesis, Queens's University, Kingston, Ont., 331 p.

Harvey, R.D., and Vitaliano, C.J., 1963, Wall-rock alteration in the Gold field district, Nevada: Geology, , p 546-579.

Hemley, R.W., and Jones, W.R., 1964, Chemical aspects of hydrothermal alteration with emphasis on hydrogen metasomatism: Economic Geology, Vol. 59, p 538-569.

Hemley, R.W., and Ellis, A.J., 1983, Geothermal systems ancient and modern: a geochemical review: Earth Science Reviews, 19, p 1-50.

Krauskopf, K.B., 1979, Introduction to geochemistry, 2nd edition, McGraw-Hill Book Comp., 601p.

Kuno, H., 1968., Origin of andesite and its bearing on the island arc structure: Bulletin Volcanology, Vol. 32, p 141-176.

Lacy, W.C., 1974, Porphyry copper deposits: Australian mineral foundation inc., Adelaide, Australia., 300p.

Levinson, A.A., 1974, Introduction of exploration geochemistry, 2nd edition, Applied Publ., Ltd., Wi;;mette, Ill., USA., 571p.

Lortie, R. L., and Clark, A. H., 1974, Stratabound, fumarolic, copper deposits in rhyolitic lavas and ash flow tuffs, Copiapo district, Atacama, Chile: Problems of ore deposition, 4th I.A.G.O.D. Symposium, Varna, Bulgaria, Vo. 1, p 256-264.

Marsh, B., 1984, On the mechanics of caldera resurgence: Journal of geophysical reserach, Vol. 89, No. B10, p 8245-8251.

Mason, B., 1966, Principles og geochemistry, 3rd edition, John Wiley & Son, N.Y., 329p.

McBride, S. L., 1972, A potassium-argon age investigation of igneous and metamorphic rocks from catamarca and La Rioja Provinces, Argentina: M.Sc. thesis, Queen's University, Kingston, Ont., 101 p.

McBride, S. L., Caelles, J. C., Clark, A. H., and Farrar, E., 1976, Paleozoic radiometric age provinces in the Andean basement, Lat. 25-30 S: Earth Planet. Sci. Letters, Vol. 29, p 373-383.

McNutt, R.H., Clark, A. H., and Zentilli, M., 1979, Lead isotopic compositions of Andean igneous rocks, latitudes 26 to 29 S: petrologic and metallogenic implications: Econ. Geology, Vol. 74, No.4, p 827-837.

Mercado, P., 1982, Mapa de Geologica, Hoja Copiapo, escala 1:100,000.

Palma, V.C., 1976, Geochemical variations along unpublished Bsc Honours thesis, Dalhousie University, Halifax, Nova Scotia, Canada, 70p.

Quirt, G. S., 1972, A potassium-argon geochronological investigation of the Andes mobile belt of North-Central Chile: Ph.D. thesis, Queen's University, Kingston, Ontario, 240 p.

Roberts, R.G., and Reardon, E.J., 1978, Alteration and ore forming processes at Mattagami Lake mine, Quebec, Canadian Journal of Earth Sciences, Vol. 15, No.1, p 1-21.

Rose, A.W., and Burt, D.M., 1979, Hydrothermal alteration, in hydrothermal ore deposits, edited by Barnes, L.H., p 173-235.

Schwartz, G.M., 1959, Hydrothermal alteration: Econ. Geology, Vol. 54, No.2, p 161-183.

Seward, T.M., 1984, The transport and deposition of gold in hydrothermal systems, in Gold '82: The geology, geochemistry and genesis of gold deposits, edited by R.P. Foster, Geological Survey of Zimbabwe, Special publication No.1, p 165-179.

Segerstorm, K., 1968, Geologia de las Hojas Copiapo y Ojos del Salado, Provincia de Atacama : Inst. Invest. Geol. Bull., 24:58.

Sillitoe, R.H., 1976, Metallic mineralization affiliated to subareal volcanism; a review, in Volcanic processes in ore genesis: The Inst. Mining and Metallurgy, The Geological Society of London, p 99-114.

Sillitoe, R.H., and Bonham Jr., H.F., 1984, Volcanic landforms and ore deposits: Economic Geology., Vol. 79, No.6, p 1286-1298.

Smith, R.L., and Bailey, R.A., 1968, Resurgent cauldrons, in Coats, R.R., et al., Studies in volcanology, Memoir 116, GSA, 678p.

Taylor, S.R., 1962, The application of trace element data to problems in petrology, in Physics and chemistry of the earth, Vol.6., p 133-213.

Thorpe, R.S. (Editor), 1984, Andesite: Orogenic andesites and related rocks, John A. Wiley, Toronto, 724p.

Vikre, P.G., 1985, Precious metal vein systems in the National District, Himbolt County, Nevada: Economic Geology, Vol. 80, No.2, p 360-393.

Walker, J., and Zentilli, M., 1984, Proposal for research grant, unpublished report, 14p.

Walker, J., Fuss, D., and Zentilli, M., 1985, Neogene volcanism in the Central Andes (26 - 28 S), IGCP project 120, magmatism of the Andes, Santiago, Chile, unpublished report, 4p.

Williams, H., and McBirney, A.R., 1979, Volcanology, Freeman, Cooper and Son, San Francisco, 395p.

Worthington, J.E., 1981, Bulk tonnage gold deposits in volcanic environments: Arizona geological society digest, Vol.XIV, p 263-270.

Zentilli, M., 1974, Geological evolution and metallogenic relationships in the Andes of northen Chile between 26 and 29 south, unpublished Ph.D thesis, Queen's University, Kingston, Ont, Canada, 460p.

Zentilli, M., and Dostal, J., 1977, Uranium in volcanic rocks from the central Andes: Jour. Volcanol. Geothermal Research, Vol.2 (1977), p 251-258.

Appendix I

Analytical methods for major element determination

Analytical methods for major element determination

(i) Si, Al, Mn, Ca, Fe (total), K and Na.

These elements were analyzed by the Atomic Absorption Spectrophotometry method, using a Perkin-Elmer, Model 530 AAS unit. Si and Al were determined by a nitrous oxide-acetylene flame while the rest by an air-acetylene flame.

Method of solution

-weigh as nearly as 0.1000 grm of rock powder (minus 100 mesh) into a digestion flask (polycarbonate centrifuge bottle, Nalgene cataloque number 3122).

-add 5 ml. concentration of HF (using Nalgene precise volume dispenser number 3700 and wearing safety hand gloves).

-place the flask on a boiling steam bath for 30 minutes (any residue should be white. If black residue remains weight out a new sample and add 1 ml. HCl and 1 ml. HNO_3 along with the HF and treat as above. add only 143 ml. distilled water afterwards).

-remove from heat and when cool add, using a measuring cylinder, 50 ml. of saturated Boric Acid solution. This solution is made as follows: weight 200 grm Boric Acid crystals. Add about 1600 ml. distilled water and heat untill dissolved. Dilute to 2 liters while still hot and store in gallon polythylene bottles.

-place back on steam bath until solution is clear .

-remove and cool. Tranfer solution to a 200 ml. volumetric flask, using a funnel and rinsing bottle 3 times with distilled water. Shake and make volume to 200 ml.

-This soluton now can be used for all the analyses.

Sample Analyses

Transfer some of the 200 ml. solution into small vials (50 ml.). Using the settings given in the A.A. instrument cook book for each element, all the analyses are done as the sample solution was made up except CaO and MgO which need further dilution.

MnO, for example:

Run standards to get rough readings for % Absorption. Get reading for sample and then the standard just lower than the sample, then the sample, and then using the next highest standard. To work out the % MnO in the sample the following formula was used.

Percentage (%) of MnO = A + B x C x D, where
A = ppm in low std.,
B = { (%A sample - % AL std.) / (%AH std. - % AL std.) }.,
C = ppm H std. - ppm L std. and D = 2/10.

(ii) CaO and MgO

Pipette 5 ml. sample solution into a 50 ml. vol. flask, add 10 ml. of Lanthanum oxide solution. Make up to 50 ml. mark with distilled water. Lanthanum oxide solution is made by : suspend 58.7 grm. spec. pure La_2O_3 in 250 ml. distilled water, carefully add 250 ml. conc. HCl. When all dissolved and cool make up to 1000 ml. in vol. flask using conc. HCl. The standard blend solutions are made up in the same way as above.

(iii) Phosphorous

Phosphorous was analysed colorimetrically. 5 ml. of sample solution was pitteted into a 50 ml. vol. flask especially prepared for this element analysis. Add 20 ml. of combine reagent solution (3N H_2SO_4, ammonium molybdate, ascorbic acid and distill water) and dilute to 50 ml. with distilled water. Measurements were made on a Bausch and Lomb Spectric 70 Spectrophotometer at 827 nm using 4 cm cells. Reagent blank readings were subtracted from each sample reading, and the results were averaged.

(iv) FeO

Weigh about 0.2 grm rock powder and transfer it to a small plastic flask. Add 5 ml. of 0.1 N ammonium vanadate and 10 ml. of HF. Place on shaker overnight. Add 10 ml. Acid mixture (H_2SO_4 + H_3PO_4) to each flask and swirl to mix. Transfer contents of flask to beaker containing 100 ml. of 5

% Boric acid solution. Rinse flask and top 3 times using 100 ml. Boric acid; add rinsings to beaker. Add 10 ml. Fe (NH_4) (SO_4)$_2$ to beaker from auto pipet. Titrate with N/20 $K_2Cr_2O_7$ (after adding more or less 15 drops of indicator) to a purple end point. Fe_2O_3 was obtained by substracting FeO (titration) from total Fe (A.A).

(v) H_2O-

Dry weighing bottles for 2 hours or overnight; cool in dessicator for 20 minutes; weigh empty with lid; put about 0.5 grm rock powder; weigh again. Dry for 2 hours at 105-110 degree celcius; cool in dessicator for 20 minutes and weigh.

Sample calculation

Bottle + sample : 18.5381 grm
Bottle + lid : 18.0371 grm
grm of rock : 0.5010 grm.
Before drying 18.5381 grm
after drying 18.5371 grm, thus loss during drying is 0.0010 gr

H_2O- percentage (%) = 0.0100 x 100 / 0.5010 .

(vi) Total H_2O

Dry penfield tubes and long funnels for 2 hours or overnight. Weigh 2.5 grm. flux and store in dessicator; weigh accurately about 0.5 grm. rock powder and store outside dessicator. Samples were weighed same day as the analysis. Mix sample and flux on large weighing paper; transfer to

bottlom bulb of penfield tube using the long funnel; Wrap double bulbs in wet cloth (in distilled water) after connecting a tube with capillary end. Put on top of a beaker with ice and water.

Heat bottom bulb over small flame of the blast burner for 10 minutes; increase the flame and heat for 3 minutes more. Cut the lower bulb off using a torch sealing the tube leave the sealed part on the beaker for 5 minutes.

Remove the wet cloth. Rinse with acetone to get rid of the water on the outer surface of the tube. Store on a metal tray for at least 5 minutes. Weigh , using the metal triangle. Dry at least for an hour in the oven at 105-110 degrees celcius. Cool on the metal tray for 10 minutes and weigh again using the triangle.

Total H_2O (%) = (wt of tube before drying - wt of tube after drying) x 100/ wt. of rock sample.

H_2O+ is obtained by substracting Total H_2O by H_2O-.

Accuracy and consistency of chemical analyses

Element	Standard value	Obtained value	Accuracy (%)
Method : A.A.S (rock standards : AGV-1 and BCR-1).			
SiO_2	59.61	58.50	98
	54.53	54.08	99
Al_2O_3	17.19	16.26	95
	13.72	13.00	95
FeO (t)	6.78	6.61	97
	13.41	13.03	97
MgO	1.52	1.50	99
	3.48	3.53	99
MnO	0.10	0.08	80
	3.53	3.48	97
CaO	4.94	5.10	97
	6.97	7.15	97
K_2O	2.92	2.72	93
	1.70	1.53	90
Method: X.R.F (rock standard : AGV-1)			
Rb	67	65	97
Ba	1200	1216	97
Sr	660	639	97
V	125	139	90
Cr	10	8	80
Ni	15	17	88
Zr	230	231	99
Cu	59	56	95
TiO_2 (%)	1.06	1.17	91
Method: N.A.A (rock standard : W-1)			
Au	5	4.3	86
Ag	<2	0.81	-
As	0.9	1.9	47
Sb	0.8	1.0	80
Se	<5	0.11	-
Mo	1	0.75	75

Rock standard values for A.A.S and X.R.F analyses are taken from Abbey, S., 1983. Rock standard values for N.A.A. are from " Geostandard Newsletter " Special issue, Govindaraju, K., Vandoeuvre-Les Nancy, FRA (Editor-in Chief), Volume III, July, 1984.

Consistency of analysis (sample duplication)

X.R.F

	GHT-20	GHT-38	% deviation
Ba	564	547	3.53
Rb	51	50	1.97
Sr	69	66	4.35
Y	43	42	2.33
Zr	155	155	0.00
Nb	12	11	8.34
Th	10	8	20.00
Pb	9	6	33.34
Ga	24	25	4.00
Zn	166	168	1.20
Cu	47	36	23.41
Ni	116	105	9.49
Ti	1.15	1.16	0.87
V	183	189	3.18
Cr	114	105	7.90

N.A.A

	GHT-274	GHT-281	
Au	21	19	9.53
As	34	38	10.53
Ag	<2	<5	-
Sb	12.2	13.7	10.95
Se	<5	<5	-
Mo	2	3	33.34
Co	30	33	9.10

Appendix II

Petrography

Petrographic description of studies rocks were carried out by the writer, using a simple student microscope. The textural terms used in this thesis follow those stated in the Igneous Petrology Laboratory Manual by Clarke, D.B. and Eddy, A.C. (1973), revised by Jamieson, R.A. (1980)*.

The grain size categories are as follows;

Coarse : > 5 millimetres diameter

Medium : 1 - 5 millimetres diameter

Fine : < 1 millimetre diameter.

* Unpublished, Department of Geology, Dalhousie University, 66p.

Sample No. WZ-16-84

Rock Name : Andesitic Ignimbrite

Texture : Porphyritic, hypocrystalline.

ROCK TYPE: Fresh and welded ignimbrite.

HANDSPECIMEN : This is a pinkish grey, medium grained rock. Very coarse crystals of hornblende and biotite (up to four millimetres long) are present. Few sulphide specks (brassy yellow color) are visible.

THIN SECTION : This is a medium-fine grained andesitic ignimbrite, containing phenocrysts of subhedral to euhedral plagioclase (An-?). These crystals show an oscillatory zoning pattern and also occur as groundmass. Some have reaction rims with the glassy groundmass. Other phenocrysts include biotite and hornblende. The latter show a greenish brown pleochroism. Subhedral clino-and orthopyroxene are prersent. opaque minerals are pyrite.

Sample No.: WZ-18-84

Rock name : Altered Andesite

Texture : Porphyritic (relict), holocrystalline

ROCK TYPE: Completely altered and partly oxidized rock with well preserved relict textures of former rock (porphyritic)

HAND SPECIMEN : This is an altered rock with whittish relicts of phenocrysts set in a very pale yellow groundmass. The rock is cut by numerous veinlets, ranging from a few millimetres to half centimetres and containing quartz and adularia. Oxidation occurs along the contact between the veinlets and host rock.

THIN SECTION : The relict of porphyritic texture which is well preserved in the hand specimen is not well defined in the section. All feldspar phenocrysts were altered into finely aggregated sericite and kaolinite. The latter is confirmed by X-ray diffraction. The groundmass consists of fine grained quartz and of feldspar microlets. Quartz and adularia aggregates form the veinlets.

Sample No : WZ-19-84

Rock name : Tuff

Texture : Microbreccia(hand specimen), hypocrystalline

ROCK TYPE : Extensively altered tuff with few pebble size clasts.

HAND SPECIMEN : This is a whittish medium grained rock, containing few pebble size and smaller clasts which indicate a volcaniclastic origin.

THIN SECTION : The rock is almost completely altered in which no original mineralogy remains. There is a rather poorly preserved relict texture which suggests the presence of former phenocrysts. The former glassy matrix was altered into fine bright green and yellow materials. Most phenocrysts are altered into isotopic materials.

Sample No.: WZ-20-84

Rock name : Diorite

Texture : Porphyritic, holocrystalline

ROCK TYPE: slightly altered intrusive rock.

HAND SPECIMEN : This is a fresh greenish grey, medium grained size intrusive rock, containing phenocrysts of feldspar and hornblende. Altered feldspars are characterized by yellowish green color.

THIN SECTION: The rock partly consists of secondary alteration products such as sericite and chlorite, phenocrysts of plagioclase (An 40-56, andesine to labradorite) and pseudomorphs. The phenocrysts are medium grained, subhedral and euhedral, showing lamellar zoins. Groundmass consists of very fine and massive feldspar and sericite. Alteration includes sericitization, and chloritization after biotite pseudomorphs of amphiboles by opaque minerals.

Sample No. WZ-21-84

Rock name : Altered diorite

Texture : Porphyritic (relict), holocrystalline

ROCK TYPE: Extensively altered intrusive rock with well preserved relict of original porphyritic texture.

HAND SPECIMEN: This is an altered diorite which still displays porphyritic texture. The original phenocrysts are mostlikely feldspar and mafics. The color of the rock is yellowish grey.

THIN SECTION: The rock consists entirely of secondary alteration products. The groundmass consists of fine plagioclase, sericite and chlorite. Porphyritic texture is the relict of plagioclase and other phenocrysts. Biotite was altered to chlorite which displays greenish pleocroism. Plagioclase was altered to sericite.

Sample No. WZ-22-84

Rock name : Altered andesite

Texture : porphyritic, hypocrystalline

ROCK TYPE : Moderately altered rock with poorly preserved relict texture of a former volcanic porphyry.

HAND SPECIMEN : This is a very light grey, partly altered medium grained rock. It is cut by tiny (~ 1 mm) veinlets. The mineralogy is not recognizable except the altered feldspar.

THIN SECTION : This is a moderately altered dacite in which its former porphyritic texture is not well preserved. Phenocrysts of plagioclase were all altered to fine grained sericite and kaolinite. Few quartz grains and coarse amphibole prisms are also present. The latter is replaced by opaque oxides. The groundmass consists of glass and minor secondary minerals such as sericite and chlorite. The veinlets which cut the rock comprise fine to medium quartz and adularia.

Sample No. WZ-23-84

Rock name : Ignimbrite

Texture : Porphyritic, hypocrystalline

ROCK TYPE: Welded ignimbrite

HAND SPECIMEN: This is a light brownish grey, medium grained rock. Mafic minerals such as biotite and hornblende are also phenocrysts.

THIN SECTION : This rock consists of predominantly medium grained, anhedral to subhedral plagiocalse phenocrysts set in a glassy matrix. Biotite and hornblende are predominant maifc minerals. Few tiny pyroxene crystals are also present. All mafics are subhedral to anhedral. Some opaque minerals are also present. Inclusions and zoning occur on plagioclase phenocrysts.

Sample No. WZ-24-84

Rock name : Ignimbrite (andesitic)

Texture : Porphyritic, hypocrystalline

ROCK TYPE : Similar to WZ-23-85

HAND SPECIMEN : This is a medium light grey, slightly altered volcaniclastic rock, containing long prisms of hornblendes and biotites. Vesicles occupy about 5 % in volmue of the rock. Fine plagioclase crystals are visible.

THIN SECTION: The rock consists of plagioclase phenocrysts and hornblende prisms set in a plagioclase microlite and glassy groundmass. The plagioclase crystals are fragmental and show twinning and oscillatory zoning pattern. K-feldspar are also present. Hornblendes occur as subhedral to anhedral phenocrysts and show a greenish brown to red brown pleocroism. Other minor minerals such as enstatite are also present.

Sample No. WZ-25-84

Rock name : Silica cap

Texture : Massive

ROCK TYPE: Siliceous or silicified rock consists of quartz , opaline and other silicas.

HAND SPECIMEN : This is a very light grey silica rock which almost entirely comprose silica minerals. A few specks of pyrite are present.

THIN SECTION : This is a silicified rock in which the former relict texture, porphyritic, is still preserved. The relicts show rectangular shape of former crystals which might be of feldspar phenocrysts replaced by silica mineral aggregates.

Sample No. WZ-26-84

Rock Name : Andesitic lava

Texture : Porphyritic, hypocrystalline

ROCK TYPE : Solid and slightly oxidized andesitic lava.

HAND SPECIMEN : This is a medium dark grey andesite in which some vesicles are partly filled by hydrous minerals, zeolite. Slight oxidation produced a fine red brown margin.

THIN SECTION : This is a porphyritic andesite, consisting of plagioclase (An 38-56), hornblende and pyroxene set in glass and lath plagioclase groundmass. The laths are oriented in the flow direction. Some of the plagioclase phenocrysts show myrmekitic texture, lamellar and partial melt zoning patterns. Hornbledes are partly pseudomorphs by oxides.

Sample No. WZ-29-84

Rock name : altered volcanic

Texture : Massive

ROCK TYPE : Completely altered rock in which no original minerals remain.

HAND SPECIMEN : This is an extensively altered lithology with

fairly well preserved relict texture of a former volcanic rock. It is pinkish grey and fine grained. Oxidation is high as indicated by staining layers in the rock.

THIN SECTION : The rock almost entirely consists of volcanic glass and isotopic feldsphatoids (?). The former is partly altered into massive shards of montmorillonite. The latter is fragmental. There are also very fine grains of high birefringence.

Sample No. WZ-30-84

Rock name : Tuff

Texture : Hypocrystalline, aphanitic

ROCK TYPE : Partly altered and oxidized pyroclastic rock with white and blue clasts in pinkish groundmass.

HAND SPECIMEN: This is a pale pink pyroclastic rock containing very light grey clasts. It is fine grained and welded.

THIN SECTION : The rock is moderately altered and oxidized lithology in which only medium size plagioclase fragments can be recognized. The groundmass consists of glass and was partly altered to montmorillonite and fine bright green and yellow materials. Clays replace feldspar minerals.

Sample No. WZ-31-84

Rock Name : Ignimbrite

Texture :

ROCK TYPE: Completely altered oxidized pyroclastic rocks.

HAND SPECIMEN : It is a greyish yellow fine grained rock with tiny whittish minerals distributed evenly.

THIN SECTION :Not available

Sample No. WZ-31a-84

Rock name : Lapilli Breccia

Texture : Aphanitic, hyporystalline

ROCK TYPE : Moderately altered and extensively oxidized rock which consists of feldspars and opaque oxides.

HAND SPECIMEN : This is a greyish orange pink fine grained rock comprising clasts from few mm to about one cm long. Vesicles are also present.

THIN SECTION : This is a moderately and oxidized rock containing medium size fragments of feldspars. The matrix consists of glass. Alteration involves devitrification of glass.

Sample No. WZ-32-84

Rock Name : Tuff

Texture : Porphyritic, hypocrystalline

ROCK TYPE : Slightly altered pyroclastic rocks.

HAND SPECIMEN: This is a very light grey, massive and fine grained rock. It is not well welded and contains many tiny vesicles.

THIN SECTION: The rock is slightly altered and mainly comprises of broken feldspars. The glassy groundmass was altered to montmorillonite while the feldspar to kaolinite (confirmed by X-ray diffraction analyses).

Sample No. WZ-33-84 and WZ-34-84

Rock name : Lapili Breccia

Texture : Porphyritic, hypocrystalline

ROCK TYPE: Moderately altered and oxidized pyroclastic rocks.

HAND SPECIMEN: This is a light brown and fine grained rock with rounded to angular white clasts up to 4 cm in diameter. The margin between the clasts and the host is reddish. WZ-34-84 is oxidized more intensely.

THIN SECTION : The rocks are altered breccias comprising anhedral and fragmental plagioclase , smooth-edge quartz and fine grained k-feldspar. The matrix is glassy. Plagioclase averages less than 1 mm long and show normal zoning. Part of the glass is devitrified.

Sample No. WZ-35-84

Rock name : Lapilli Breccia

Texture : Porphyritic, hypocrystalline

ROCK TYPE : Moderately altered and oxidized pyroclastic rock.

HAND SPECIMEN: This is a very pale orange and altered breccia containing white clasts which occupy 30 % of the rock and range in size from 1 cm to 5 cm in diameter. The clasts are subrounded and angular. Vesicles are small and take up to 20 % of the rock.

THIN SECTION : The rock comprises broken plagioclase and K-feldspar phenocrysts. Minor minerals are opaque oxides. The groundmass is glass which is partly devitrified.

Sample No. WZ-36-84

Rock name : Breccia

Texture : Hypocrystalline

ROCK TYPE : Moderatly latered and oxidized quartz-feldspar pyroclastic rock.

HAND SPECIMEN : Is is a fine grained welded pyroclastic rock containing coarse clasts. Oxidation formed a greyish orange (iron-rich) layer while the other part is very light grey.

THIN SECTION : The rock consists of fragmental plagioclase laths (< 2 mm). Very fine aggregates of quartz are also present. the glassy groundmass is partly devitrified. Alteration produced montmorillonite.

Sample No. WZ-40-84

Rock Name : Andesite

Texture : Porphyritic, hypocrystalline

ROCK TYPE : Solid porphyritic andesite with vesicles (< 10 %).

HAND SPECIMEN : This is a medium dark grey porphyritic andesite with mafic phenocrysts clearly visible in hand specimen. The rock is slightly oxidized, but only confined to marginal part.

THIN SECTION : The rock comprises plagioclase, hornblende and pyroxene as the major constituents. The groundmass consists of tiny plagioclase microlites and glass. Plagioclase phenocrysts are anhedral to subhedral and show corroded texture. No An content can be determined. Some show reaction rim along the edges. Some hornblende are rimmed by oxide opaques. Pyroxene minerals are hypersthene and augite.

Sample No. WZ-107-84

Rock name : Biotite-hornblende andesite.

Texture : Porphyritic, hypocrystalline

ROCK TYPE : Fresh and solid andesitm with vesicles (~10%).

HAND SPECIMEN : Is is a porphyritic andesite with feldspar and mafic phenocrysts clearly visible in hand specimen. The rock is medium grey with slightly oxidized vesicles.

THIN SECTION : This is a biotite-hornblende andesite comprising plagioclase phenocrysts, coarse biotite and hornblende prisms and few pyroxene. The matrix consists of feldspar microlites and glass. Plagioclase phenocrysts are anhedral to subhedral and have corroded texture. A single biotite, slightly altered, measures 1 cm long. Hornblendes and biotites are anhedral to subhedral and some are rimmed by opaques. Hornblende shows greenish brown to reddish brown pleocroism.

Sample No. WZ-114-84

Rock name : Ignimbrite (Dacitic)

Texture : Porphyritic, hypocrystalline

ROCK TYPE : Solid porphyritic rock with minor oxidation.

HAND SPECIMEN : This is a medium grey rock with plagioclase and mafics predominating the mineralogy. Quartz is minor. Vesicles are filled by late stage minerals.

THIN SECTION : The rock is slightly altered and its plagioclase phenocrysts show corroded texture. Alteration occurs along the marginal contact with the groundmass. Mafics are rimmed by opaque oxides. Enstatite and augite are also present. The groundmass consists of glass and plagioclase microlites.

Sample No. WZ-117-84

Rock Name : Altered andesite

Texture : Porphyritic (relict), holocrystalline

ROCK TYPE : Completely altered porphyritic rock and is cut by tiny veinlets.

HAND SPECIMEN : This is a medium grey porphyritic rock containing altered white colored phenocrysts. The rock is hard and silicified.

THIN SECTION : The rock is completely altered in which no original minerals remain. The original texture, porphyritic, is preserved as relict. Fine grained dickite aggregates replace phenocrysts. Groundmass consists of dickite, quartz and plagioclase microlites. The veinlets, 2 cm wide, consists of quartz and adularia.

Sample No. WZ-118-84

Rock Name : Quartz-alunite vein

Texture : Massive

ROCK TYPE : Vein with numerous very pale yellow minerals forming tiny veinlets.

HAND SPECIMEN : This is a medium grey and very pale yellow vein. The vein bordering with silicified porphyritic lithology. The yellowish veinlets range from few mm to 1/2 cm wide.

THIN SECTION : Quartz and adularia form crustified texture in the vein and veinlets. The very pale yellow minerals are alunite which are fine grained, massive and low birefringence. The silicified rock is porphyritic.

Sample No.WZ-119-84

Rock name : Silica Cap

Texture : massive

ROCK TYPE: Solid, yellow and hard amorphous capping rock.

HAND SPECIMEN: This is the so called capping rock, which is characterized by amorphous minerals and quartz grains. The latter replaces pre-existing minerals.

THIN SECTION: The whole rock consists of aphanitic materials and of minor quartz and rutile grains. The former has low birefringence and forms pepper-like texture. Replacement is extensive, especially by quartz. Some rutile and quartz aggregate to form " veinlets ".

Sample No. WZ-120-84

Rock name : Alunite-quartz vein

Texture : massive

HAND SPECIMEN: This vein shows alterating small bands of grey quartz and yellow amorphous minerals. White alunite is also present.

THIN SECTION : This vein consists of aphanitic minerals which form the groundmass, of sericite, quartz and rutile. The aphanitic materials show low birefringence, pepper-like texture, colorless and replacing former phenocrysts. They might be dickite or halloysite. Sericite flakes also replace phenocrysts.

Sample No. WZ-121-84

Rock name : Altered andesite

Texture : Porphyritic, holocrystalline

ROCK TYPE : Completely altered lithology with fairly well preserved texture (relict) of a porphyritic rock.

HAND SPECIMEN : This is a medium grey and strongly altered porphyry. The white phenocryst relict ranges from 2 to 3 mm long.

THIN SECTION : The rock is an extremely altered lithology in which no original minerals remain. The original phenocrysts were altered to prehnite, which shows its typical bow-tie structure. The average dimension is 3 x 2 millimetres. The groundmass consists of interlocking fine quartz and other minerals.

Sample No. WZ-122-84

Rock name : Quartz-alunite vein

Texture :

ROCK TYPE : Alunitized quartz vein containing very pale yellow veinlets.

HAND SPECIMEN : This is a vein rock in which alunite grew in the fractures forming clayed veinlets. The quartz vein is medium grey. The rock also contains about 5 % of black patches of unknown minerals.

Sample No. WZ-128-84

Rock name : Andesite

Texture : Porphyritic, hypocrystalline

ROCK TYPE : Solid andesitic flow

HANDSPECIMEN : This is a medium dark grey andesite with phenocrysts of plagioclase clearly visible.

THIN SECTION: This is a porphyritic andesite, composing plagioclase phenocrysts, biotite, pyroxene and opaque minerals in a glassy groundmass. Most of feldspar phenocrysts show sieve texture. Twinning is poorly developed. Most crystals are anhedral to subhedral.

Appendix III

X-Ray Diffraction patterns of clay minerals

Identification of some clay minerals by X-ray diffraction was carried out by the writer in the Department of Geology, Dalhousie University, using a Phillips X-Ray Diffractometer.

The following are the setup of the X-ray diffractometer:

Radiation	: copper alpha
Filter	: nickel
Kv/mA	: 40/20
Scan Speed	: 1/2 degree per minute
Chart speed	: 1 cm per minute
Range (C.P.S)	: 1 x 1000 for natroalunite, chlorite and kaolinite.
	: 2 x 400 for jarosite and dickite.

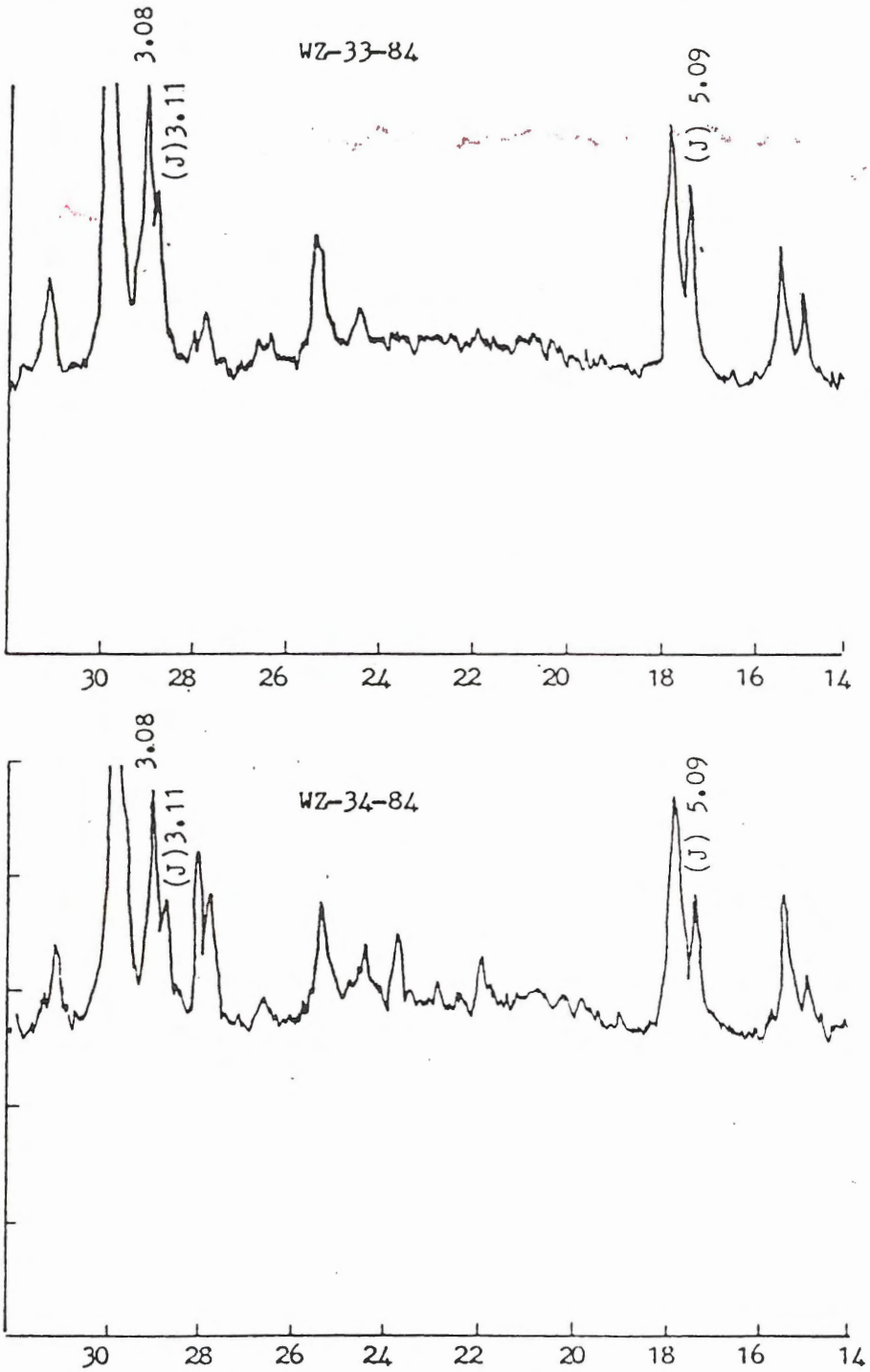

Jarosite pattern

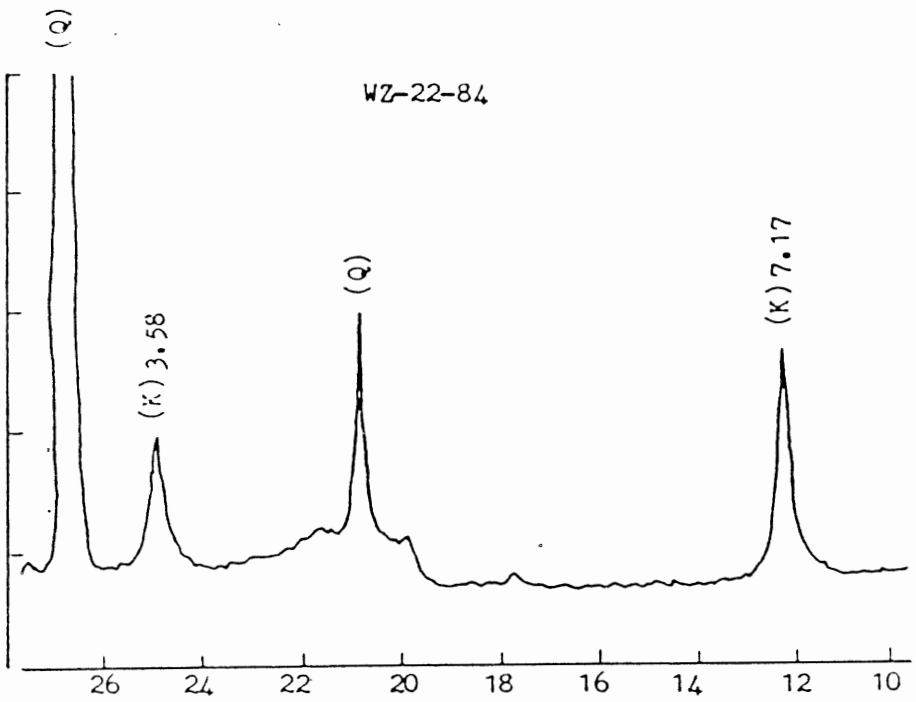

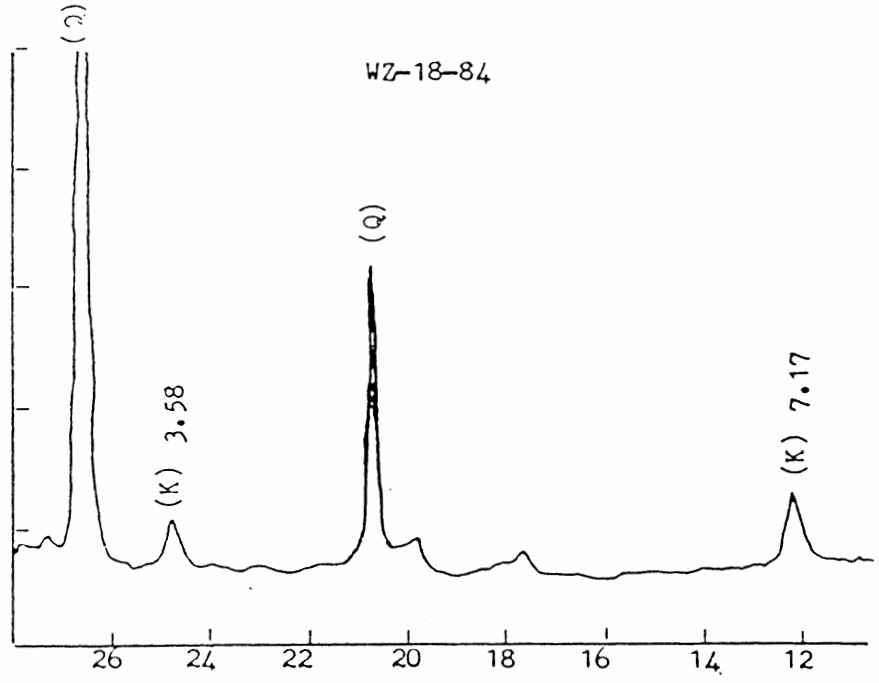

Kaolinite pattern

K: Kaolinite, Q: Quartz

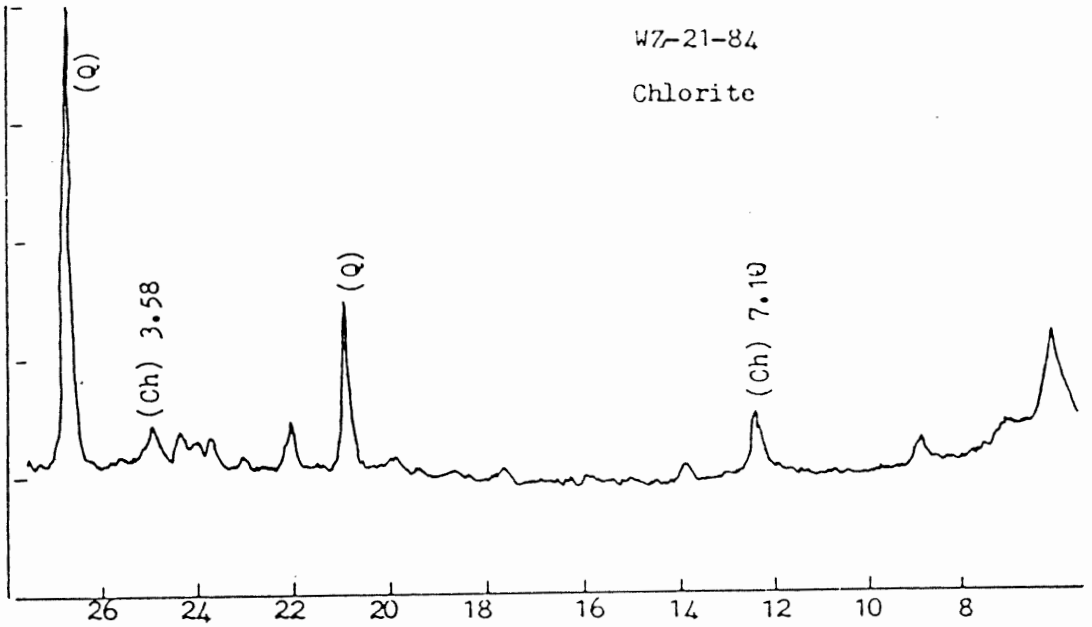
WZ-21-84
Chlorite
(Q)
(Ch) 3.58
(Q)
(Ch) 7.10
26
24
22
20
18
16
14
12
10
8

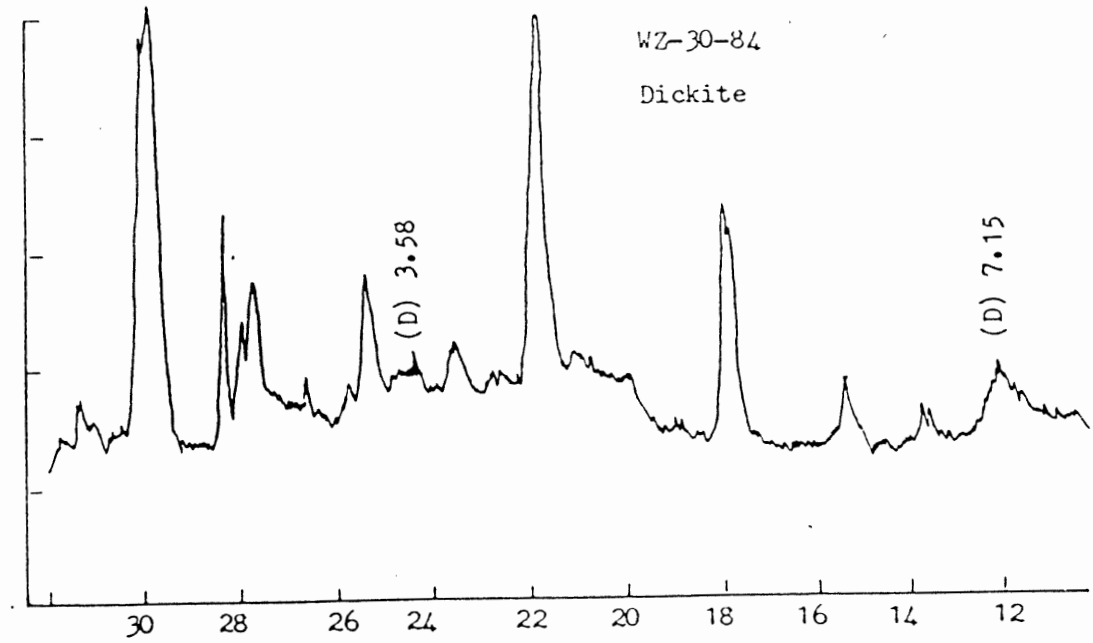
WZ-30-84
Dickite
(D) 3.58
(D) 7.15
30
28
26
24
22
20
18
16
14
12

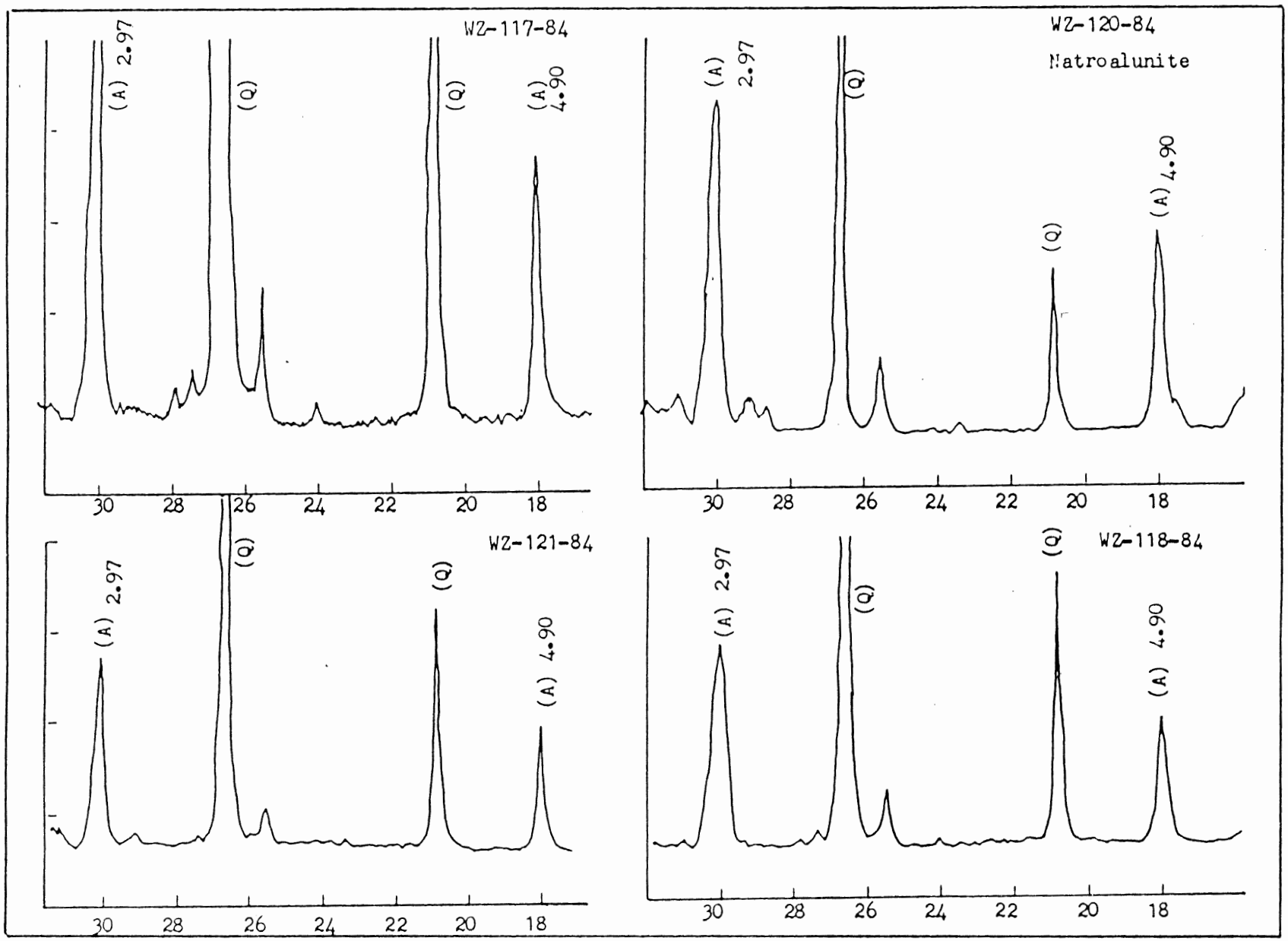
WZ-117-84
(A) 2.97
(Q)
(Q)
(A) 4.90
30 28 26 24 22 20 18
WZ-120-84
Natroalunite
(A) 2.97
(Q)
(Q)
(A) 4.90
30 28 26 24 22 20 18
WZ-121-84
(A) 2.97
(Q)
(Q)
(A) 4.90
30 28 26 24 22 20 18
WZ-118-84
(A) 2.97
(Q)
(Q)
(A) 4.90
30 28 26 24 22 20 18

Appendix IV

Method of calculation for elemental gains and losses

This method is after that of Coleman (1982), who introduces the Ti-constant method which does not require the volume factor. The constant element, Ti (or any other element), must nevertheless be proved to be immobile. The weight of each elemetal oxide in the altered rocks is calculated by multiplying its weight percentage by the ratio of the weight percentage of Ti in the fresh rock to that in the altered rock; i.e.

Gain or loss = { [Ti(f)/Ti(a)] x E(a) } - E(f),

where E(f) is the element in fresh rock, Ti(f) is the Ti in fresh rock, Ti(a) is the Ti in altered rock and E(a) is the element in altered rock. The resulting value in the brackets is the recalculated value of the element in the altered rock.

The calculated values are equivalent to the amount remaining after the alteration of 100 gr of fresh rock. The resulting calculation for each altered rock is given in the following pages.

	Fresh Analyses	Altered Analyses	Recalculated Values	Gains or Losses (-)
Si	.60410E+2	.500500E+02	.387179E+02	-.216921E+02
Ti	.82000E+0	.106000E+01	.820000E+00	-.355271E-14
Al	.17570E+2	.117000E+01	.905094E+00	-.166649E+02
Fe	.49600E+1	.315300E+02	.243911E+02	.194311E+02
Mn	.80000E-1	.100000E-01	.773585E-02	-.722642E-01
Mg	.26000E+1	0.	0.	-.260000E+01
Ca	.56300E+1	.100000E+00	.773585E-01	-.555264E+01
Na	.38900E+1	.280000E+00	.216604E+00	-.367340E+01
K	.20500E+1	.500000E-01	.386792E-01	-.201132E+01
P	.26000E+0	.253000E+01	.195717E+01	.169717E+01
H*	.32000E+0	.132100E+02	.102191E+02	.989906E+01
Rb	.64000E+2	.700000E+01	.541509E+01	-.585849E+02
Ba	.66800E+3	.784000E+03	.606491E+03	-.615094E+02
Sr	.72100E+3	.400000E+02	.309434E+02	-.690057E+03
Cu	.31000E+2	.360000E+02	.278491E+02	-.315094E+01
WZ-19-84				
Si	.60410E+2	.463200E+02	.404068E+02	-.200032E+02
Ti	.82000E+0	.940000E+00	.820000E+00	-.355271E-14
Al	.17570E+2	.104000E+01	.907234E+00	-.166628E+02
Fe	.49600E+1	.355000E+02	.309681E+02	.260081E+02
Mn	.80000E-1	.100000E-01	.872340E-02	-.712766E-01
Mg	.26000E+1	0.	0.	-.260000E+01
Ca	.56300E+1	.500000E-01	.436170E-01	-.558638E+01
Na	.38900E+1	.500000E-01	.436170E-01	-.384638E+01
K	.20500E+1	.400000E-01	.348936E-01	-.201511E+01
P	.26000E+0	.274000E+01	.239021E+01	.213021E+01
H*	.32000E+0	.133000E+02	.116021E+02	.112821E+02
Rb	.64000E+2	.600000E+01	.523404E+01	-.587660E+02
Ba	.66800E+3	.769000E+03	.670830E+03	.282979E+01
Sr	.72100E+3	.380000E+02	.331489E+02	-.687851E+03
Cu	.31000E+2	.420000E+02	.366383E+02	.563830E+01
WZ-29-84				
Si	.60410E+2	.495100E+02	.688105E+02	.840050E+01
Ti	.82000E+0	.590000E+00	.820000E+00	-.355271E-14
Al	.17570E+2	.230800E+02	.320773E+02	.145072E+02
Fe	.49600E+1	.489000E+01	.679627E+01	.183627E+01
Mn	.80000E-1	.100000E-01	.138983E-01	-.666100E-01
Mg	.26000E+1	0.	0.	-.260000E+01
Ca	.56300E+1	.410000E+00	.569830E+00	-.506016E+01
Na	.38900E+1	.249000E+01	.346067E+01	-.429322E+00
K	.20500E+1	.367000E+01	.510068E+01	.305067E+01
P	.26000E+0	.210000E+00	.291864E+00	.318644E-01
H*	.32000E+0	.162500E+02	.225847E+02	.222647E+02
Rb	.64000E+2	.820000E+02	.113966E+03	.499661E+02
Ba	.66800E+3	.528000E+03	.733830E+03	.658305E+02
Sr	.72100E+3	.708000E+03	.984000E+03	.263000E+03
Cu	.31000E+2	.170000E+02	.236271E+02	-.737288E+01
WZ-30-84				

Si	.60410E+2	.730500E+02	.809473E+02	.205373E+02
Ti	.82000E+0	.740000E+00	.820000E+00	-.710543E-14
Al	.17570E+2	.320000E+01	.354595E+01	-.140241E+02
Fe	.49600E+1	.128300E+02	.142170E+02	.925703E+01
Mn	.80000E-1	.100000E-01	.110811E-01	-.689189E-01
Mg	.26000E+1	0.	0.	-.260000E+01
Ca	.56300E+1	.80000E-1	.886486E-01	-.554135E+01
Na	.38900E+1	.210000E+00	.232703E+00	-.365730E+01
K	.20500E+1	.311000E+01	.344622E+01	.139622E+01
P	.26000E+0	.830000E+00	.919730E+00	.659730E+00
H*	.32000E+0	.595000E+01	.659324E+01	.627324E+01
Rb	.64000E+2	.170000E+02	.188378E+02	-.451622E+02
Ba	.66800E+3	.792000E+03	.877622E+03	.209622E+03
Sr	.72100E+3	.806000E+03	.893135E+03	.172135E+03
Cu	.31000E+2	.130000E+02	.144054E+02	-.165946E+02

WZ-31-84

Si	.60410E+2	.473000E+02	.969650E+02	.365550E+02
Ti	.82000E+0	.400000E+00	.820000E+00	-.355271E-14
Al	.17570E+2	.253400E+02	.519470E+02	.343770E+02
Fe	.49600E+1	.734000E+01	.150470E+02	.100870E+02
Mn	.80000E-1	.100000E-01	.205000E-01	-.595000E-01
Mg	.26000E+1	0.	0.	-.260000E+01
Ca	.56300E+1	.720000E+00	.147600E+01	-.415400E+01
Na	.38900E+1	.269000E+01	.551450E+01	.162450E+01
K	.20500E+1	.694000E+01	.142270E+02	.121770E+02
P	.26000E+0	.560000E+00	.114800E+01	.888000E+00
H*	.32000E+0	.874000E+01	.179170E+02	.175970E+02
Rb	.64000E+2	.820000E+02	.168100E+03	.104100E+03
Ba	.66800E+3	.456000E+03	.934800E+03	.266800E+03
Sr	.72100E+3	.106300E+04	.217915E+04	.145815E+04
Cu	.31000E+2	.360000E+02	.738000E+02	.428000E+02

WZ-31a-84

Si	.60410E+2	.645300E+02	.912321E+02	.308221E+02
Ti	.82000E+0	.580000E+00	.820000E+00	-.355271E-14
Al	.17570E+2	.201000E+02	.284172E+02	.108472E+02
Fe	.49600E+1	.265000E+01	.374655E+01	-.121345E+01
Mn	.80000E-1	.100000E-01	.141379E-01	-.658621E-01
Mg	.26000E+1	.780000E+00	.110276E+01	-.149724E+01
Ca	.56300E+1	.170000E+00	.240345E+00	-.538966E+01
Na	.38900E+1	.362000E+01	.511793E+01	.122793E+01
K	.20500E+1	.297000E+01	.419897E+01	.214897E+01
P	.26000E+0	.400000E-01	.565517E-01	-.203448E+00
H*	.32000E+0	.561000E+01	.793138E+01	.761138E+01
Rb	.64000E+2	.880000E+02	.124414E+03	.604138E+02
Ba	.66800E+3	.506000E+03	.715379E+03	.473793E+02
Sr	.72100E+3	.463000E+03	.654586E+03	-.664138E+02
Cu	.31000E+2	.200000E+01	.282759E+01	-.281724E+02

WZ-32-84

Si	.60410E+2	.490200E+02	.788165E+02	.184065E+02
Ti	.82000E+0	.510000E+00	.820000E+00	-.355271E-14
Al	.17570E+2	.180200E+02	.289733E+02	.114033E+02
Fe	.49600E+1	.132200E+02	.212557E+02	.162957E+02
Mn	.80000E-1	.100000E-01	.160784E-01	-.639216E-01
Mg	.26000E+1	0.	0.	-.260000E+01
Ca	.56300E+1	.460000E+00	.739608E+00	-.489039E+01
Na	.38900E+1	.152000E+01	.244392E+01	-.144608E+01
K	.20500E+1	.713000E+01	.114639E+02	.941392E+01
P	.26000E+0	.121000E+01	.194549E+01	.168549E+01
H*	.32000E+0	.895000E+01	.143902E+02	.140702E+02
Rb	.64000E+2	.610000E+02	.980784E+02	.340784E+02
Ba	.66800E+3	.493000E+03	.792667E+03	.124667E+03
Sr	.72100E+3	.226200E+04	.363694E+04	.291594E+04
Cu	.31000E+2	.400000E+02	.643137E+02	.333137E+02

WZ-33-84

Si	.60410E+2	.445200E+02	.629421E+02	.253207E+01
Ti	.82000E+0	.580000E+00	.820000E+00	-.355271E-14
Al	.17570E+2	.222400E+02	.314428E+02	.138728E+02
Fe	.49600E+1	.140100E+02	.198072E+02	.148472E+02
Mn	.80000E-1	.100000E-01	.141379E-01	-.658621E-01
Mg	.26000E+1	.100000E-01	.141379E-01	-.258586E+01
Ca	.56300E+1	.580000E+00	.820000E+00	-.481000E+01
Na	.38900E+1	.247000E+01	.349207E+01	-.397931E+00
K	.20500E+1	.605000E+01	.855345E+01	.650345E+01
P	.26000E+0	.32000E+0	.452414E+00	.192414E+00
H*	.32000E+0	.909000E+01	.128514E+02	.125314E+02
Rb	.64000E+2	.660000E+02	.933103E+02	.293103E+02
Ba	.66800E+3	.506000E+03	.715379E+03	.473793E+02
Sr	.72100E+3	.104000E+04	.147034E+04	.749345E+03
Cu	.31000E+2	.460000E+02	.650345E+02	.340345E+02

WZ-34-84

Si	.60410E+2	.555200E+02	.892675E+02	.288575E+02
Ti	.82000E+0	.510000E+00	.820000E+00	-.355271E-14
Al	.17570E+2	.230900E+02	.371251E+02	.195551E+02
Fe	.49600E+1	.512000E+01	.823216E+01	.327216E+01
Mn	.80000E-1	.100000E-01	.160784E-01	-.639216E-01
Mg	.26000E+1	.190000E+00	.305490E+00	-.229451E+01
Ca	.56300E+1	.970000E+00	.155961E+01	-.407039E+01
Na	.38900E+1	.361000E+01	.580431E+01	.191431E+01
K	.20500E+1	.379000E+01	.609373E+01	.404373E+01
P	.26000E+0	.240000E+00	.385882E+00	.125882E+00
H*	.32000E+0	.651000E+01	.104671E+02	.101471E+02
Rb	.64000E+2	.630000E+02	.101294E+03	.372941E+02
Ba	.66800E+3	.569000E+03	.914863E+03	.246863E+03
Sr	.72100E+3	.103400E+04	.166251E+04	.941510E+03
Cu	.31000E+2	.240000E+02	.385882E+02	.758824E+01

WZ-35-84

Si	.60410E+2	.557100E+02	.543836E+02	-.602643E+01
Ti	.82000E+0	.840000E+00	.820000E+00	-.355271E-14
Al	.17570E+2	.173900E+02	.169760E+02	-.594048E+00
Fe	.49600E+1	.160500E+02	.156679E+02	.107079E+02
Mn	.80000E-1	.100000E-01	.976190E-02	-.702381E-01
Mg	.26000E+1	.100000E-01	.976190E-02	-.259024E+01
Ca	.56300E+1	.240000E+00	.234286E+00	-.539571E+01
Na	.38900E+1	.303000E+01	.295786E+01	-.932143E+00
K	.20500E+1	.497000E+01	.485167E+01	.280167E+01
P	.26000E+0	0.	0.	-.260000E+00
H*	.32000E+0	.818000E+01	.798524E+01	.766524E+01
Rb	.64000E+2	.550000E+02	.536905E+02	-.103095E+02
Ba	.66800E+3	.536000E+03	.523238E+03	-.144762E+03
Sr	.72100E+3	.161400E+04	.157557E+04	.854571E+03
Cu	.31000E+2	.590000E+02	.575952E+02	.265952E+02

WZ-36-84

Si	.60410E+2	.75910E+2	.616299E+02	.121990E+01
Ti	.82000E+0	.101000E+01	.820000E+00	-.355271E-14
Al	.17570E+2	.159700E+02	.129657E+02	-.460426E+01
Fe	.49600E+1	.790000E+00	.641386E+00	-.431861E+01
Mn	.80000E-1	.100000E-01	.811881E-02	-.718812E-01
Mg	.26000E+1	.150000E+00	.121782E+00	-.247822E+01
Ca	.56300E+1	.900000E-01	.730693E-01	-.555693E+01
Na	.38900E+1	.106000E+01	.860594E+00	-.302941E+01
K	.20500E+1	.259000E+01	.210277E+01	.527723E-01
P	.26000E+0	.400000E-01	.324752E-01	-.227525E+00
H*	.32000E+0	.337000E+01	.273604E+01	.241604E+01
Rb	.64000E+2	.610000E+02	.495248E+02	-.144752E+02
Ba	.66800E+3	.332000E+03	.269545E+03	-.398455E+03
Sr	.72100E+3	.720000E+02	.584554E+02	-.662545E+03
Cu	.31000E+2	.290000E+02	.235446E+02	-.745545E+01

WZ-18-84

Si	.60410E+2	.591500E+02	.584373E+02	-.197265E+01
Ti	.82000E+0	.830000E+00	.820000E+00	-.355271E-14
Al	.17570E+2	.175400E+02	.173287E+02	-.241325E+00
Fe	.49600E+1	.589000E+01	.581904E+01	.859036E+00
Mn	.80000E-1	.160000E+00	.158072E+00	.780723E-01
Mg	.26000E+1	.322000E+01	.318120E+01	.581205E+00
Ca	.56300E+1	.443000E+01	.437663E+01	-.125337E+01
Na	.38900E+1	.352000E+01	.347759E+01	-.412410E+00
K	.20500E+1	.134000E+01	.132386E+01	-.726145E+00
P	.26000E+0	.220000E+00	.217349E+00	-.426506E-01
H*	.32000E+0	.368000E+01	.363566E+01	.331566E+01
Rb	.64000E+2	.330000E+02	.326024E+02	-.313976E+02
Ba	.66800E+3	.684000E+03	.675759E+03	.775904E+01
Sr	.72100E+3	.456000E+03	.450506E+03	-.270494E+03
Cu	.31000E+2	.100000E+01	.987952E+00	-.300120E+02

WZ-20-84

Si	.60410E+2	.662200E+02	.517147E+02	-.869533E+01
Ti	.82000E+0	.105000E+01	.820000E+00	-.355271E-14
Al	.17570E+2	.174000E+02	.135886E+02	-.398143E+01
Fe	.49600E+1	.513000E+01	.400629E+01	-.953714E+00
Mn	.80000E-1	.120000E+00	.937143E-01	.137143E-01
Mg	.26000E+1	.187000E+01	.146038E+01	-.113962E+01
Ca	.56300E+1	.130000E+00	.101524E+00	-.552848E+01
Na	.38900E+1	.309000E+01	.241314E+01	-.147686E+01
K	.20500E+1	.630000E+00	.492000E+00	-.155800E+01
P	.26000E+0	.900000E-01	.702857E-01	-.189714E+00
H*	.32000E+0	.385000E+01	.300667E+01	.268667E+01
Rb	.64000E+2	.270000E+02	.210857E+02	-.429143E+02
Ba	.66800E+3	.363000E+03	.283486E+03	-.384514E+03
Sr	.72100E+3	.184000E+03	.143695E+03	-.577305E+03
Cu	.31000E+2	.237000E+03	.185086E+03	.154086E+03

WZ-21-84

Si	.60410E+2	.722600E+02	.543607E+02	-.604927E+01
Ti	.82000E+0	.109000E+01	.820000E+00	-.355271E-14
Al	.17570E+2	.191900E+02	.144365E+02	-.313349E+01
Fe	.49600E+1	.700000E+00	.526606E+00	-.443339E+01
Mn	.80000E-1	.100000E-01	.752294E-02	-.724771E-01
Mg	.26000E+1	.170000E+00	.127890E+00	-.247211E+01
Ca	.56300E+1	.80000E-1	.601835E-01	-.556982E+01
Na	.38900E+1	.170000E+00	.127890E+00	-.376211E+01
K	.20500E+1	.182000E+01	.136917E+01	-.680826E+00
P	.26000E+0	.110000E+00	.827523E-01	-.177248E+00
H*	.32000E+0	.538000E+01	.404734E+01	.372734E+01
Rb	.64000E+2	.400000E+02	.300917E+02	-.339083E+02
Ba	.66800E+3	.258000E+03	.194092E+03	-.473908E+03
Sr	.72100E+3	.245000E+03	.184312E+03	-.536688E+03
Cu	.31000E+2	.800000E+01	.601835E+01	-.249817E+02

WZ-22-84

Si	.60410E+2	.870300E+02	.951528E+02	.347428E+02
Ti	.82000E+0	.750000E+00	.820000E+00	-.355271E-14
Al	.17570E+2	.833000E+01	.910746E+01	-.846253E+01
Fe	.49600E+1	.500000E-01	.546060E-01	-.484533E+01
Mn	.80000E-1	0.	0.	-.800000E-01
Mg	.26000E+1	0.	0.	-.260000E+01
Ca	.56300E+1	.160000E+00	.174933E+00	-.545506E+01
Na	.38900E+1	.104000E+01	.113706E+01	-.377629E+01
K	.20500E+1	.171000E+01	.186960E+01	-.180400E+00
P	.26000E+0	.700000E-01	.765333E-01	-.183466E+00
H*	.32000E+0	.194000E+01	.212106E+01	.180106E+01
Rb	.64000E+2	.250000E+02	.273333E+02	-.366666E+02
Ba	.66800E+3	.114000E+03	.124640E+03	-.543360E+03
Sr	.72100E+3	.125000E+03	.136666E+03	-.584333E+03
Cu	.31000E+2	.172000E+03	.188053E+03	.157053E+03

WZ-117-84

Si	.60410E+2	.735100E+02	.621425E+02	.173247E+01
Ti	.82000E+0	.970000E+00	.820000E+00	-.355271E-14
Al	.17570E+2	.166900E+02	.141091E+02	-.346093E+01
Fe	.49600E+1	0.	0.	-.496000E+01
Mn	.80000E-1	0.	0.	-.800000E-01
Mg	.26000E+1	0.	0.	-.260000E+01
Ca	.56300E+1	.490000E+00	.414227E+00	-.521577E+01
Na	.38900E+1	.182000E+01	.153856E+01	-.235144E+01
K	.20500E+1	.246000E+01	.207959E+01	.295876E-01
P	.26000E+0	.350000E+00	.295876E+00	.358763E-01
H*	.32000E+0	.381000E+01	.322082E+01	.290082E+01
Rb	.64000E+2	.100000E+01	.845361E+00	-.631546E+02
Ba	.66800E+3	.748000E+03	.632330E+03	-.356701E+02
Sr	.72100E+3	.170000E+03	.143711E+03	-.577289E+03
Cu	.31000E+2	.340000E+02	.287423E+02	-.225773E+01

WZ-121-84

H* : Water. E+1 : Power to 1, i.e. x10. Gains or losses are in grams per 100 grams for major elements and in parts per million for trace elements.